5-2014

Analysis of Snake Creek Burial Cave Mustela fossils using Linear & Landmark-based Morphometrics: Implications for Weasel Classification & Black-footed Ferret Conservation

Nathaniel S. Fox III
East Tennessee State University

Analysis of Snake Creek Burial Cave *Mustela* fossils using Linear & Landmark-based Morphometrics: Implications for Weasel Classification & Black-footed Ferret Conservation

---

A thesis

presented to

the faculty of the Department of Geosciences

East Tennessee State University

In partial fulfillment

of the requirements for the degree

Master of Science in Geosciences

---

by

Nathaniel S. Fox

May 2014

Dr. Steven C. Wallace, Chair

Dr. Jim I. Mead

Dr. Blaine W. Schubert

Keywords: *Mustela*, weasels, morphometrics, classification, conservation, Pleistocene, Holocene

ABSTRACT

Analysis of Snake Creek Burial Cave *Mustela* fossils using Linear & Landmark-based Morphometrics: Implications for Weasel Classification & Black-footed Ferret Conservation

by

Nathaniel S. Fox

Two discreet methods of geometric morphometrics were applied to evaluate the taxonomic utility of each in classifying the craniomandibular region of several *Mustela* species. Use of both linear measurements and 2-dimensional landmarks proved successful in discriminating between extant *M. nigripes* (black-footed ferret) and *Neovison vison* (American mink), in addition to the extant North American weasel species (*M. erminea*, *M. frenata*, *M. nivalis*). Methods were then used to classify Late Pleistocene *Mustela* spp. fossils collected from Snake Creek Burial Cave (SCBC) of eastern Nevada. Data acquired for unknown predicted group memberships varied markedly among methods and specimens. Nevertheless, results support the presence of *M. nigripes* and all 3 weasel taxa among the SCBC paleofauna.

ACKNOWLEDGMENTS

I would like to thank my thesis committee and East Tennessee State University faculty members: Drs. Steven Wallace, Jim Mead, and Blaine Schubert for their imperative revisions and feedback towards this manuscript. I am also indebted to the following collections personnel: Sandy Swift (Collections Manager, East Tennessee State University), Judith Chupasko (Curatorial Associate and Collections Manager, Harvard Museum of Comparative Zoology), Mark Omura (Curatorial Assistant, Harvard Museum of Comparative Zoology), and Suzanne Peurach (Collection Manager, Smithsonian National Museum of Natural History) for their generous hospitality and assistance in data collection. Furthermore, this study would not have been possible without materials provided through the research of Emily Mead and Dr. Jim Mead who facilitated the groundwork. I must also thank Dr. Steven Wallace, Dr. Eileen Ernenwein, Dr. Andrew Joyner, and Eric Lynch for their assistance with the variety of morphometric and geospatial programs used herein. Lastly, I give special thanks to my family, friends, and colleagues for their continued support throughout the development of this project.

TABLE OF CONTENTS

Page

LIST OF TABLES

Table Page

LIST OF FIGURES

Figure Page

CHAPTER 1

INTRODUCTION

Snake Creek Burial Cave (SCBC), located in White Pine County, Nevada (Fig. 1), is a karst-derived vertical sinkhole that spans 3 meters at the entrance (Heaton 1987). The cave is positioned within a small ridge along a series of alluvial channels draining from southern Snake Range (Mead and Mead 1989). As a natural trap, SCBC offers insight into a relatively sparse (Lawlor 1998) and inadequately understood Late Pleistocene valley-bottom paleocommunity of the Great Basin (Grayson 1987; Mead and Mead 1989). Radiocarbon and uranium isotope series analyses taken from *in-situ* microtine rodents have produced ages ranging from 9,460 +/- 160 to 15,100 +/- 700 years BP, extending from latest Pleistocene (Rancholabrean Land Mammal Age) into the Early Holocene (Bell and Mead 1998). Few descriptions of this chronologic unit have been reported within surrounding areas of the Great Basin, thus contributing to the significance of this locality (Mead and Mead 1989). Among the many species identified through preliminary investigation, SCBC yields an unprecedented diversity of up to 8 mustelids (Mead and Mead 1989). Reported taxa include: *Martes americana* (American marten), *M. nobilis* (extinct noble marten), *Mustela erminea* (ermine), *M. frenata* (long-tailed weasel), *M. nigripes* (black-footed ferret), *M. nivalis* (least weasel), *Neovison vison* (American mink), and *Gulo gulo* (wolverine). Of these species, *M. nigripes*, *M. nivalis*, and *Gulo gulo* were formerly absent among Rancholabrean-age Great Basin localities (Mead and Mead 1989).

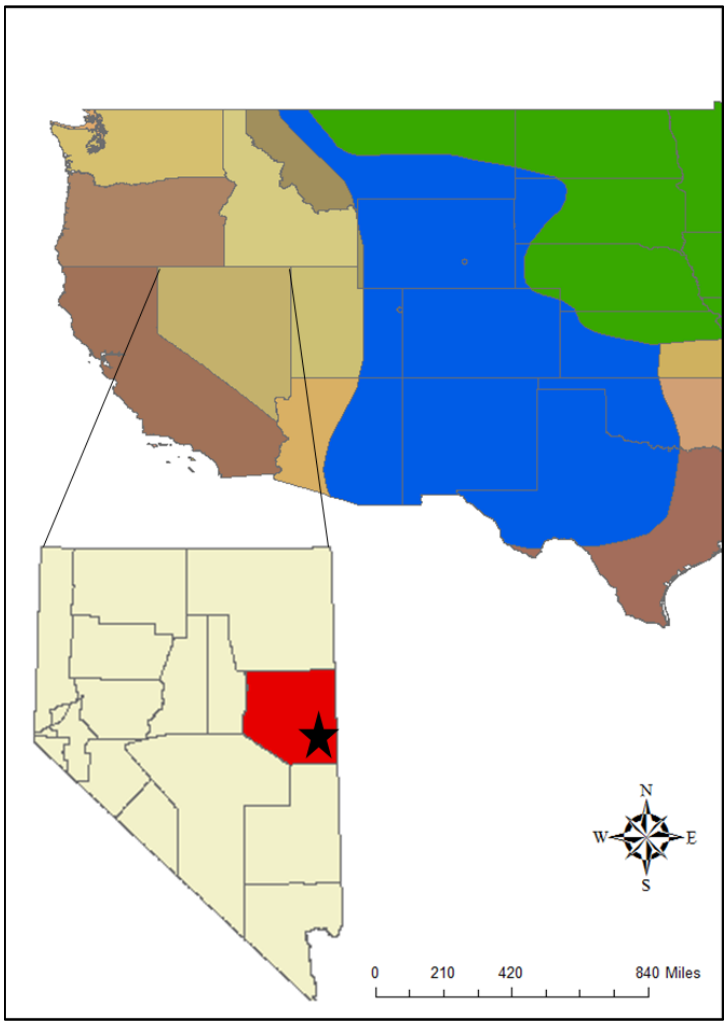

Figure 1. Map of the western United States including historic distributions of *Mustela nigripes* and *M. nivalis* as illustrated in blue and green respectively. White Pine County is depicted in red with a black star indicating the relative location of SCBC. Species range data from: Patterson et al. (2007).

Confirmed occurrence of *M. nigripes* within SCBC would expand the historic distribution of this taxon further westward (Mead and Mead 1989) (Fig. 1). Interestingly, *Cynomys* spp., the principal dietary component of living black-footed ferrets (Clark 1986), are notably absent from this locality despite extensive sorting of an estimated 30,000 vertebrate specimens (Mead and Mead 1989). Quantitative verification of *M. nigripes* from this *Cynomys*-lacking paleontological locality may prompt innovative methods for management and reintroduction of contemporary black-footed ferrets in wild habitats (e.g., Owen et al. 2000). Preliminary description of these mustelids, however, acknowledged that collected materials of *M. nigripes* and "*M.*" *vison*, now *Neovison vison* (Abramov 2000; Wozencraft 2005), would benefit from reexamination due to general morphologic similarities between these taxa (Mead and Mead 1989).

Additionally, over 90 weasel-sized fossils have been collected from SCBC as well. Confirmation of *M. nivalis* among these specimens would extend this taxon markedly westward of its modern distribution (Mead and Mead 1989) (Fig. 1). However, differentiating the skeletons of North American weasels can prove considerably challenging due to excessive morphological similarly, intraspecific variation, and interspecific size overlap among *M. nivalis*, *M. erminea*, and *M. frenata* (McNab 1971; Kurose et al. 2005; King and Powell 2007). Such difficulties are often amplified when dealing with disarticulated or fragmentary skeletal elements (Kurtén 1968). Given that isolated crania and dentaries of all 3 weasel taxa are tentatively described from this locality, a comprehensive examination of the material is warranted (Mead and Mead 1989). Consequently, the objective of this study is to classify individual specimens of *Mustela* spp. collected from SCBC through the use of various geometric morphometric techniques. Note that the term "weasel" is used herein to include all North American *Mustela* species of the subgenus

Mustela; *M.* (*Mustela*) *erminea*, *M.* (*Mustela*) *frenata*, and *M.* (*Mustela*) *nivalis*, in exclusion of *M.* (*Putorius*) *nigripes*.

CHAPTER 2

BACKGROUND

Evolutionary History

Mustela is a specialized genus of carnivorous mammals within the diverse family Mustelidae (Hosoda et al. 2000; Heptner et al. 2002; Koepfli et al. 2008) (Fig. 2). Origins of the family, which includes 59 extant species and 22 genera (Wozencraft 2005; Kurose et al. 2008; Koepfli et al. 2008) date back to the early Oligocene in North America, Europe, and Asia (Brown 1966; Ewer 1973). Phylogenetic time estimates for this split between mustelid and procyonid lineages are calibrated at approximately 28.5 Mya (Bininda-Emonds et al. 1999; Sato et al. 2003; Koepfli et al. 2008; Sato et al. 2012). Most studies suggest that mustelid diversification occurred in Eurasia (Kurtén and Anderson 1980; Sato et al. 2012), with intercontinental speciation and adaptive radiation occurring through several dispersal events (Hosoda et al. 2000; Koepfli et al. 2008). Following the Mid-Miocene Climatic Optimum, 2 major bursts of diversification likely occurred within the Mustelidae (Koepfli et al. 2008). An initial event during the Late Miocene (8.8-12.5 Mya) is thought to have given rise to most extant lineages (Brown 1966; King 1989; Marmi et al. 2004; Koepfli et al. 2008). While a second event in the Pliocene (1.8-5.3 Mya) likely resulted in rapid generic and species-level diversification (Marmi et al. 2004; Koepfli et al. 2008). This secondary event is thought to have occurred in response to northern climatic cooling throughout the Pliocene (King 1989; Koepfli et al. 2008). During the Late Miocene, forests were gradually replaced by grasslands resulting in the abrupt radiation of voles and other field rodents (King 1989; King and Powell 2007; Koepfli et al. 2008). Consequently, members of the genus *Mustela* likely evolved from a forest dwelling,

martin-like ancestor in response to open niches for exploiting narrow subterranean rodent burrows (King and Powell 2007).

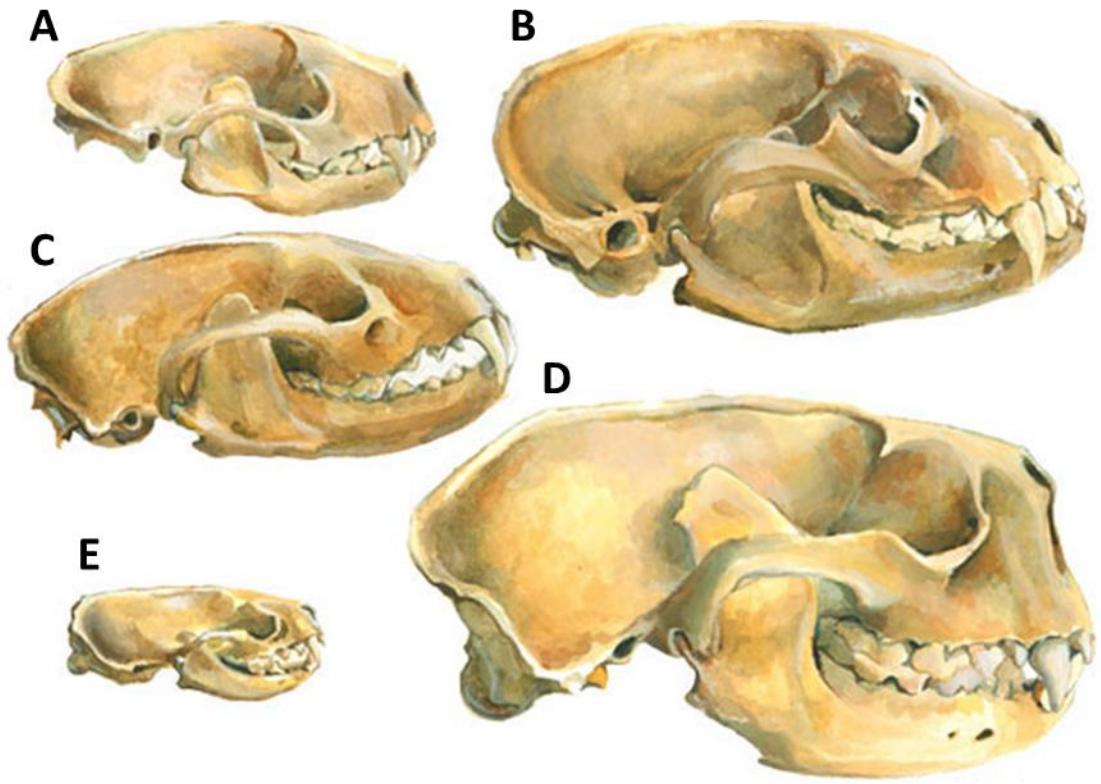

Figure 2. Right lateral skull profiles of *Mephitis mephitis* (A), *Taxidea taxus* (B), *Martes pennanti* (C), *Enhydra lutris* (D), and *Mustela frenata* (E) exemplifying the morphologic diversity within the Musteloidea. Illustration from: Harrington (2013).

Ancestral species of *Mustela* are thought to have entered North America during the Late Miocene through Eurasia (Kurtén and Anderson 1980; Heptner et al. 2002; King and Powell 2007; Koepfli et al. 2008). The first record of fossil weasels that closely resemble extant forms appear in the Late Pliocene, represented by *M. plioerminea* of Eurasia (Anderson 1989; King 1989; King and Powell 2007) and *M. rexrodensis* from the Blancan of North America (Hibbard 1950; Kurtén and Anderson 1980; King and Powell 2007). However, intercontinental relationships remain poorly understood for many of these extinct forms (Heptner et al. 2002; Koepfli et al. 2008). Extant *Mustela* spp. exhibit a primarily circumboreal distribution throughout much of the Holarctic (King 1989). Currently, this genus includes 17 extant species (Abroamov 2000; Wozencraft 2005) making it the most diverse within the Order Carnivora (Abroamov 2000; Kurose et al. 2008). Members of this group are among the most diminutive of the Mustelidae (Fig. 2), with *M. nivalis* acknowledged as the smallest living carnivoran (Anderson 1989; Hosoda et al. 2000; Heptner et al. 2002; Flynn et al. 2005). *Mustela* taxa range in size from 125 mm (35g) for *M. nivalis* (Hall 1981; Ewer 1973; Sheffield and King 1994; Hosoda et al. 2000) to 565 mm in body length for *M. eversmanni* (Heptner et al. 2002).

Within this heterogeneous group, *Mustela* species include weasels, minks, and polecats: *M. africana* (Amazon weasel), *M. altaica* (Mountain weasel), *M. erminea* (ermine or stoat), *M. eversmanni* (steppe polecat), *M. felipei* (Columbian weasel), *M. frenata* (long-tailed weasel), *M. itatsi* (Japanese weasel), *M. kathiah* (yellow-belled weasel), *M. lutreola* (European mink), *M. lutreolina* (Indonesian mountain weasel), *M. nigripes* (black-footed ferret), *M. nivalis* (least weasel), *M. nudipes* (Malayan weasel), *M. putorius* (European polecat), *M. siberica* (Siberian weasel), *M. strigidorsa* (black-stripped weasel) and *M. subpalmata* (Egyptian weasel). Of these taxa, 4 are indigenous to North America (*M. erminea*, *M. frenata*, *M. nigripes*, and *M. nivalis*) as

well as the closely related American mink, *Neovison vison* (Abroamov 2000; Wozencraft 2005). Although considerable osteologic similarities occur among some of these species, marked differences are exhibited by others (Heptner et al. 2002). Consequently, discrete morphologic and phylogenetic "groups" are acknowledged. These groups have been separated into multiple subgenera, though a definitive number and their species membership remains debated (Kurose et al. 2008). Previous authors have proposed from 2 (Heptner et al. 2002), to as many as 9 subgenera within *Mustela* (Abroamov 2000). From a conservative standpoint, at least 2 subgenera exist; the distinctive polecats (subgenus *Putorius*), and all other species (Heptner et al. 2002; Koepfli et al. 2008). Members of subgenus *Putorius* include: *M. eversmanni* (steppe polecat), *M. putorius* (European polecat), and *M. nigripes* (black-footed ferret) (Abroamov 2000; Wozencraft 2005). However, other subgenera proposed within *Mustela* include: *Gale, Lutreola, Kolonokus, Pocockictis, Grammogale, Cabreragale*, and *Cryptomustela* (Abroamov 2000).

Phylogeny

Within the Mustelidae, up to 15 subfamilies have been proposed (Pocock 1921). Five subfamilies were traditionally supported by Simpson (1945) including: Mustelinae (weasels, ferrets, mink, martins, and wolverine), Lutrinae (otters), Mellivorinae (honey-badger), Melinae (true badgers), and Mephitinae (skunks). Each of these groups was considered monophyletic with respect to several morphological characters including scent gland enlargement, loss of the upper second molar, and loss of the carnassial notch on the upper fourth premolar (Bryant et al. 1993; Dragoo and Honeycutt 1997; Marmi et al. 2004). Although, it is now acknowledged that the Mephitinae diverged prior to the mustelid-procyonid split due to recent molecular and phylogenetic inferences, ultimately forming a discrete family; Mephitidae (Dragoo and Honeycutt 1997; Marmi et al. 2004; Flynn et al. 2005; Wozencraft 2005; Koepfli et al. 2008).

Koepfli et al. (2008) recently proposed 8 mustelid subfamilies that include: Lutrinae (otters), Mustelinae (weasels and ferrets), Galictinae, Taxidiinae (American badger), Helictidinae (ferret badgers), Martinae (martins, fishers, and wolverines), Melinae (hog badger and European badger), and Mellivorinae (honey badger). Nevertheless, only 2 cohesive subfamilies are commonly acknowledged at present: Mustelinae and Lutrinae (Wozencraft 2005).

Subfamily Mustelinae is generally considered non monophyletic (Bryant et al. 1993; Dragoo and Honeycutt 1997; Bininda-Emonds et al. 1999; Hosoda et al. 2000; Koepfli et al. 2003; Sato et al. 2003; Flynn et al. 2005; Koepfli et al. 2008; Sato et al. 2012), although there is little consensus on whether the group is paraphyletic or polyphyletic. Synapomorphies have been difficult to establish among mustelids due to their retention of several plesiomorphic traits (Anderson 1989; Dragoo and Honeycutt 1997). However, the Mustelinae are especially problematic due to their historic usage as a "waste-basket" group for taxa of complicated phylogenetic orientation (Anderson 1989; Dragoo and Honeycutt 1997; Koepfli and Wayne 2003). Among these systematically ambiguous taxa is *Neovison vison*, historically grouped within genus *Mustela*. More recently, it has been reported that *N. vison* is an outgroup to *Mustela* spp., splitting between 5 and 14 Mya (Bininda-Emonds et al. 1999; Hosoda et al. 2000; Sato et al. 2003; Kurose et al. 2008). These extensive temporal estimates stem from differences in methodology. Karyosystematic analyses (Grafodatsky et al. 1976; Mandahl and Fredga 1980); mitochondrial DNA of the cytochrome-*b* region (Hosoda et al. 2000; Kurose et al. 2000; Kurose et al. 2008); nuclear interphotoreceptor retinoid binding protein analyses (Sato et al. 2003); and multigene Bayesian inference (Koepfli et al., 2008) yield estimates ranging from 10-14 Mya (Hosoda et al. 2000); to 4.6-7.3 Mya divergence periods (Koepfli et al. 2008).

While *N. vison* is currently placed basal to *Mustela* spp. (Abramov 2000; Kurose et al. 2000; Wozencraft 2005; Kurose et al. 2008); alternate studies reject the discreet generic status of this taxon (Marmi et al. 2004; Sato et al. 2012; Abramov et al. 2013), or its assignment as a lone outgroup (Koepfli et al. 2008; Harding and Smith 2009) (Figs. 3-4). Harding and Smith (2009) addressed that several of the previous analyses that demonstrated generic divergence between *N. vison* and *Mustela* spp. were biased in respect to their geographic selection and species diversity, often in exclusion of endemic New World taxa. Their study using Bayesian and likelihood inferences from the cytochrome-*b* gene that included the enigmatic South American species *M. africana* and *M. felipei*, grouped *N. vison* among these New World taxa (Harding and Smith 2009) (Fig. 3). Moreover, these authors proposed that endemic New World weasels (*M. frenata, M. africana, M. felipei*) and *N. vison* all warrant phylogenetic placement outside the Old World *Mustela* spp. (Harding and Smith 2009). Likewise, a recent analysis integrating these South American taxa produced a monophyletic tree of *Mustela* spp., with endemic North American taxa (including *N. vison*) forming a distinct subgroup (Abramov et al. 2013) (Fig. 3).

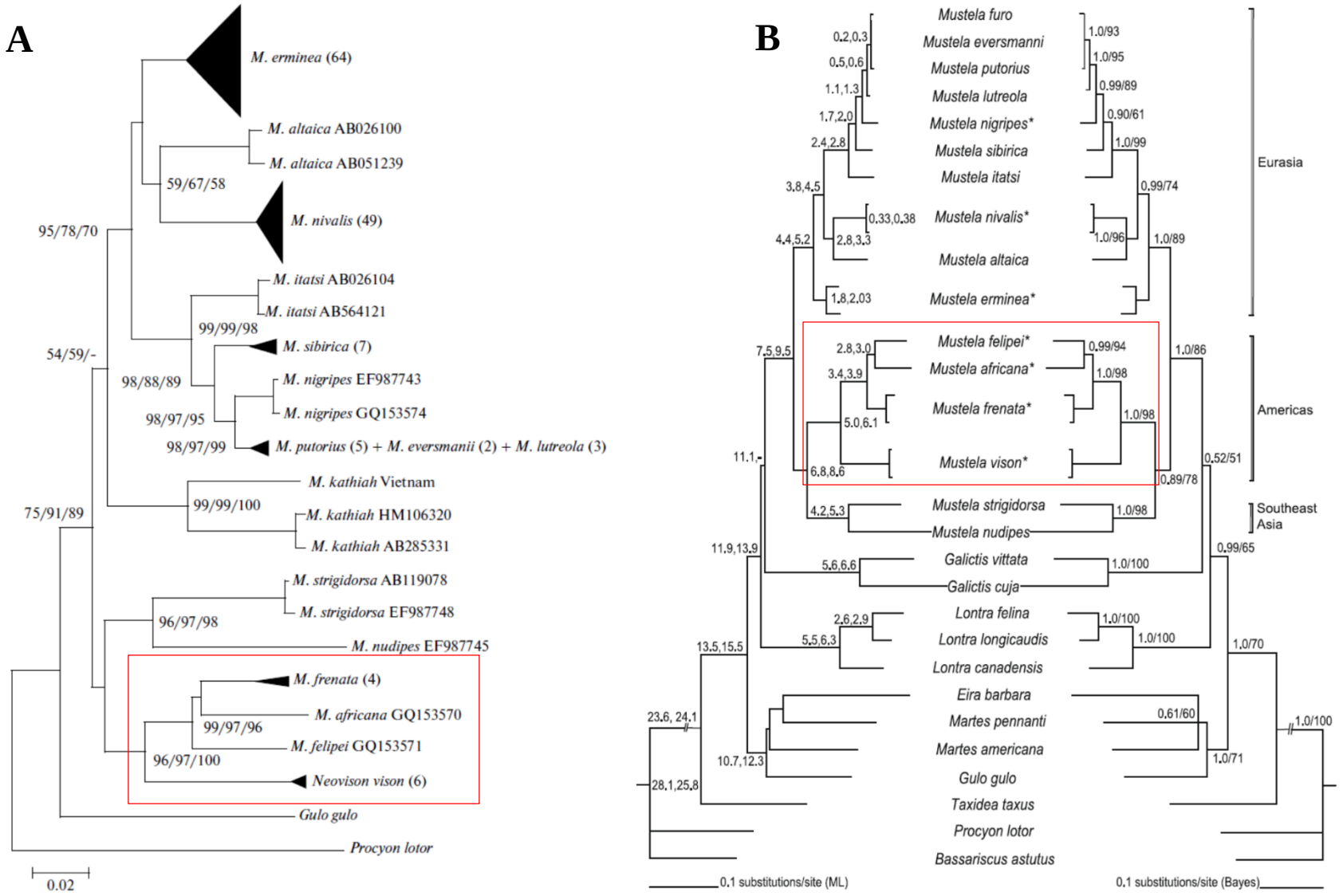

Figure 3. Two recent cladistic analyses grouping *Neovison vison* within endemic New World taxa (*M. africana*, *M. felipei*, *M. frenata*). Modified from: A) Abramov et al. (2013), B) Harding and Smith (2009).

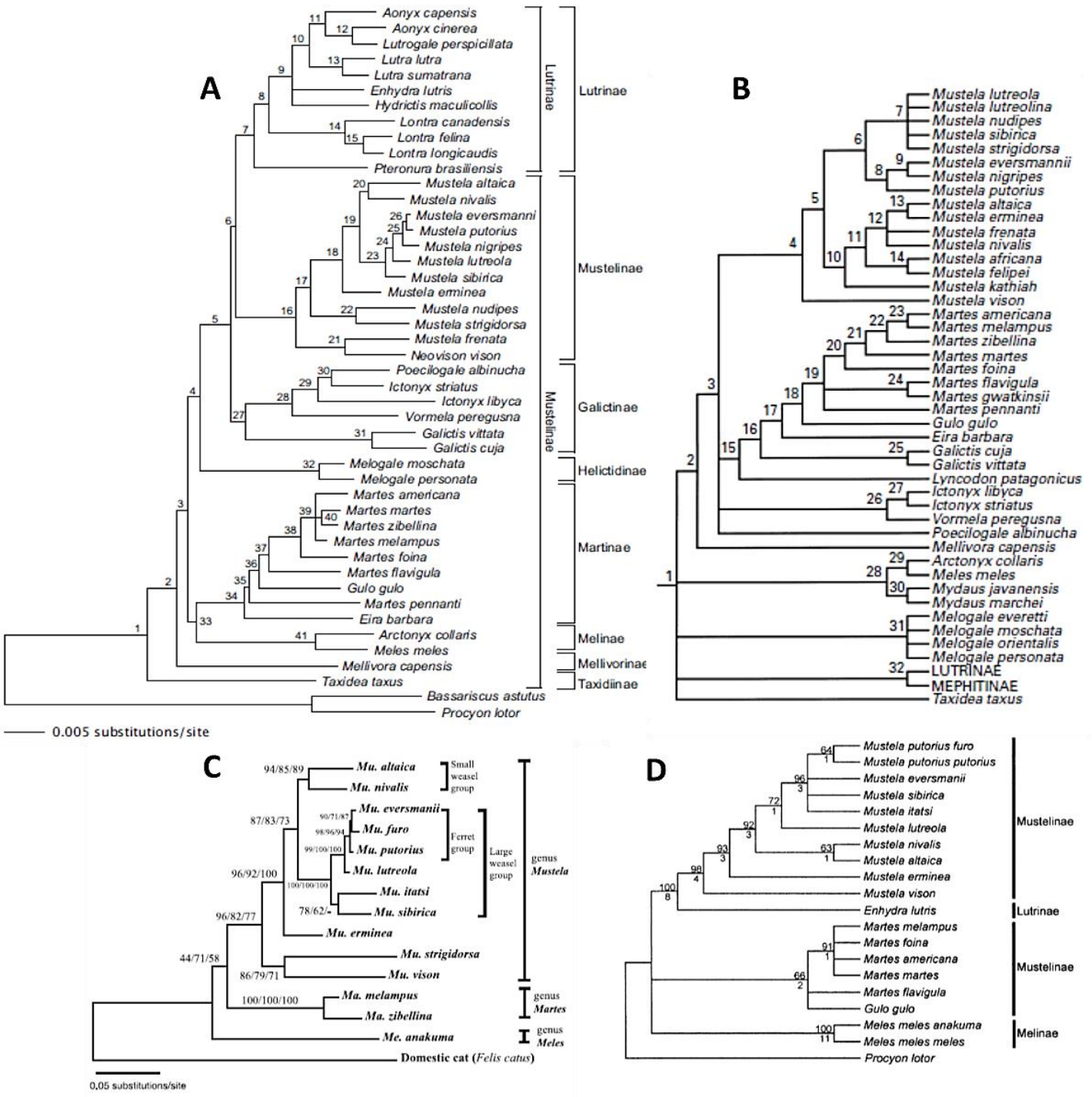

Figure 4. Mustelidae phylogenies published over the past 15 years. Modified from: A) Koepfli et al. (2008) with Lutrinae most closely related to Mustelinae and *Mustela frenata* + *Neovison vison* basal to Mustelinae. B) Bininda-Emonds et al. (1999) with *Martes* spp. + *Gulo gulo* as closest outgroup to *Mustela* spp. C) Kurose et al. (2008) with *Martes* spp. closest to *Mustela* spp., and *M. strigidorsa* and *N. vison* basal to genus *Mustela*. D) Sato et al. (2003) with Lutrinae more closely related to *Mustela* spp. than *Martes* spp.

Additional disagreement remains with the ancestry and divergence periods of *Mustela* spp. and their sister groups. Some authors support a *Martes*/*Gulo* group as most closely related (excluding *N. vison*) (Dragoo and Honeycutt 1997; Bininda-Emonds et al. 1999; Hosoda et al. 2000; Kurose et al. 2008), while others support a closer phylogenetic relationship of the Lutrinae (i.e., *Lontra* and *Enhydra*) to *Mustela* spp. (Sato et al. 2003; Marmi et al. 2004; Flynn et al. 2005; Koepfli et al. 2008; Harding and Smith 2009) (Fig. 4). Nevertheless, divergence estimates vary markedly among all (Fig. 4). Consequently, until phylogenetic consensus is reached, temporal ranges and systematic positioning of *N. vison* and other taxa both closely related to, and within the genus *Mustela*, remain unclear and are beyond the scope of this project.

Characters of *Mustela*

Despite their somewhat ambiguous phylogeny, several conditions are recognized for taxonomically differentiating members of the Mustelidae and Mustelinae. For instance, all mustelids exhibit a reduction or loss of the anterior premolar, loss of the second and third upper molars, loss of the third lower molar, and reduction of the second lower molar (Anderson 1989). Within the genus *Mustela*, dental formulas are as follows: I 3/3: C 1/1: P 3/3: M 1/2 = 34 (Ewer 1973; King and Powell 2007). Moreover, the upper and lower detentions of *Mustela* spp. exhibit highly sectorial modifications (King and Powell 2007), with upper fourth premolars exhibiting a simplistic deuterocone (Hall 1981). Upper first molars of these taxa express a markedly expanded protocone, while the metaconid of the lower first molars is absent (Hall 1981). Their lower first molars also exhibit a comparatively elongate trigonid relative to the trenchant talonid (Hall 1981), with a prominent occlusal recess in the lower carnassial notch (King and Powell 2007). Additionally, the lower incisors are markedly compacted, with medial teeth often overlapping into a posterior row (King and Powell 2007).

Cranial features shared by *Mustela* spp. include a relatively small, narrow, flattened, and overall elongate skull (Heptner et al. 2002; King and Powell 2007). Furthermore, they exhibit a short, blunt rostrum and markedly elongate parietals that are slightly expanded near the occipital region (Kurtén and Anderson 1980; Heptner et al. 2002). Sagittal crests are often well-developed, while the zygoma are comparatively thin (King and Powell 2007) and demonstrate a weak lateral flare relative to other carnivora (Heptner et al. 2002). Hard palates in these taxa are located posterior to the upper first molars (Hall 1981), while the glenoid (mandibular) fossa is partially enclosed by the postglenoid process, greatly inhibiting lateral movement of the dentary (Anderson 1989; King and Powell 2007). Auditory bullae are markedly inflated and elongate, while the mastoid and paraoccipital processes remain weakly developed and narrowed towards the tympanum (Hall 1981; Heptner et al. 2002). Crests and protuberances throughout the skull are relatively subtle with minimal convexity near the orbital region (Heptner et al. 2002). In sexually mature individuals cranial sutures exhibit complete fusion (King and Powell 2007). Lastly, the coronoid processes of the jaw are proportionally large relative to the total length of the dentary (King and Powell 2007).

Body shape within the genus *Mustela* is serpent-like, exhibiting thin and elongate torsos exaggerated by short and stubby limbs that extend less than half the total body length (Moors 1980; Hall 1981; Anderson et al. 1986; Heptner et al. 2002; King and Powell 2007). Tail lengths vary greatly among species, ranging from less than one quarter, to more than half of the total body length (Hall 1981; King and Powell 2007). Orbits are relatively large, while the external ears are small, rounded, and widely separated (Heptner et al. 2002). Cervical vertebrae are elongate and robustly developed for strong muscular attachment (King and Powell 2007). Atlas and axis vertebrae are particularly well-developed and highly modified, markedly larger than the

rest of the vertebral column (King and Powell 2007). Total vertebrae include: 7 cervical, 14-15 thoracic, 5-6 lumbar, 2-4 sacral, and 11-33 caudal (King and Powell 2007). Gait and stance is digitigrade, supported by broad palms and soles that include 5 digits on each foot (Hall 1981; Anderson 1989; Heptner et al. 2002; King and Powell 2007). Limb and pelvic girdles are relatively gracile and medially compacted, no more laterally splayed than the width of the skull (King and Powell 2007). Furthermore, male *Mustela* can be identified by morphology of the baculum that exhibit prominent urethral grooves and a well-developed distal hook (Heptner et al. 2002; Baryshnikov et al. 2003). Moreover, the head of the baculum is either flattened, cup-shaped, or absent (Baryshnikov et al. 2003).

In regard to soft tissue characters, anal scent glands are present in all *Mustela*, though the strength and odor can vary significantly among taxa (Hall 1981; Heptner et al. 2002). Members are covered in a densely compacted silky pelage somewhat evenly spread throughout the length of the body (Anderson 1989; Heptner et al. 2002). Fur color varies markedly both among and within species ranging from 2-toned to monotone, and light color to dark (Heptner et al. 2002; King and Powell 2007). In many weasels the dorsal portions of these coats range in color from tan to dark brown in the summer, while the ventral regions range from pure white to dark yellow (King and Powell 2007). Weasels living in colder climates will express a whitish pelage phase in winter, while those in milder climates will remain darker (King and Powell 2007). Some species and subspecies form distinct facial patterns such as the black "mask" of *M. nigripes* (Hillman and Clark 1980; Anderson et al. 1986) or the white and brown markings of *M. frenata* in the southwestern United States (Fagerstone 1987; King and Powell 2007). Marked seasonal dimorphism is expressed in fur length and density, especially within populations at northern latitudes (Heptner et al. 2002, King and Powell 2007). The majority of *Mustela* spp. and closely

related taxa are terrestrial, though many are excellent climbers and swimmers as well (Brown 1966; Hosoda et al. 2000; King and Powell 2007). Locomotion is often characterized by quick arcading half-bounds facilitated by loose articulation of the vertebral column (e.g. Heptner et al. 2002; King and Powell 2007 and references therein).

North American Species Diagnosis

Mustela erminea, Linnaeus 1758; common name(s): ermine or stoat

Distribution and origins: exhibits circumboreal dispersal throughout much of the Holarctic (King 1983). Ranges from Ireland across Europe and into Russia, Algeria, the Middle East, and Japan (Ewer 1973; King 1983). In the New World this taxon can be found throughout much of North America, reaching as far northeast as Greenland, and continuing westward into Alaska (Ewer 1973; King 1983; Heptner et al. 2002) (Fig. 11). *Mustela erminea* fossils have not been reported prior to the Pleistocene (Hall 1981, King 1983). The oldest confirmed specimens of this taxon date to approximately 0.6 Mya and are common throughout European deposits around the Last Glacial Maximum (Kurtén 1968; King and Powell 2007). *Mustela erminea* is thought to have originated in Europe, evolving from *M. palerminea* during the Middle Pleistocene, which likely descended from *M. plioerminea* of the Late Pliocene (Kurtén 1968; King 1983). In a recent census 37 extant subspecies of *M. erminea* were acknowledged (Wozencraft 2005).

Diagnostic characters: total length is 225-340 mm and 190-290 mm for males and females respectively (Hall 1981). Pelage ranges from monotone white to dark brown on the dorsum with a whitish venter, dorsal, and ventral colors are well-delimited (Hall 1981; King and Powell 2007). Furthermore, the distal tail of *M. erminea* is black irrespective to season (Hall 1981; Heptner et al. 2002; King and Powell 2007). Skull width at the canines is markedly less

than the interorbital distance, while the supraorbital area is slightly elevated (Heptner et al. 2002) (Fig. 5). Postglenoid length is greater than 46% and 48% of the condylobasal length in males and females respectively (Hall 1981). Length between mastoid processes is around half the condylobasal length (Heptner et al. 2002) (Fig. 5). Tail length is 30-45% of the total body length (King and Powell 2007) encompassing 16-19 caudal vertebrae (King 1983). The baculum of male *M. erminea* does not curve upward anteriorly as in other members of its genus, and exhibits a markedly elongate 'S' shape (Heptner et al. 2002). Skull length is approximately 9-24% greater in males than in females (King 1983). Overall, their morphology is strikingly similar to that of the least weasel. As stated by Heptner et al. (2002, p. 997); "In its general proportions, manner of posture and movement, the ermine is entirely similar to the weasel and represents a somewhat enlarged copy of it". Tail length aside, however, *M. erminea* usually differs from *M. nivalis* in the following aspects: skull is relatively more elongate (particularly in the frontal and nasal regions), the braincase is generally less inflated, the postorbital constriction is usually more extensive and narrowed, cranial processes and crests are more abruptly defined overall, anterior portions of the sagittal crest are generally better developed, infraorbital foramina are rounded and comparatively large, anterior slope of the facial region is generally steeper, dentition is, overall, more strongly developed (particularly in the upper carnassials), upper canines are comparatively elongate and thin, and lower canines are generally more massive (Heptner et al. 2002).

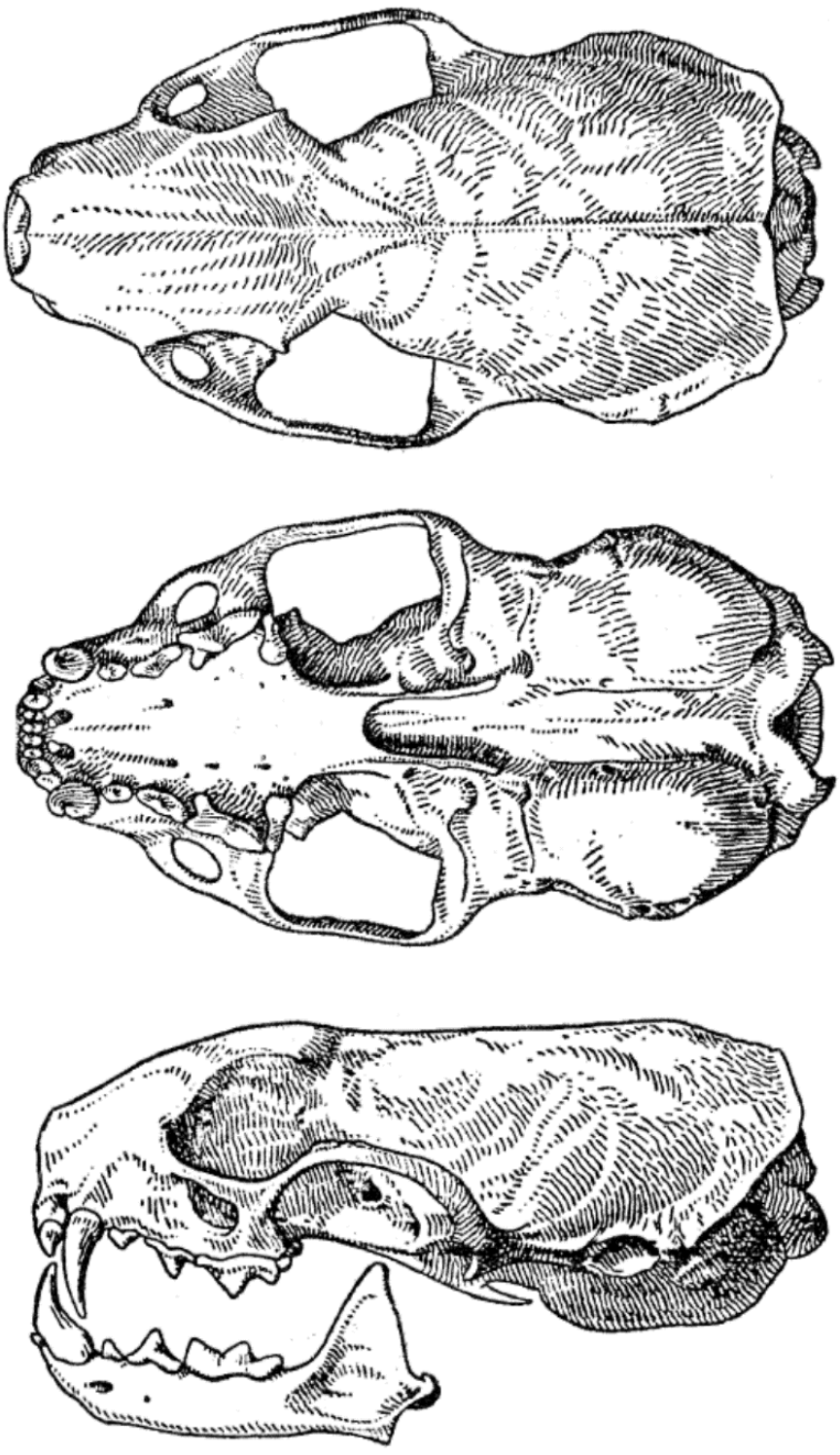

Figure 5. *Mustela erminea* skull in dorsal (top), ventral (center), and left lateral (bottom) views. Image is not to scale. Modified from King (1983).

Mustela frenata Lichtenstein, 1831; common name(s): long-tailed weasel or bridled weasel

Distribution and origins: although restricted to the New World, this species demonstrates the most expansive distribution of any mustelid in the western Hemisphere (Sheffield and Thomas 1997). Ranges through much of the United States, Central America, and into northwestern South America (Ewer 1973; Sheffield and Thomas 1997) (Fig. 11). Southern boundaries of this taxon reach Peru and the Bolivian Andes (Sheffield and Thomas 1997; Heptner et al. 2002). The fossil record of *M. frenata* is more temporally extensive than of *M. erminea* or *M. nivalis* given that specimens have been recovered from North American deposits prior to 2 Mya (King and Powell 2007). *Mustela rexroadensis* from the Blancan of North America may be ancestral to *M. frenata*, though these inferences remain speculative (Hibbard 1950; Kurtén and Anderson 1980; King and Powell 2007). While similar in morphology and behavior, *M. frenata* and *M. erminea* are thought to have diverged more than 4 Mya, the latter originating in the Old World, the former in the New World (King and Powell 2007). Forty-two extant subspecies of *M. frenata* are currently acknowledged (Wozencraft 2005).

Diagnostic characters: largest of the 3 North American weasel taxa overall (King and Powell 2007). Total length ranges from 300-550 mm (Hall 1981). Postglenoid length is less than 46% and 47% of the condylobasal length in males and females respectively (Hall 1981; Sheffield and Thomas 1997). The distal tail exhibits a prominent black tip, yet is less extensive then in most *M. erminea* subspecies (Hall 1981). Tail length encompasses 40-70% of the total body length including 19-33 caudal vertebrae (King and Powell 2007). *M. frenata* usually displays a brown dorsum in summer with a lightly tinted, often yellowish, venter (Hall 1981). Only northern subspecies of this taxon exhibit white pelage in winter (Hall 1981). *M. frenata* usually differs morphologically from *M. erminea* in exhibiting greater skull rugosity and a more elongate rostrum (Kurtén and Anderson 1980) (Fig. 6). Additionally, there is greater geographic variation

in pelage and relative anatomic proportions among *M. frenata* than in *M. erminea or M. nivalis* (Hall 1981; Fagerstone 1987; Sheffield and Thomas 1997).

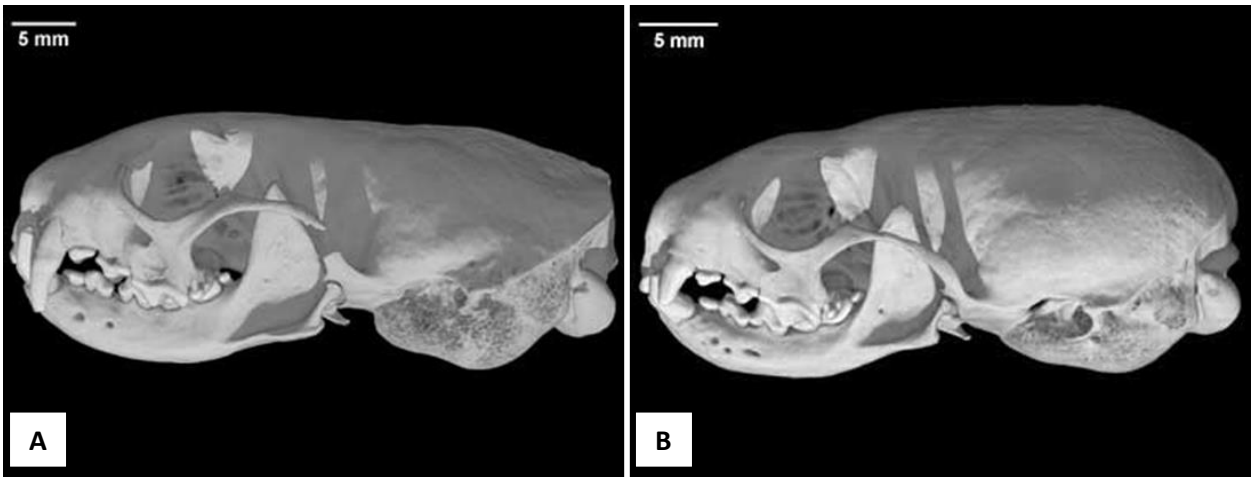

Figure 6. A) Male *Mustela frenata* skull (USNM 52702) in lateral view, B) female *M. frenata* skull (USNM 95054) in lateral view. From: Digital Morphology (2002-2005).

Mustela nigripes Audubon and Bachman, 1851; common name(s): black-footed ferret, American polecat

Distribution and origins: formerly dispersed throughout mid-western North America from Alberta and Saskatchewan, down into the Great Plains, intermontane areas of the Rocky Mountains, and the southwestern United States (Hillman and Clark 1980; Anderson et al. 1986; Owen et al. 2000). Range almost coincides in full with that of *Cynomys* spp. (Hillman and Clark 1980; Hall 1981). This taxon is often considered obligate to the genus *Cynomys* for both food and shelter (Hall 1981). Nearing extinction due to steady population declines throughout the 20th century, the last known wild individuals were captured from 1985 to 1987 and subsequently bred in captivity (Seal et al. 1989; Klebanoff et al. 1991; Biggens et al. 2011a). The oldest substantiated black-footed ferret fossils from Colorado date between 400,000-850,000 yr BP (Youngman 1994). Prehistoric *M. nigripes* likely colonized North America from Asia during glacial period dispersal events through Beringia (Kurtén and Anderson 1980; Youngman 1994). This species shares close phylogenetic affinity to the Siberian polecat *M. eversmanii*, some authors have considered these taxa conspecific (Anderson 1977; Kurtén and Anderson 1980; Wozencraft 2005). No extant subspecies of *M. nigripes* are currently acknowledged (Wozencraft 2005).

Diagnostic characters: roughly mink sized, pelage exhibits a whitish-yellow buff with a black distal tail and feet (Hillman and Clark 1980; Hall 1981). Winter coat is marginally lighter than in summer (Hall 1981). Tail includes 17 vertebrate encompassing 22-25% of the total body length (Hillman and Clark 1980; Hall 1981). Females are approximately 10% smaller than males (Hall 1981). Size notwithstanding, *M. nigripes* can be differentiated from weasels of the subgenus *Mustela* in lacking a prominent dorsal-ventral boundary (Hillman and Clark 1980).

Furthermore, *M. nigripes* exhibit a distinct black mask across the orbital region (Hall 1981). This species can be distinguished anatomically from weasels in demonstrating a proportionally shorter, broader, and more robust skull (Anderson et al. 1986; Abramov 2000), as well as more angular mastoid processes (Hillman and Clark 1980) (Fig. 7). Additional cranial characters include: a longer rostrum than the length of the braincase (Abramov 2000); a relatively shallow facial slope, well-developed postorbital processes, an exaggerated postorbital constriction, a relatively narrow basioccipital region, relatively pronounced lateral flaring of the zygoma, and more obliquely compressed auditory bullae (Anderson et al. 1986), that diverge posteriolaterally (Abramov 2000) (Fig. 7). With regard to the mandible, their dentaries are proportionally short and robust (Anderson et al. 1986) (Fig. 7). Moreover, the inferior margins of the jaw angle are markedly broad and compressed, while the masseteric fossa projects anteriorly towards the medial portion of the m_1 talonid. Lastly, p_2 and m_2 alveoli often exhibit fusion, and the mental foramina generally number around 4 per dentary (Anderson et al. 1986) (Fig. 7).

This taxon can be differentiated from *Neovison vison* by the presence of a well-developed tube enclosing the foramen ovale that extends posteriolaterally to the anterior margin of the auditory bullae (Anderson et al. 1986). Additional variations include: a wider palatal region between the upper canines, more inflated auditory bullae, a larger external opening of the auditory meatus, smaller infraorbital foramina, a shorter and broader P^3, a shorter P^4 protocone, and a less expanded M^1 lingual lobe (Anderson 1977). Furthermore, *M. nigripes* exhibit relatively shorter and thicker mandibles, comparatively shorter and wider premolars (Anderson 1977); a more narrowed m_1 talonid, lack of an incipient metaconid on the m_1, a markedly diminutive and circular m_2, and limb elements which tend exhibit less curvature and more rugosity than the mink (Anderson et al. 1986).

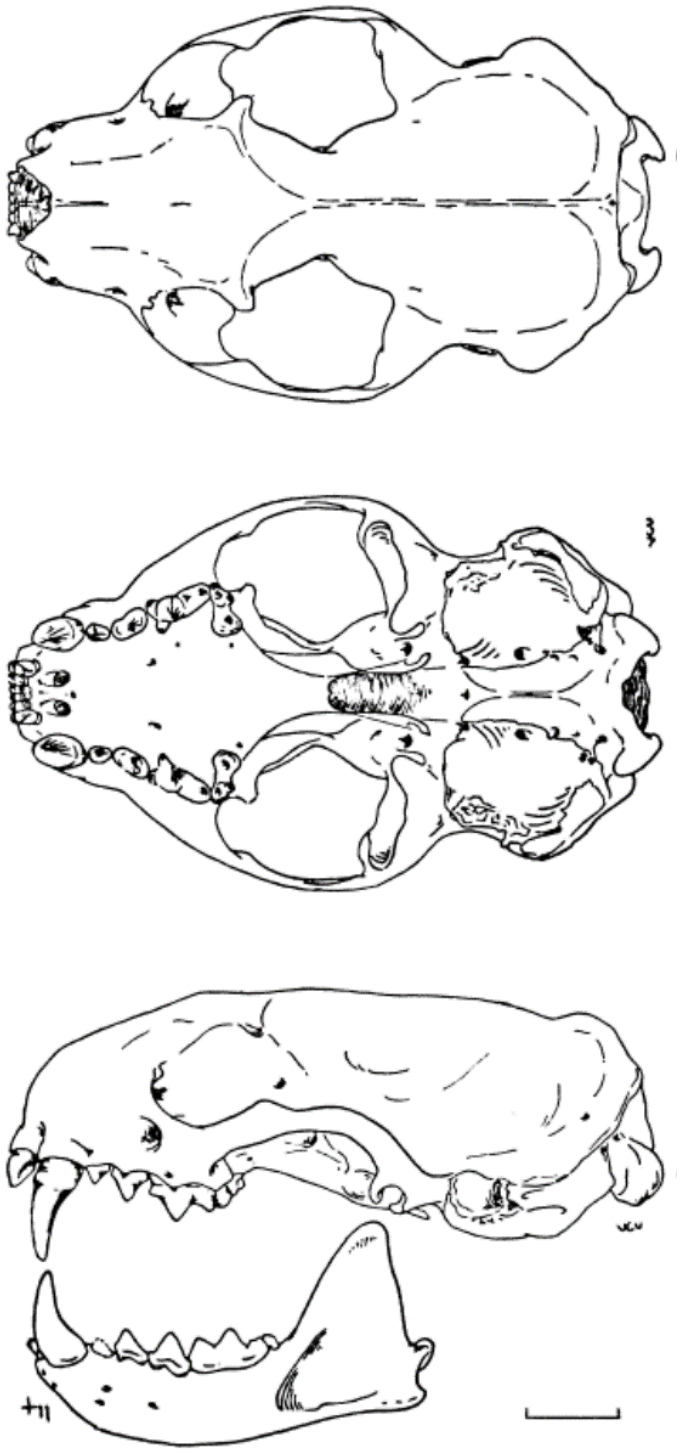

Figure 7. *Mustela nigripes* skull in dorsal (top), ventral (center), and left lateral (bottom) views. Scale bar = 1cm. Modified from Hillman and Clark (1980).

Mustela nivalis Linnaeus, 1766; common name(s): weasel, least weasel, or common weasel

Distribution and origins: range extends throughout the Palaearctric region, covers most of Europe, Asia Minor, northeastern Siberia, Japan, and North Africa from Morocco to Egypt. (Ewer 1973, Wozencraft 2005; Lin et al. 2010). In the New World this taxon inhabits much of central and north central North America (Ewer 1973) (Fig. 11). *M. nivalis* is established in the fossil record by .5 Mya from Pleistocene deposits of central Europe, western Europe, and Italy (Kurtén 1968; King and Powell 2007). This taxon is thought to have evolved from *M. praenivalis* found within Middle Pleistocene deposits of Europe (Kurtén 1968). *M. praenivalis* likely descended from an ancestral taxon; *M. pliocaenica* from the Late Pliocene of Europe as well (Kurtén 1968; King and Powell 2007). Eighteen extant subspecies of *M. nivalis* are currently acknowledged (Wozencraft 2005) and exhibit marked global phenotypic plasticity (Saarma and Tumanov 2006; King and Powell 2007; Lin et al. 2010). Accordingly, these subspecies have been divided into several broad-scale geographic morphotypes. Heptner et al. (2002) proposed 3 *M. nivalis* groups including: small weasels of the *pygmaea-rixosa* group, large weasels of the *boccamela* group, and intermediate sized weasels of the *nivalis* group.

Diagnostic characters: smallest of the 3 North American weasels overall (Sheffield and King 1994; King and Powell 2007). *M. nivalis* exhibit a total length of less than 250 mm and 225 mm in males and females respectively (Hall 1981). While demonstrating marked intercontinental plasticity, this taxon also displays the least amount of intraspecific variation in size relative to *M. erminea* and *M. frenata* of the New World (Ralls and Harvey 1985). Pelage is monotone white to dark brown on the dorsum, with dorsal and ventral colors well-delimited. Distal portions of the tail lack a black tip as in *M. erminea* or *M. frenata* (Hall 1981; Heptner et al. 2002). Tail length is less than 25% of the total body length, including 11-16 caudal vertebrae (King and Powell 2007).

Additionally, the mastoid breath is often greater or equal to the maximum breadth of the braincase (Hall 1981), while the skull width above the canines is approximately equal to the interorbital distance (Heptner et al. 2002) (Fig. 8). Often differs from *M. erminea* in the following aspects: area above the interorbitals is relatively flat versus sloped, distance between the auditory bullae is greater than in the ermine, and the facial profile is generally more "infantile" in appearance as expressed by a shorter rostrum, and a relatively inflated braincase (Heptner et al. 2002) (Fig. 8). It is worth mentioning, however, that marked intraspecific variation is expressed in these two species (Heptner et al. 2002). Moreover, juvenile and young adult ermine will often portray more '(least) weasel-like' characters (Heptner et al. 2002).

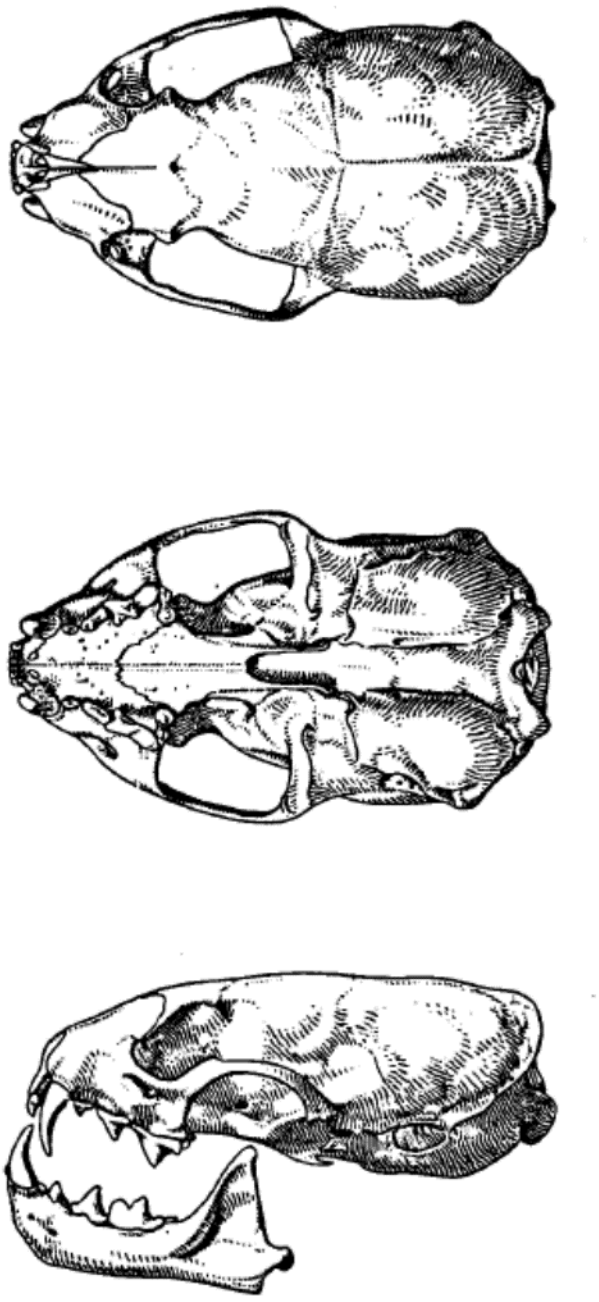

Figure 8. *Mustela nivalis* skull in dorsal (top), ventral (center), and left lateral (bottom) views. Image is not to scale. Modified from Sheffield and King (1994).

Neovison "*Mustela*" *vison* Schreber, 1777; common name(s): American mink

Distribution and origins: ranges throughout Canada and most of the contiguous United States excluding Arizona and arid parts of California, Nevada, New Mexico, western Texas, and Utah (Lariviére 1999) (Fig. 9). Moreover, this taxon has been introduced throughout much of western Europe, Russia, and eastern Asia (Lariviére 1999). Earliest fossils of *N. vison* have been recovered from Irvingtonian-age deposits of the United States (Kurtén and Anderson 1980; Anderson 1989; Lariviére 1999). 15 extant subspecies of *N. vison* are currently acknowledged (Wozencraft 2005). Some authors argue that the extinct sea mink *Mustela macrodon* is a subspecies of this taxon as well (e.g. Wozencraft 2005 and references therein).

Diagnostic characters: exhibits a total body length greater than 300mm (Lariviére 1999). Pelage is often homogeneously brown with minor white markings throughout the venter, particularly near the chin (Hall 1981; Lariviére 1999). Fur is generally darkest at the distal tail, and medially along the dorsum (Hall 1981), though coloration does not alter seasonally or ontogenetically as in several weasel taxa (Lariviére 1999). Additionally, this taxon is markedly larger and more robust than North American weasels (*M. erminea*, *M. frenata*, and *M. nivalis*). Female *N. vison* average 10% smaller (Hall 1981), and 50% lighter than males, while the length of the upper toothrow exceeds 20mm and 17.8mm in males and females respectively (Lariviére 1999). Tail length is approximately 33% of the body length (Lariviére 1999), and includes 18-20 caudal vertebrae (Hall 1981). Digits also exhibit webbed skin at the base (Lariviére 1999).

The skull of *N. vison* is somewhat flattened, with uneven spreading of the zygoma. Lambdoidal ridges are well-developed in adults, extending to the posterior boundary of the condyle (Lariviére 1999) (Fig. 10). These crania are sexually dimorphic in size but not shape (Lariviére 1999). Auditory bullae are moderately inflated (Lariviére 1999) yet flatter than in *M.*

nigripes (Anderson 1977) (Fig. 10). This taxon can be further distinguished from *M. nigripes* in exhibiting a markedly expanded M^1 lingual lobe (Anderson 1977), broader occipital region, larger infraorbital foramen, and wider m_1 talonid (Kurtén and Anderson 1980) (Fig. 10). Lastly, an incipient metaconid is present on the lower first molar of *N. vison*, yet not in *M. nigripes* (Kurtén and Anderson 1980; Hall 1981; Lariviére 1999).

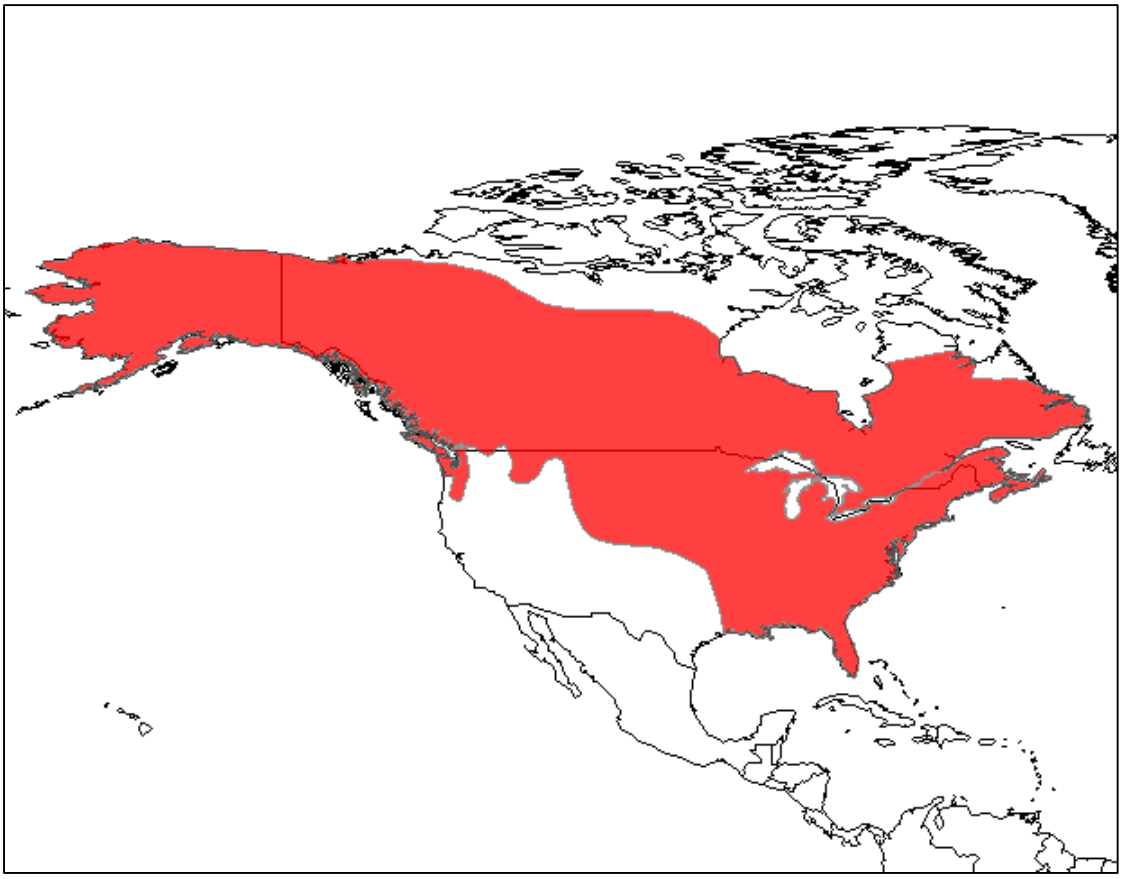

Figure 9. North American distribution (red) of the American mink *Neovison vison*. Species range data from: Patterson et al. (2007).

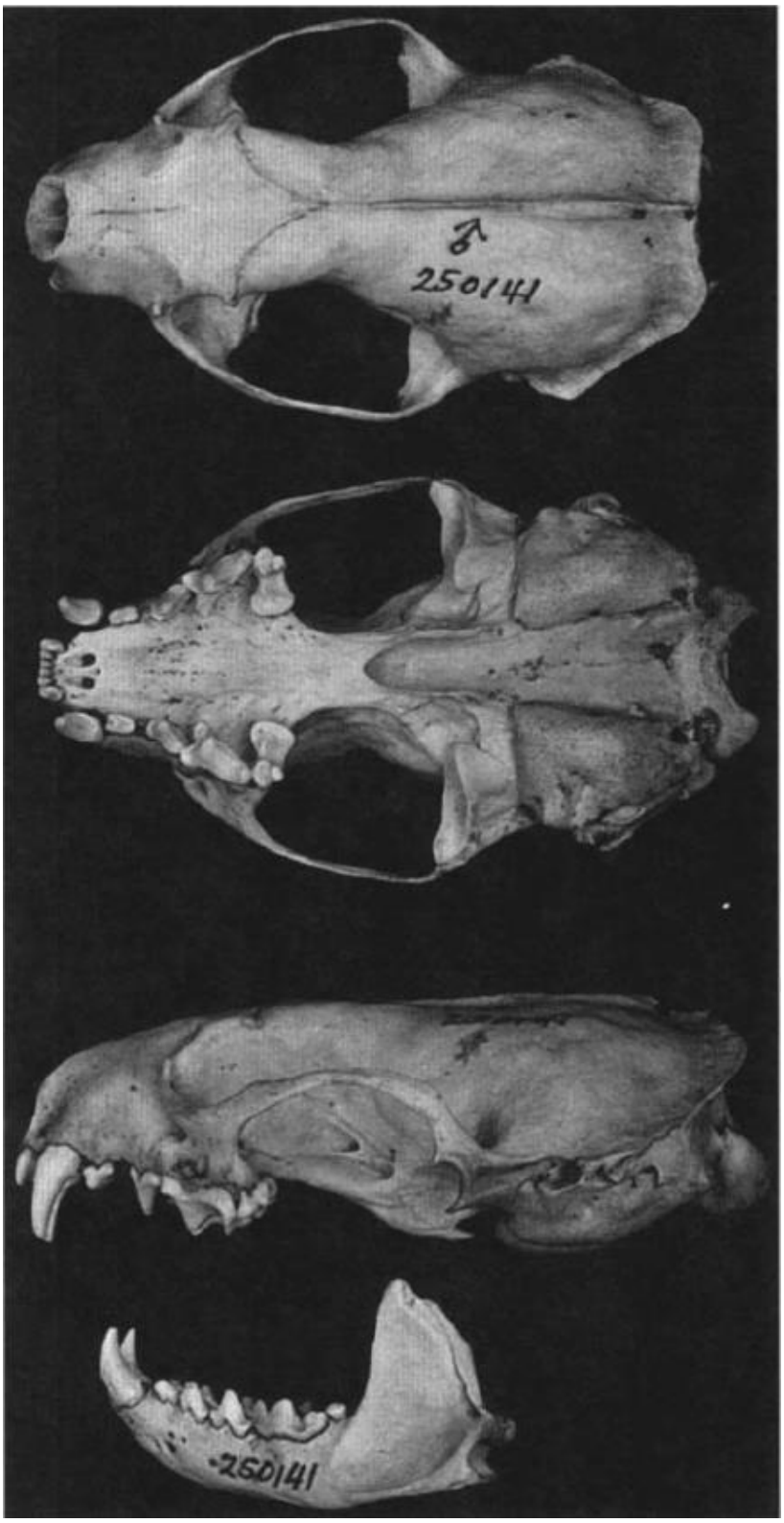

Figure 10. *Neovison vison* skull in dorsal (top), ventral (center), and left lateral (bottom) views. Image is not to scale. Modified from Lariviére (1999).

Modern Ecology

Habitats

Weasels, ferrets, and polecats occupy a wide geographic range and variety of habitats including: arctic tundra, steppes and plains, high altitude mountain ranges, talus slopes, tropical forests, and deserts (Anderson 1989; Heptner et al. 2002). These *Mustela* taxa are globally dispersed throughout much of Eurasia and North America, as well as parts of South America and north Africa (Anderson 1989). Two or more sympatric species will often coexist despite similar ecological requirements, especially within the northern Holarctic region (Ralls and Harvey 1985; Erlinge and Sandell 1988; King 1989) (Fig. 11). Northern limits for the New World distribution of this genus reach the Arctic Archipelago and northeastern Greenland at approximately 70˚ N latitude, continuing westward into Alaska (Heptner et al. 2002) (Fig. 11). Their southern range breeches South America, extending from Venezuela to Columbia, down through Peru, and terminating with the occupancy of *M. frenata* in western Bolivia (Heptner et al. 2002) (Fig. 11). Old World distributions of *Mustela* taxa encompass nearly all of Europe excluding: Iceland, the Arctic Islands, and Mediterranean isles (Heptner et al. 2002). Their Old World northern boundaries reach the New Siberian Islands, and the Asian mainland, while their southern limits in the Middle East include: Syria, Palestine, and northern Iraq (Heptner et al. 2002). African *Mustela* spp. distributions are limited to the extreme northeast (parts of Egypt, Algeria, and Tunisia), as well as Morocco (Heptner et al. 2002).

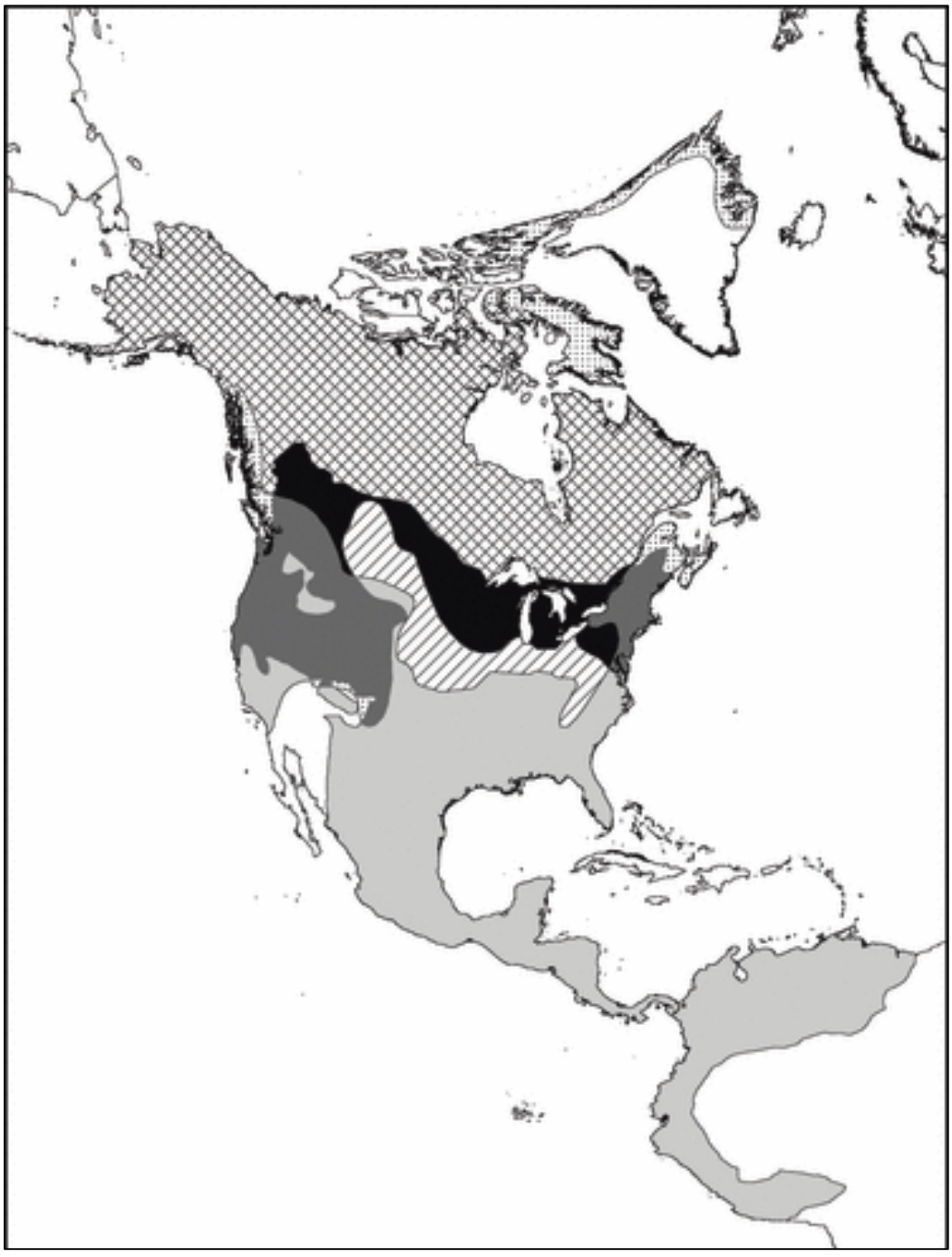

Figure 11. Distribution of New World weasels. In descending latitude: dots = *Mustela erminea* alone; crosshatch = *M. erminea* + *M. nivalis*; black = all 3 species; diagonal lines = *M. frenata* + *M. nivalis*; dark grey = *M. frenata* + *M. erminea*; light grey = *M. frenata* alone. From Meiri et al. (2011).

Diet

Members of *Mustela* are strictly carnivorous and primarily miophagous (Rosenzweig 1966; Heptner et al. 2002). Their diets generally consist of rodents and lagomorphs ranging from shrew-size to large-ground squirrels (Rosenzweig 1966; Murphy and Dowding 1995; Heptner et al. 2002). Although, reptiles, birds, and amphibians are occasionally supplemented as well (Moors 1980; King 1989; Murphy and Dowding 1995; Heptner et al. 2002). In most cases, prey dispatch involves a killing bite to the nape of the neck (Kurtén and Anderson 1980; Dayan and Simberloff 1994; Meiri et al. 2011). These taxa rely heavily on local rodent population sizes, though specific dependence can vary significantly among species (Korpimäki et al. 1991). For example, *M. nivalis* are acknowledged as small rodent specialists, primarily dependent on *Microtus* spp. (King and Moors 1979; Korpimäki et al. 1991; Aunapuu and Oksanen 2003). Likewise, *M. nigripes* are considered obligate to *Cynomys* spp. based on scat remains and extensive overlap throughout their historic ranges (Hillman and Clark 1980; Klebanoff et al. 1991). However, *M. erminea* can function as semi-generalists, and, to an extent, will include alternative prey when rodent populations diminish (King and Moors 1979; Korpimäki et al. 1991; Aunapuu and Oksanen 2003).

Such reliance on local rodent communities are primarily attributed to the energetic demands (Moors 1980; King 1989); and limited mobility of *Mustela* spp. due to size and shape constraints (Korpimäki et al. 1991). Their elongate physique and relatively short fur creates excessive surface area exposure, thus resulting in poor heat retention and a fast basal metabolic rate (King 1989). In order to accommodate this caloric demand, *Mustela* spp. facilitate vast ranges to maximize their likelihood of prey encounters despite intermittent rodent abundances (King 1989; Korpimäki et al. 1991). Within these ranges weasels and ferrets hunt under dense

vegetation and in narrow subterranean burrows, while frequenting rodent dens for shelter, thermal buffering, and periodic meals (King 1989). After successful kills, weasels will often drag prey back to their dens, cashing multiple carcasses in times of prey abundance (King 1989). Nevertheless, using large ranges enables an energetic tradeoff. While increasing the likelihood of prey capture, expansive territories result in energetically demanding hunting strategies as consequence of diminutive size and physically taxing foraging techniques (King 1989). Thus, energetic costs associated with elongate body shape, expansive territories, and specialized hunting strategies, make *Mustela* spp. physiologically vulnerable (Moors 1980; King 1989). This exchange ultimately leads to reproductive uncertainty, given that supplementary energy can only be reserved for reproduction when rodent populations are abundant (King 1989; Korpimäki et al. 1991).

Physiology and Population Dynamics

Within Mammalia life expectancy is often scaled to size (King 1989; Levine 1997; King and Powell 2007). While a resting human heart will beat approximately 70 times per minute (Levine 1997), the pulse of a weasel averages at around 400-500 beats per minute (King 1989). Given that mammalian bodies tend to exhibit similar thresholds for maximum heartbeats per lifetime (King 1989; Levine 1997), the average lifespan of a wild weasel is somewhat short-lived, ranging from less than 1 year to about 2 years in the wild depending on species (Sandell 1989; King and Powell 2007). To accommodate for relatively short life expectancies, *Mustela* spp. are born with innate hunting abilities and experience rapid ontogenetic growth (King 1989). This shift towards *r*-selected reproduction facilitates a high risk-high reward strategy that yields marked population variability and turnover throughout generations (King 1989). Such lifestyles result in prolific reproduction during times of rodent abundance (Korpimäki et al. 1991).

Conversely, weasels maturing during periods of low prey density often die before reproducing because sexually mature weasels rarely live into a second breeding season (King 1989; Sandell 1989). These events can be particularly devastating to species such as *M. erminea*, which exhibit delayed implantation (King and Moors 1979; Sandell 1989; Korpimäki et al. 1991; King and Powell 2007). Direct dependence on rodent population sizes, along with frequent sympatry and competition among *Mustela* spp., ultimately leaves weasels highly susceptible to localized extinctions (King and Moors 1979; Powell and Zielinski 1983).

Sexual Dimorphism

All *Mustela* taxa exhibit marked sexual dimorphism, though to various levels depending on species (Moors 1980; Ralls and Harvey 1985; Gittleman and Van Valkenburgh 1997; Berdnikovs 2005). In every instance females represent the smaller sex (Moors 1980; Gittleman and Van Valkenburgh 1997; Meiri et al. 2011). Female size reduction is thought to diminish their energetic requirements, thus permitting more energy expenditure towards rearing offspring (Moors 1980; Ralls and Harvey 1985), which can exceed 5 times their normal daily caloric requirements (Sandell 1989). While reproductively efficient, this spike in energy disbursement may be negatively correlated with female longevity, which is markedly less than that of male weasels (Sandell 1989). It has also been proposed that sexual selection favors smaller size in females to facilitate more rapid sexual maturity (Erlinge 1979; Ralls and Harvey 1985). Conversely, male weasels that exhibit polygonous or promiscuous mating strategies (Erlinge 1979; Moors 1980; Ralls and Harvey 1985; Gittleman and Van Valkenburgh 1997) are markedly larger, often by a factor of 10-20% in condylobasal length (King 1983); and 1.5-2 times the body weight of females (Erlinge 1979; Moors 1980; Sandell 1989).

Sexual selection may favor large body size in male *Mustela* taxa due to its advantages in competing for females, thus maximizing the number of mates per breeding season from April through June (Ralls and Harvey 1985; King 1989; Sandell 1989). However, size increase does not remain favorable outside of the breeding season. Larger bodies require more energy to maintain, consequently, increased size becomes detrimental due to the already high energetic requirements of weasels, especially during stressful winter seasons (King 1989; Sandell 1989). Furthermore, maximum body size can vary markedly within sexes, particularly for male *Mustela* spp. (Ralls and Harvey 1985; King 1989). Some authors attribute this phenomenon to periodic fluctuates in food supply, resulting in differential nutritional uptake and growth (Ralls and Harvey 1985; King 1989). In such events males often appear to be more strongly affected than females (Ralls and Harvey 1985). Accordingly, size variability in both male and female weasels is likely a compromise between factors of sexual selection (Gittleman and Van Valkenburgh 1997) and energetic/seasonal optima which differ markedly between sexes (King 1989; Sandell 1989).

Furthermore, it has been proposed that size discrepancies among *Mustela* spp. may result from intraspecific niche partitioning (Erlinge 1979; Moors 1980, Dayan et al. 1989; Sandell 1989; McDonald 2002). In these circumstances males and females of a given taxon form 2 distinct "morphospecies" for exploiting discreet resources (Erlinge 1979; Dayan et al. 1989; Dayan and Simberloff 1994). Such phenomena are thought to reduce intraspecific competition through differential prey exploitation (Erlinge 1979; Dayan et al. 1989). Under this hypothesis female size reduction may have evolved to prey on smaller taxa by exploiting niches that remain inaccessible, or are energetically inefficient for males (Erlinge 1979; Ralls and Harvey 1985; King 1989). For example, Brickner et al. (2014) found that 39% of stable isotope signatures

collected from female *M. nigripes* reintroduced to Shirley Basin, WY correlated with mice and other small-bodied mammals as opposed to larger prairie-dogs (*Cynomys leucurus*). However, only 24% and 28% of isotopic data from male and juvenile black-footed ferrets respectively correlated with *Cynomys*-divergent prey (Brickner et al. 2014). Results imply that body size may be heavily influenced on intraspecific resource partitioning and foraging plasticity given that male *M. nigripes* can weigh over 20% more than females (Brickner et al. 2014).

Geographic Variation and Distribution

In addition to sexual variation, interregional body size and morphology differs markedly throughout *Mustela* spp. as well. Though size gradations are quite prominent among geographic subspecies of weasels, such occurrences cannot be explained as simple effects of latitudinal change (Bergmann's rule) (McNab 1971; Ralls and Harvey 1985; King 1989, Meiri et al. 2011). Bergmann's rule states that within warm-blooded vertebrates, larger populations of a given species will inhabit higher latitudes (colder climates) to maximize their surface-to-volume ratios, while analogous species at lower latitudes (warmer climates) will exhibit smaller body sizes where heat conservation is less fundamental (McNab 1971). Weasels, however, often violate this rule given that *M. frenata* and *M. nivalis* show little correlation between size and latitude in the New World (McNab 1971; Ralls and Harvey 1985; King and Powell 2007). Only *M. erminea* follow the trend of Bergmann's rule, and only in the New World (Ralls and Harvey 1985; King and Powell 2007). In North America for example, the smallest members of *M. erminea* reside in the southwestern United States, yet the same species of the Old World are smallest in northeastern Eurasia (King 1989; King and Powell 2007). Ecological dynamics such as foraging efficiency, ambient temperature on metabolism (King 1989; Sandell 1989), elevation (King and Powell 2007), and presence of sympatric predators (Rosenzweig 1966; McNab 1971; Erlinge and

Sandell 1988; Dayan et al. 1989; McDonald 2002) all appear to be critical factors of geographic size in weasels. Some authors have proposed that diminutive *Mustela* spp. living at high latitudes must remain small for sustaining the ability to frequent shelters such as rodent burrows, thus minimizing aerial exposure (King 1989; King and Powell 2007). In such regions, maximizing access to thermal buffers through size reduction may outweigh the benefits of a larger surface-to-volume ratio for thermoregulation (King 1989).

Despite influences of biogeography and sexual dimorphism, some authors believe that interregional variation among coexisting *Mustela* spp. may be attributed to additional factors such as interspecific niche partitioning (Rosenzweig 1966; Dayan and Simberloff 1994). Parallel to the framework of intraspecific variation, interspecific partitioning suggests that taxa fulfilling similar ecological niches may use different resources in areas of sympatry to avoid interference and competition (Rosenzweig 1966; Dayan and Simberloff 1994; Meiri et al. 2011). Consequently, these species may amplify phenotypic, ecological, or behavioral differences in the presence of other closely-related taxa, yet in allopatry, these characteristics will be unexpressed or reduced (Brown and Wilson 1956; Dayan and Simberloff 1994; Meiri et al. 2011). In such instances species will be more similar to each other in allopatry than in sympatry, resulting in a phenomenon termed character displacement (Brown and Wilson 1956; Meiri et al. 2011).

Rosenzweig (1966) was among the earlier authors to address concepts related to character displacement. He suggested that exploitation of discreet prey sizes, differential hunting capabilities, and interspecific aggression may account for the gradational size changes that enable closely related carnivores to coexist. In a hypothetical example, Rosenzweig (1966) proposed that *M. frenata* may be able to sustain population size among more specialized predators like *M. nivalis* through differential prey exploitation and interference aggression. In

some cases these encounters result in predation of the smaller taxon (*M. nivalis*) by the larger one (*M. frenata*) (Rosenzweig 1966; Erlinge and Sandell 1988). Interspecific size discrepancies may therefore be amplified in such regions to maintain community equilibrium (Rosenzweig 1966).

Likewise, McNab (1971) stated that latitudinal size increase expressed by North American *M. erminea*, while often recognized as Bergmann's rule, could alternatively be the result of character release from sympatric *M. frenata* as the former taxon moves north of the latter's range extent. However, Ralls and Harvey (1985) countered against this character displacement hypothesis, stating that in North America, both sexes of *M. frenata* and *M. erminea* covary in size, and that latitude is a more reliable size proxy for *M. erminea* than temperature or prey size. These authors determined that *M. erminea* increases in size northward notwithstanding the presence or absence of *M. frenata* or *M. nivalis*, thus implying that sympatric size gradations are merely coincidental with latitude (Ralls and Harvey 1985). Accordingly, these authors attributed interspecific size variation in *Mustela* spp. to biogeographic influences, sexual dimorphism due to sexual selection, and possibly intraspecific partitioning rather than character displacement (Ralls and Harvey 1985).

However, Dayan et al. (1989) and Dayan and Simberloff (1994) found evidence for stepwise character displacement among *Mustela* spp. in North America and the United Kingdom respectively. Studies demonstrated equal size ratios for skull length and upper canine diameter among sympatric species guilds irrespective of regional variation throughout North America (Dayan et al. 1989) and Great Britain, though not in Ireland (Dayan and Simberloff 1994). These phenomena were primarily attributed to inter-and intraspecific character displacement facilitated by differential prey exploitation (Dayan et al. 1989). Those authors acknowledged, however, that

empirical evidence was lacking and that sexual selection and interference may contribute to this incidence as well (Dayan et al. 1989; Dayan and Simberloff 1994). Conversely, a *post hoc* analysis conducted by McDonald (2002) offered little support for interspecific prey partitioning among mustelids from Great Britain and Ireland. Results failed to establish compelling relationships between predator and prey sizes among sympatric species after incorporating local dietary information warranted by the research of Dayan and Simberloff (1994). However, empirical data did reveal that male mustelids consistently implemented larger prey than females, thus supporting an intraspecific niche partitioning hypothesis (McDonald 2002). Whether resource partitioning is the primary mechanism influencing canine size or a secondary effect derived from sexual selection could not be determined, though the latter inference was favored (McDonald 2002). Furthermore, McDonald (2002) suggested that even size ratios in mustelid canines may result from additional influences such as interspecific aggression (Rosenzweig 1966; King and Moors 1979; Erlinge and Sandell 1988) or character convergence (Grant 1972; Heptner et al. 2002; Meiri et al. 2011).

Meiri et al. (2011) tested for community-wide character displacement in Holarctic weasels while correcting for latitudinal clines using canine diameter as proxy. Under the assumption that character displacement is in effect, they predicted *M. erminea* would be smallest in sympatry with *M. frenata* (largest weasel taxon), largest in sympatry with *M. nivalis* (smallest taxon) and intermediately sized when allopatric. Likewise, they anticipated that *M. frenata* would be larger in sympatry with *M. erminea* then in allopatry (Meiri et al. 2011). Surprisingly, the results illustrated that *M. frenata* decreases in size when sympatric with *M. erminea* and/or *M. nivalis* (Meiri et al. 2011). While *M. erminea* canine size decreases in the presence of *M. frenata* as expected, they decrease more so in the presence of *M. nivalis* than in allopatry (Meiri

et al. 2011). Although *M. nivalis* remains small in the presence of *M. frenata*, they too violate the assumption of character displacement by increasing canine diameter when sympatric with *M. erminea* only (Meiri et al. 2011). Consequently, Meiri et al. (2011) established little support for community-wide character displacement after correcting for clinal variation. Alternately, these data are more indicative of character convergence among sympatric *Mustela* spp. (Meiri et al. 2011). In their conclusion, the authors proposed a differential explanation, suggesting that morphological convergence in canine diameter may have evolved independently as adaptations for locally homogenous prey (Meiri et al. 2011). This hypothesis implies that coexistence may be achieved through differential use of microhabitat structures (Meiri et al. 2011).

In summary, size gradations exhibited throughout sympatric weasels may be attributed, but not limited to, one or more of the following comprehensive factors: a) sexual dimorphism due to sexual selection, b) sexual dimorphism due to intraspecific resource partitioning, c) variation due to biogeographic influences, d) character displacement due to interspecific resource partitioning, e) character displacement due to interspecific aggression/intraguild predation, and f) localized character convergence. Although these phenomena have been extensively analyzed, consensus as to which factor(s) primarily facilitate size discrepancies are not yet agreed. It is worth mentioning, however, that the vast majority of published quantitative studies have focused on measurements of skull length, upper dentition, and full body ratios, while reports on alternative anatomical features are notably lacking. Incorporating more systematically controlled qualitative experiments, and using differential characters in quantitative analyses may accordingly shed new light on this topic in future analyses.

CHAPTER 3

DISTINGUISHING *MUSTELA NIGRIPES* AND *NEOVISON VISON* DENTARIES THROUGH LINEAR MORPHOMETRICS

Introduction

Once broadly dispersed throughout the grasslands of mid-western North America, *Mustela nigripes* (black-footed ferret) was teetering on the brink of extinction by the late 1940s due to a steady decline in viable habitat, marked prey reduction, and rapid disease outbreaks including sylvatic plague and canine distemper (Seal et al. 1989; Klebanoff et al. 1991; Biggins et al. 2011a). Between 1985 and 1987 the last known population of just 18 individuals near Meeteetse, Wyoming (Fig. 12) was captured, and therefore, extirpated from the wild in an effort to prevent their complete extinction (Seal et al. 1989; Biggins et al. 1999; Cain et al. 2011). Despite inherit risks and consequences associated with reproduction in captivity (Seal et al. 1989), conservation efforts made significant progress in the years to follow. By fall of 1989, captive breeding programs had increased the living ferret population to 118 individuals (Klebanoff et al. 1991), with numbers subsequently increasing to over 400 by the year 2000 (Owen et al. 2000).

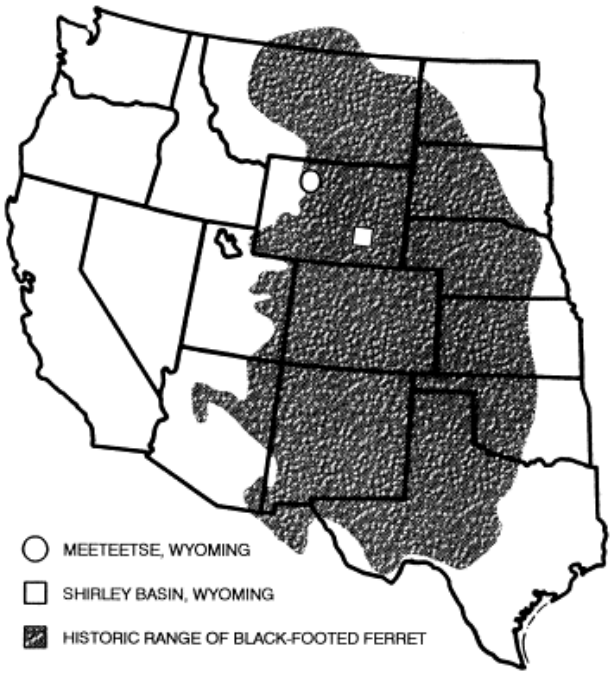

Figure 12. Location of the last known wild population of *Mustela nigripes* near Meeteetse, WY (circle) relative to its historic range (shaded region). Square signifies one of the first successful ferret reintroduction sites in Shirley Basin, WY. Modified from Biggens et al. (1999).

Definitive goals of these breeding programs are to gradually reintroduce black-footed ferrets back into wild habitats (Seal et al. 1989; Jachowski and Lockhart 2009). While demonstrating some success in facilitating self-sustained populations (Jachowski and Lockhart 2009) (Fig. 13), this has proven a daunting objective overall (Clark 1986; Biggins et al. 1999; Owen et al. 2000). Complications of reintroduction arise from a variety of sources including: anthropogenic habitat modification, natural catastrophes, hunting and trapping, avian and mammalian predators, niche competition, lack of obligatory prey (Hillman and Clark 1980; Clark 1986), and disease susceptibility due to low genetic diversity (Altizer et al. 2003; Cain et al. 2011). Of these constraints, lack of suitable habitat and continued degeneration of prairie-dog colonies are considered to be among the principal factors limiting black-footed ferret reintroduction (Jachowski and Lockhart 2009; Biggins et al. 2011a; Eads et al. 2011).

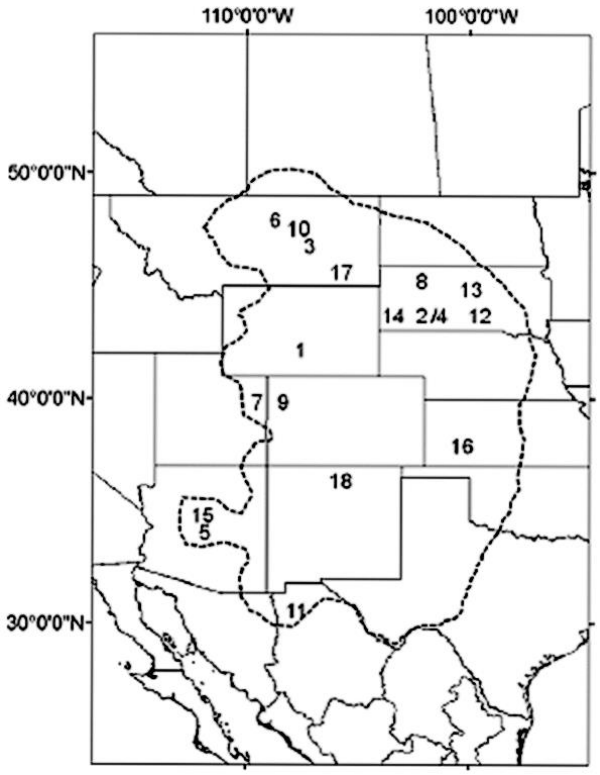

Figure 13. Map of the Great Plains indicating the 18 black-footed ferret reintroduction sites labeled in chronologic order from 1991-2008. All sites are all located within the historic range of *M. nigripes* (dashed lines). 1=Shirley Basin, WY; 2=Badlands National Park, SD; 3=UL Bend National Wildlife Refuge, MT; 4=Conata Basin, SD; 5=Aubrey Valley, AZ; 6=Fort Belknap Indian Reservation, MT; 7=Coyote Basin, UT; 8=Cheyenne River Indian Reservation, SD; 9=Wolf Creek, CO; 10=40-Complex, MT; 11=Janos, Chihuahua, MX; 12=Rosebud Indian Reservation, SD;13=Lower Brule Indian Reservation, SD; 14=Wind Cave National Park, SD; 15=Espee Ranch, AZ; 16=Logan County, KS; 17=Northern Cheyenne Indian Reservation, MT; 18=Vermejo Ranch, NM. Modified from Jachowski and Lockhart (2009).

At present, 99% of viable prairie habitats have been agriculturally modified or destroyed by humans (Seal et al. 1989). Unfortunately, while prairie-dogs (*Cynomys* spp.) are traditionally thought to comprise over 90% of extant black-footed ferret diets based on historic observations and scat analysis (Campbell et al. 1987; Klebanoff et al. 1991), 90-97% of prairie dog towns have disappeared. Historic accounts of *M. nigripes* are seldom documented apart from *Cynomys* spp. colonies due to extensive overlap among their recent distributions (Hillman and Clark 1980; Nowark 1999). Accordingly, black-footed ferrets are considered dependent on prairie-dogs as their obligate prey taxa (Klebanoff et al. 1991; Biggins et al. 1999; Eads et al. 2011). Unfortunately, these rodents are often considered agricultural pests, and are frequently destroyed by farmers and ranchers (Anderson et al. 1986; Klebanoff et al. 1991). Such degradation of prairie-dog colonies results in black-footed ferret habitat fragmentation, where population migration and gene flow become stagnant through isolation (Flesness 1989).

Reintroducing *M. nigripes* into wild habitats is further complicated from a demographic perspective since these ferrets are thought to require at least 50 hectares of prairie-dog town per individual, and approximately 50 individuals to facilitate self-sustaining populations (Flesness 1989). Therefore, *Cynomys*-rich habitat areas of at least 2500 hectares are often considered essential for reintroduction (Flesness 1989). However, protected lands containing active prairie-dog colonies are frequently smaller than 1000 hectares (Flesness 1989). Even the moderately sized Meeteetse expanse only encompasses 2,886.5 hectares (Flesness 1989), therefore implying it is unsustainable for a black-footed ferret population of over 55-60 individuals.

While *Cynomys* spp. are acknowledged as the primary food source of *M. nigripes*, reports verify that this highly specialized mesopredator will occasionally integrate alternative prey as well (Campbell et al. 1987; Owen et al. 2000; Biggins et al. 2011b; Brickner et al. 2014).

Additional species consumed may include: *Spermophilus* spp. (ground squirrels), *Sylvilagus* spp. (cotton tail rabbits), *Peromyscus* spp. (deer mice) (Hillman and Clark 1980); *Lemmiscus curtatus* (sage brush vole), *Microtus* spp. (true voles), *Lepus townsendii* (white-tailed jackrabbit) (Campbell et al. 1987; Owen et al. 2000); Geomyids (pocket gophers), and *Dipodomys ordii* (kangaroo rats) (Biggins et al. 2011b). Moreover, Brickner et al. (2014) acknowledge that historic black-footed ferret consumption of *Cynomys* spp. could have been overestimated given their more diurnal lifestyles relative to many other rodent genera. Likewise, scatological analyses yielding >90% prairie-dog elements may have been an artifact of taphonomic bias as well due to the comparatively more robust materials associated with these large ground-squirrels relative to smaller rodents (Brickner et al. 2014). A recent analyses of stable carbon and nitrogen isotope ratios from blood and hair materials suggest that reintroduced black-footed ferrets in Shirley Basin, WY exhibit markedly greater foraging plasticity than previously acknowledged (Brickner et al. 2014). From that study, only 76%, 72%, and 61% of *M. nigripes* isotopic ratios were recovered with white-tailed prairie-dog signatures (*Cynomys leucurus*) in males, juveniles, and females respectively (Brickner et al. 2014). Interestingly, the remainder of stable isotope percentages correlated with other local ground-squirrels, small mammals, and mice (Brickner et al. 2014). Incidentally, Shirley Basin happens to be among the most longstanding, and successful *M. nigripes* reintroduction sites as well (Brickner et al. 2014) (Fig. 13).

Moderate dietary plasticity in black-footed ferrets appears to extend into prehistoric times as well. Stomach contents from a well-preserved *M. nigripes* mummy discovered in the Yukon Territory of Canada produced a food bolus attributed to a small mammal (Youngman 1994). Possible identified taxa included: *Ochotona* sp., *Spermophilus* sp., *Lemmus* sp., *Dicrostonyx* sp., and *Microtus* sp., though the latter genus is most likely based on guard hair patterns (Youngman

1994). Radiocarbon dating of this specimen produced an age of 39,560 +/- 490 BP (Youngman 1994), indicating that some *M. nigripes* incorporated alternative prey to *Cynomys* spp. during the Pleistocene as well. Additionally, an experiment conducted by Vargas and Anderson (1996) placed black-footed ferret kits into three groups during their presumed olfactory imprinting period at 60-90 days of age. Each group was fed differential portions of prairie-dog meat throughout this phase of development. Results indicated that ferrets with the greatest inclination for hunting prairie-dogs as adults were individuals fed the most prairie-dog meat as kits. These data imply that current prey selection among *M. nigripes* are not intrinsic to the species, but rather a preference acquired through postnatal influence (Vargas and Anderson 1996). Despite these inferences, however, many captive breeding programs continue to precondition extant black-footed ferrets around prairie-dogs exclusively as part of their prerelease reintroduction protocol.

Initiating a more comprehensive examination of prehistoric *M. nigripes* fossils may therefore improve our understanding of black-footed ferret dietary preferences through time and space. Doing so may facilitate more informed decision-making with regard to the modern conservation of this taxon. For example, confirmation of *M. nigripes* among the prairie-dog lacking Snake Creek Burial Cave (SCBC) assemblage of eastern Nevada (Mead and Mead 1989), juxtaposed with data compiled on other *Cynomys*-absent localities (Anderson et al. 1986; Owen et al. 2000) would support interpretations of dietary plasticity in prehistoric black-footed ferrets. Such evidence could suggest new methods for the management of reintroduced ferret populations by facilitating the consumption of alternate rodent taxa, thus reducing their dependency on depleted prairie-dog resources. Due to these potential implications for modern conservation of the black-footed ferret, validation or rejection of *M. nigripes*, and the American

mink *Neovison vison*, is warranted among the SCBC paleofauna. Principal objectives of this study are to classify the undifferentiated ferret-sized mustelid fossils housed within East Tennessee Vertebrate Paleontology (ETVP) collections to species level despite morphological similarities and extensive size overlap between the black-footed ferret and American mink (Fig. 14).

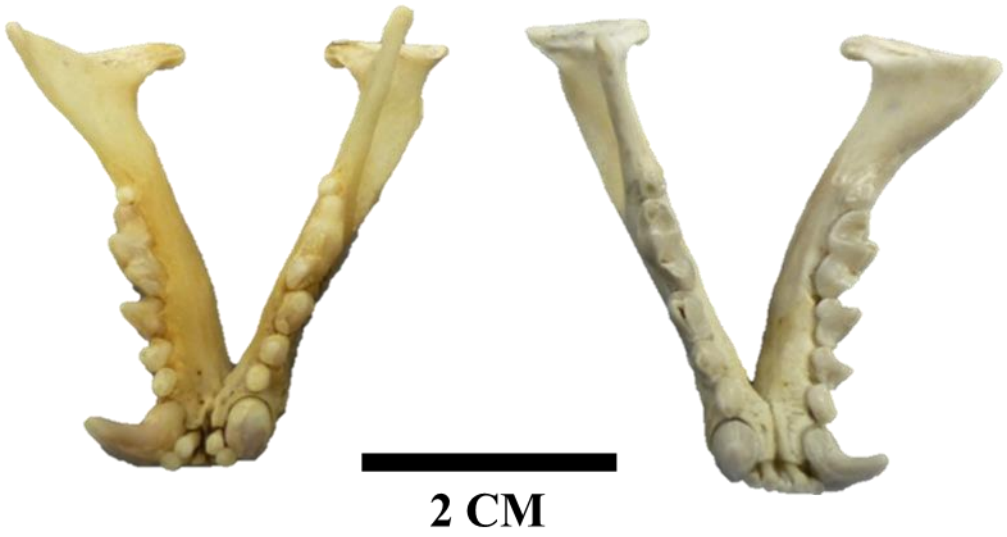

Figure 14. Occlusal view of extant captive-bred black-footed ferret, *Mustela nigripes* ETVP7310 (left) and American mink, *Neovison vison* ETVP5542 (right) mandibles.

Abbreviations

BFC: Blue Fish Caves, **BFF:** black-footed ferret, **BMC:** Big Manhole Cave, **BP:** years before present, **CAM:** Cudahy Ash Mine, **CWC:** Cottonwood Canyon, ***C*:** *Cynomys* spp., **DA:** discriminant analysis, **EHOL:** Early Holocene, **ETVP:** East Tennessee Vertebrate Paleontology, **HOPL:** Holocene-Pleistocene, **IC:** Isleta Cave, **JC:** Jaguar Cave, **JanC:** January Cave, **LBEC-LGLA:** Little Box Elder Cave-Late Glacial, **LBEC-PREB:** Little Box Elder Cave-Pre-Boreal, **LCCC:** Little Canyon Creek Cave, ***L*:** *Lemmiscus* spp., **LHOL:** Late Holocene, **LPLE:** Late Pleistocene, ***Ma*:** *Marmota* spp., **MF:** number of mental foramina per dentary, **MH:** Medicine Hat, **MHOL:** Middle Holocene, ***Mi*:** *Microtus* spp., **MPLE:** Middle Pleistocene, **NALMA:** North American Land Mammal Age, **OCR:** Old Crow River, **PC:** Porcupine Cave, **PCA:** principal component analysis, **SCBC:** Snake Creek Burial Cave, **SFLF:** Smith Falls Local Fauna, ***S:*** *Spermophilus* spp.

Materials and Methods

Eleven fossil dentaries (NAUQSP 8711/115B-NAUQSP 8711/125B) from SCBC tentatively labeled "*M. nigripes*/*vison*" were reevaluated from 10 linear measurements (Table 1, Fig. 15). Measurements were also taken from extant black-footed ferret and mink specimens to achieve species-level classification. Characters were selected based on quantitatively significant degrees of interspecific variation as noted in former studies (e.g., Anderson 1977; Anderson et al. 1986; Mead et al. 2000) and measured using digital calipers (Mitutoyo Absolute IP67). All measurements were conducted twice to the nearest 0.01mm and only recorded when within < 0.1mm deviation; averages (of the two) were then used for this analysis. In addition to continuous variables, one discreet character; the number of mental foramina per dentary was noted as well. Only adult individuals were measured; identified by lack of visible cranial sutures and fully erupt lower dentition. All measurements were taken from left mandibles, unless right features were available exclusively.

Table 1. Ten linear measurements of the dentary included for geometric morphometric analysis in extant *Mustela nigripes* (n=38), *Neovison vison* (n=21), and Snake Creek Burial Cave specimens (n=11).

TDL: total dentary length
DP_p3: dentary depth at the lower third premolar
DP_m1: dentary depth at the lower first molar
p4_H: height of the lower fourth premolar
p4_W: labial-lingual width of the lower fourth premolar
m1_L: anteroposterior length of the lower first molar
m1_TalW: labial-lingual width of the talonid from the lower first molar
m2_D: diameter (greatest occlusal distance) of the lower second molar
m2_W: labial-lingual width of the lower second molar
MTR: length of the mandibular toothrow from the lower second premolar to the lower second molar

Note than all nine variables below TDL were standardized using the length of the dentary to reduce size bias prior to statistical analysis. Furthermore, an independent sample t-test was run against the TDL of extant *M. nigripes* and *N. vison* specimens to verify that morphometric analyses were appropriate for discrimination. Results generated *p*-values greater than .05, thus rejecting the null hypothesis and confirming that separation between these taxa cannot be quantified by size exclusively. Dental measurements were taken from teeth only. In the absence or degradation of a tooth, species averages were used as opposed to dimensions of the alveolus.

Morphometric data were collected from 21 specimens of *N. vison* and 38 of *M. nigripes* housed within ETVP collections (Fig. 14, Appendix A). Stepwise discriminant and principal component analyses were conducted (SPSS version 21) to determine whether the 10 variables selected could effectively separate *M. nigripes* from *N. vison*. Missing values for both extant and fossil taxa were replaced with group-specific averages prior to statistical analysis. Independent variables were then standardized using the length of the dentary to reduce intraspecific size bias. It is worth mentioning that while many studies include canine width as a morphometric variable (Anderson et al. 1986; Mead et al. 2000; Owen et al. 2000; Wisely et al. 2002b), this character was not selected due to extensive sexual dimorphism in canine size among mustelids (Moors 1980; Gittleman and Van Valkenburgh 1997; Santymire et al. 2012). Accordingly, lower canine data were removed in an effort to reduce interspecific overlap resulting from intraspecific variation among sexes.

TDL measurements were attainable from 8 of the 11 SCBC jaws, and inclusive first molar data (m1_L and m1Tal_W) from 10 of the 11 specimens due to the well-preserved condition of these fossils (Table 2, Fig. 16). Variables were standardized for 3 specimens missing the anterior portion of the jaw by estimating TDLs based on their dentary length up to the p3 alveolar ridge (Table 2). TDL percentages for this measurement were averaged over complete SCBC specimens at 77.9% of the jaw length. Only one specimen (NAUQSP 8711/116B) retained an m_2 (Table 2, Fig. 16), while no fossils maintained a complete lower toothrow (p_2-m_2). Consequently, MTR was removed as an independent variable in subsequent analyses. Photographs and concise descriptions of each SCBC specimen are illustrated in Appendix A.

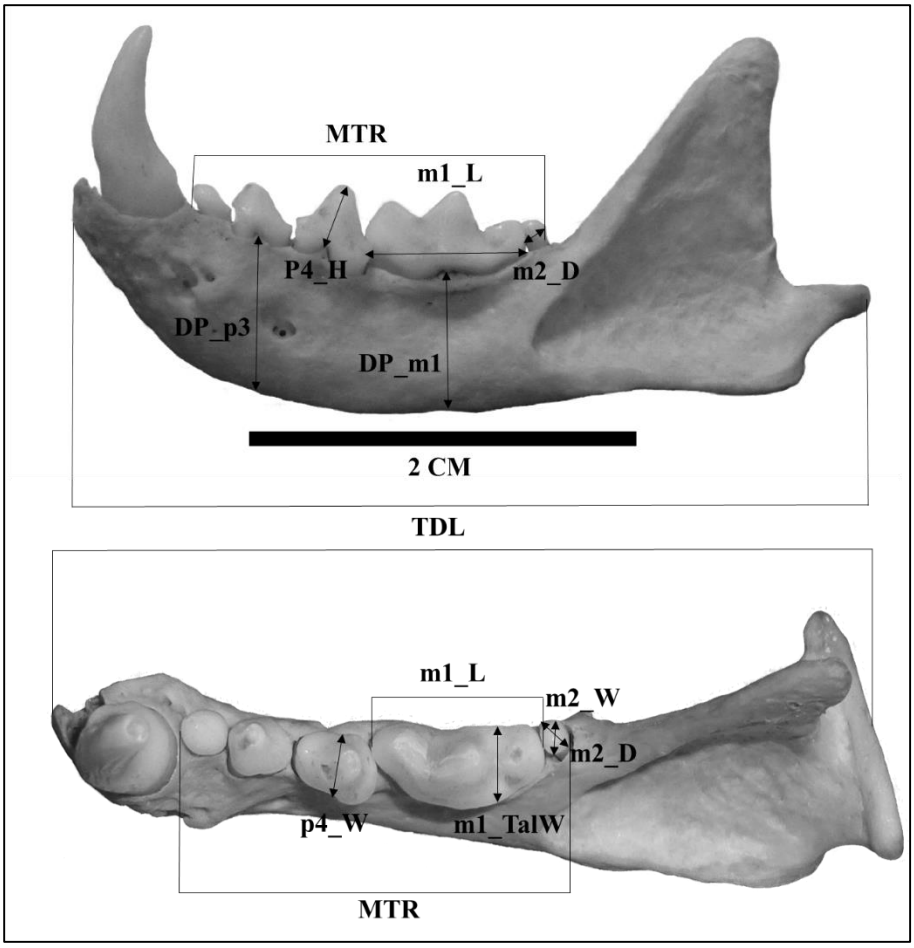

Figure 15. Left dentary of captive-bred *Mustela nigripes* ETVP7271 illustrating 10 linear measurements applied to extant *M. nigripes*, *Neovison vison*, and SCBC specimens in lateral (top) and occlusal (bottom) views. Symbols correspond with abbreviations in Table 1.

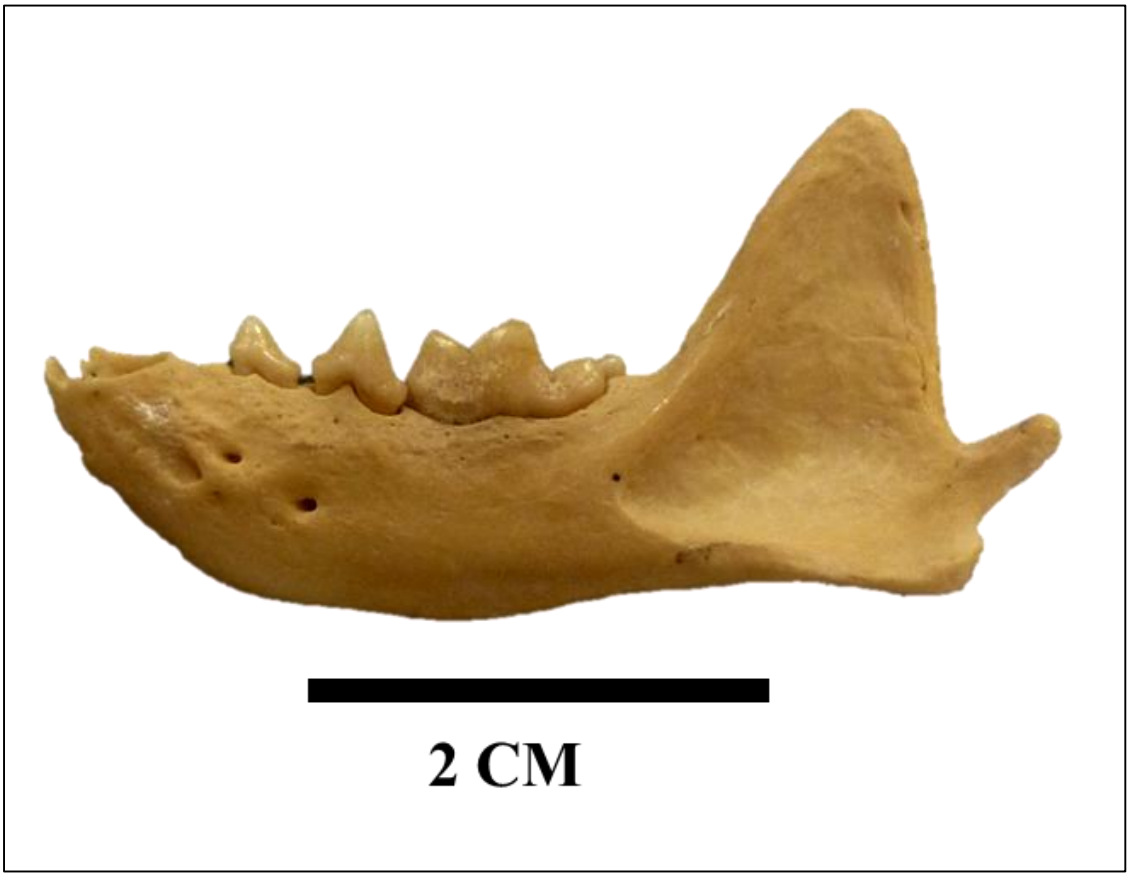

Figure 16. Typical Snake Creek Burial Cave specimen NAUQSP8711/116B in lateral profile.

Due to their extensive range and geographic variation (Hall 1981; Mead et al. 2000), extant *N. vison* specimens were sampled from several states throughout the U.S. including Arkansas, Nebraska, Maine, Colorado, Alaska, and Iowa in an attempt to minimize regional and subspecies biases. For obvious reasons, all *M. nigripes* specimens were sampled from the Wyoming Captive Breeding program. While no recent subspecies of *M. nigripes* are currently acknowledged (Anderson 1989; Wozencraft 2005), morphological variation has been reported among pre- and post bottlenecked samples of extant black-footed ferrets (Wisely et al. 2002b; S. Wallace, personal communication, 4/24/2013). This condition is often exhibited in founder populations due to a decrease in genetic diversity (Wisely et al. 2002a; Cain et al. 2011). Nevertheless, captive-bred *M. nigripes* should serve as adequate proxies for the purpose of discriminating against *N. vison* given that intraspecific differences are often greatly surpassed by interspecific variation (e.g., assumptions in Wallace 2006).

Table 2. Linear measurements for Snake Creek Burial Cave dentaries (n=11).

NAUQSP ID #	Side	TDL	DP_p3	DP_m1	p4_H	p4_W	m1_L	m1_TalW	m2_D	m2_W
8711/115B	left	41.19*	9.80	8.25			8.77	2.39		
8711/116B	left	42.67	10.01	8.88	3.31	2.49	8.55	2.38	1.62	1.66
8711/117B	right	42.12	9.17	8.20	3.56	2.35	9.02	2.39		
8711/118B	right	39.75	8.97	8.53	3.03	2.27	7.91	2.30		
8711/119B	left	39.38	8.90	8.35	2.94	2.25	7.85	2.31		
8711/120B	right	42.36	9.68	8.52			8.66	2.36		
8711/121B	left	38.99*		7.76	3.23	2.22	8.10	2.40		
8711/122B	left	40.21	8.75	7.61	3.51	2.57	8.61	2.31		
8711/123B	right	35.07	7.87	6.91	3.18	2.07	7.98	2.14		
8711/124B	right	42.73	8.85	7.77			9.03	2.58		
8711/125B	left	37.59*	8.01	5.61	2.83	1.94				

Note that MTR has been eliminated as an independent variable due to insufficient characters. Morphometric symbols correspond with abbreviations in Table 1, while *TDL are estimations from incomplete specimens. All numerical values are represented in millimeters.

Results

Several variables within the stepwise DA proved successful in separating extant *M. nigripes* from *N. vison*. Results yielded 100% predicted group memberships for both original and cross-validated cases (Fig. 17). These data were statistically significant at $p = .000$, with a Wilks' Lamba value of .034. A single function with an Eigenvalue of 28.66 accounted for 100% of the total variance in data. Variables selected for discriminating these taxa in descending significance were: m1_TalW, m1_L, DP_p3, and m2_W. The initial 2 components of the PCA generated distinct group clusters for *N. vison* and *M. nigripes*, with more variation exhibited in the former taxon (Fig. 18). These components explained 74.176% of total variance in data at 59.403% and 14.773% respectively. With effective separation established, analyses were re run incorporating the 11 SCBC specimens. Stepwise DA scores grouped fossil specimens exclusively among extant *M. nigripes* (Fig. 19). The first 3 components of this PCA accounted for 82.877% of the variance in data at 55.365%, 14.636%, and 12.877% respectively. Results illustrate all SCBC specimens clustering within the morphospace of extant *M. nigripes* (Fig. 20).

Furthermore, several conditions were noted among mustelid specimens notwithstanding morphometric evaluation. TDLs acquired from group averages indicate that extant *N. vison* demonstrate the smallest jaws overall, while SCBC specimens exhibit the largest dentaries (Table 3). Observations in the number of mental foramina per dentary (MF) also demonstrate marked variation between extant taxa (Table 3). MF values in *N. vison* were lower than *M. nigripes*, averaging less than 2.5 per dentary versus > 4 in the latter taxon (Table 3). However, these values in SCBC fossils averaged between extant taxa at ~ 3.3 MF per side (Table 3).

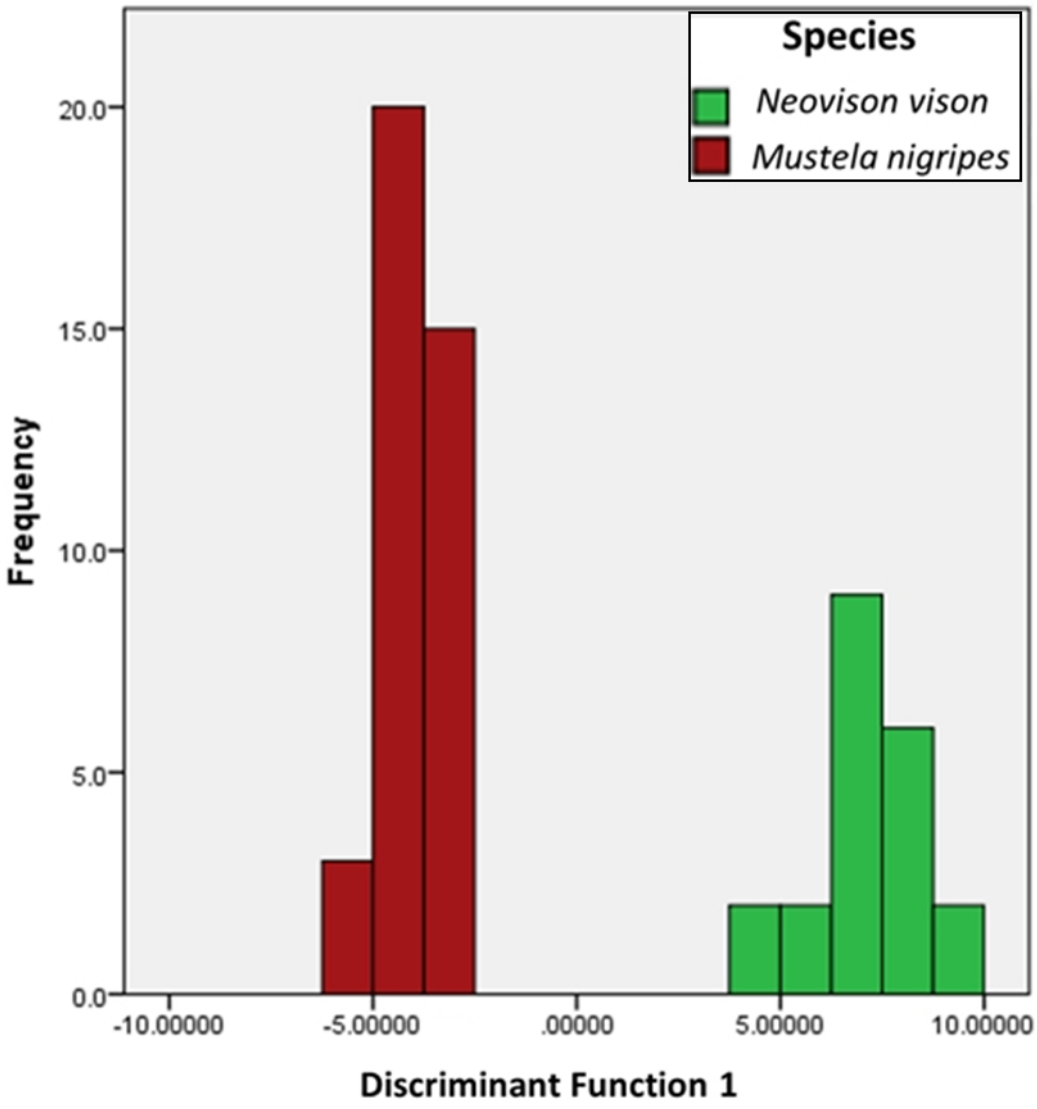

Figure 17. Stepwise discriminant scores for extant East Tennessee Vertebrate Paleontology specimens. Green: *Neovison vison* (n=21), Red: *Mustela nigripes* (n=38).

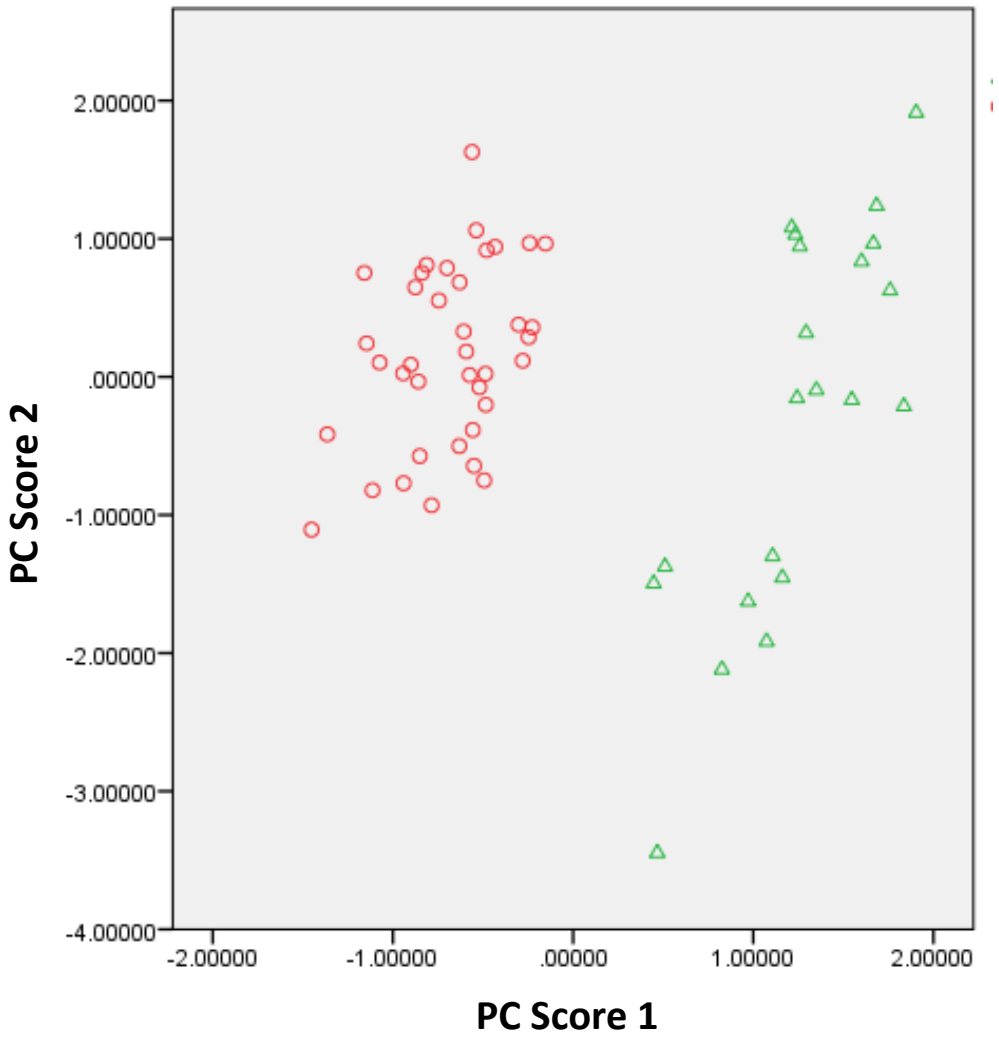

Figure 18. First two principal component scores for extant East Tennessee Vertebrate Paleontology specimens. Triangles = *Neovison vison* (n=21), circles = *Mustela nigripes* (n=38).

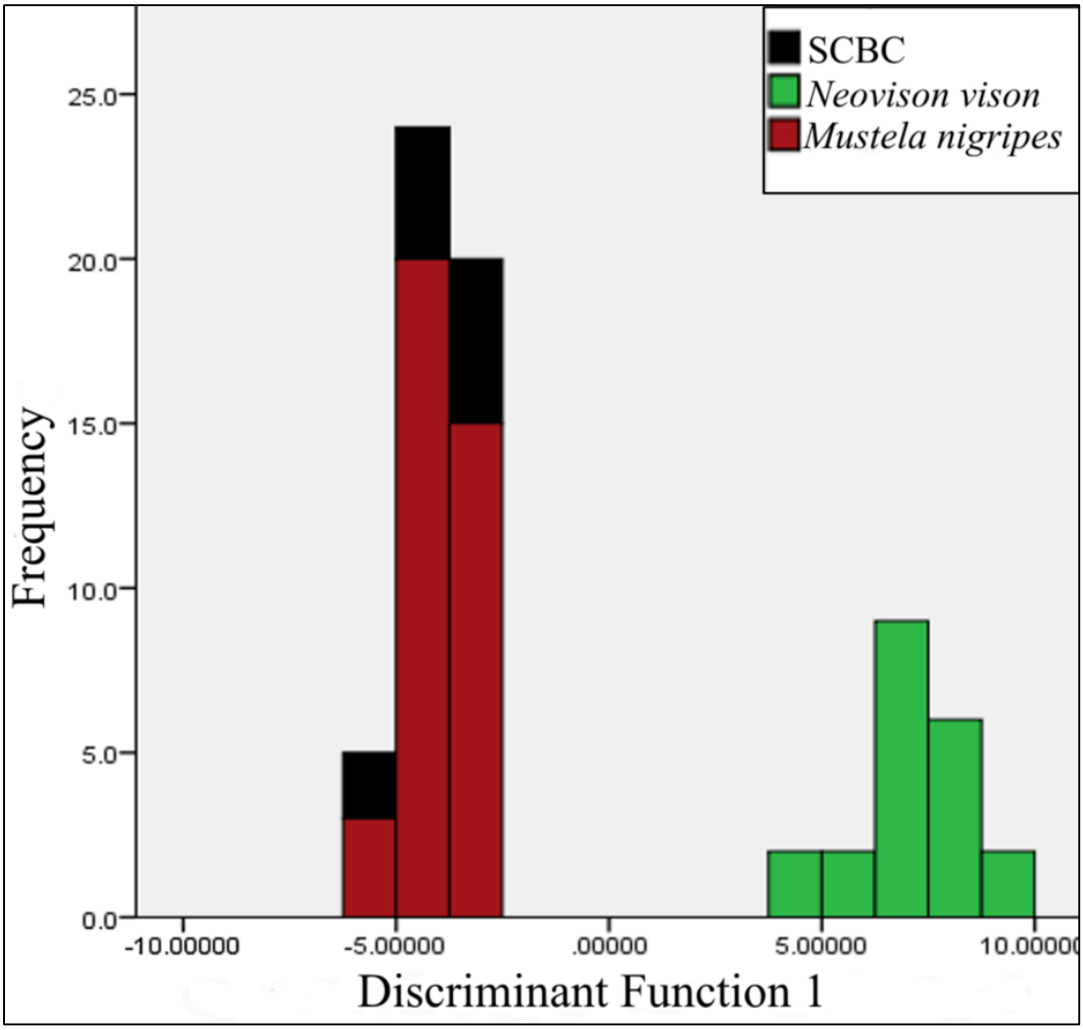

Figure 19. Stepwise discriminant scores for extant *Neovison vison* (n=21), extant *Mustela nigripes* (n=38), and Snake Creek Burial Cave fossils (n=11).

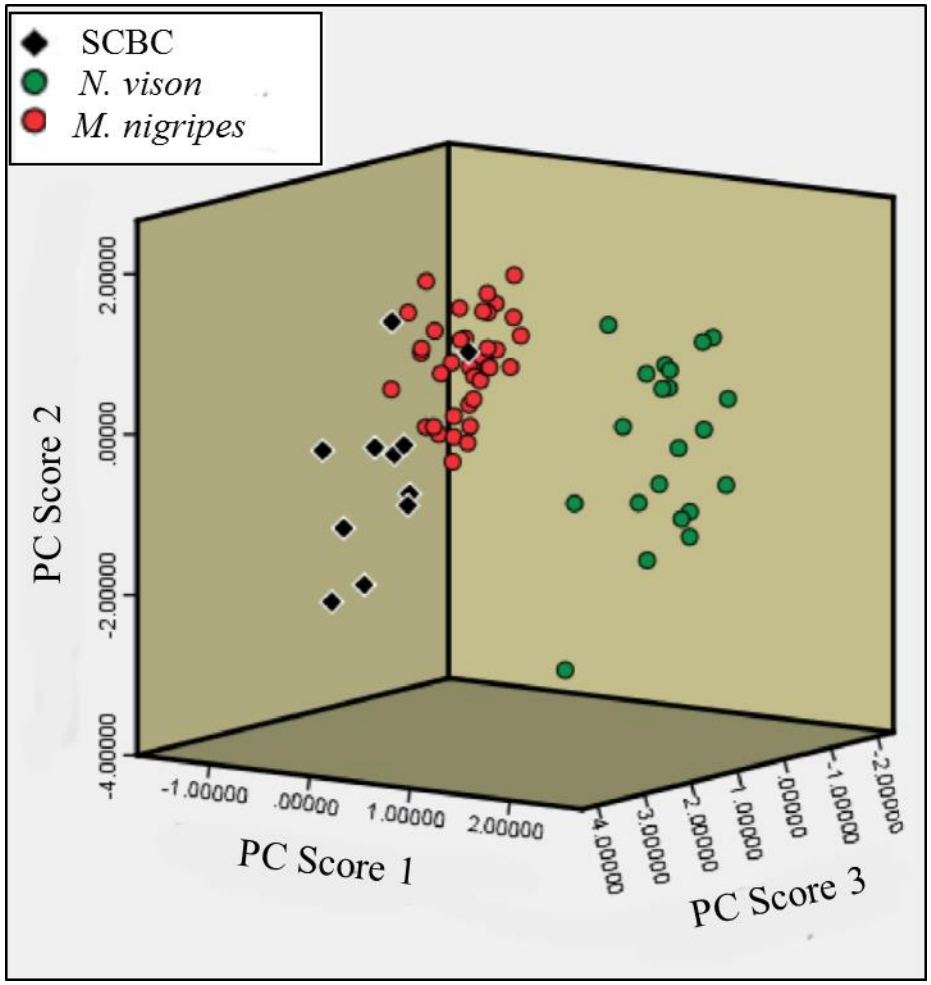

Figure 20. First three principal component scores for *Neovison vison* (green dots), *Mustela nigripes* (red dots), and Snake Creek Burial Cave fossils (black diamonds).

Table 3. Mean dentary lengths (TDL) and number of mental foramina per dentary side (MF) for *Mustela nigripes*, *Neovison vison*, and fossil specimens.

Population	Ave TDL	Ave MF
Neovison vison	38.819 (n = 21)	2.49 (n = 41)
Mustela nigripes	40.044 (n = 38)	4.27 (n = 76)
Snake Creek Burial Cave	40.536 (n = 8)	3.28 (n = 9)

TDL measurements represent collective averages for male, female, and unsexed specimens with values given in millimeters. Mean MF values were averaged from all available left and right dentaries of each population. TDL estimates from incomplete specimens are not included.

Discussion

Captive, Wild, and Prehistoric Observances

In regard to body size Wisely et al. (2002b) noted that mandibles of captive black-footed ferrets averaged ~5% and ~ 6% smaller for males and females respectively compared to species averages for historic specimens (pre-bottlenecked). Likewise, Anderson et al. (1986) recorded Pleistocene *M. nigripes* as 2.9% smaller (males and females combined) on average than their extant wild descendants. Mean TDLs acquired from this analysis signify SCBC dentaries as having the greatest average of these 3 groups at 1.2% larger than extant captive *M. nigripes* specimens (Table 3). Conversely, wild *N. vison* specimens demonstrate the lowest TDL average at 3.1% less than captive-bred *M. nigripes* and ~ 4.2% less than the SCBC population (Table 3).

Furthermore, Anderson et al. (1986) observed that MF on *M. nigripes* dentaries usually average 4 per side. Mean MF observed in extant *M. nigripes* of this study were comparable with those findings (Table 3). Nevertheless, MF values of SCBC specimens averaged indiscriminately between *M. nigripes* and *N. vison*. Therefore, while MF may be used as a proxy for differentiating extant taxa, it remains inconclusive thus far for distinguishing fossil specimens as either *M. nigripes* or *N. vison*. Such values would be expected if SCBC specimens represent a mixed sample of *M. nigripes* and *N. vison*, however, these inferences would conflict with morphometric data (Figs. 19, 20). Admittedly, historic pre bottlenecked *M. nigripes* may have served more applicably for these observations given the possibility of morphologic bias in captive-bred specimens (Wisely et al. 2002b). It is also worth noting that factors of both taphonomy and inadequate sample size may have contributed to the ambiguity of these data in fossil representatives.

Anderson et al. (1986) also reported that *M. nigripes* frequently exhibit pre mortem tooth loss characterized by fused alveoli. Such phenomena were correspondingly exhibited by extant *M. nigripes* analyzed within this study. While dental pathologies were prominent in many of the captive-bred specimens, fusion of the m_2 alveolus was particularly common as exemplified by a marked reduction in m_2 data acquired for *M. nigripes* vs. *N. vison* (Appendix A). This condition was likewise observed within a significant percentage of SCBC specimens (Table 2). Whether this occurrence is a secondary effect of diminutive size in the m_2 of prehistoric and extant *M. nigripes*, or consequence of raising modern specimens in captivity may be worth investigating, though it is beyond the scope of this study.

Morphometric Classification

Results of both stepwise DA and PCA group the eleven SCBC specimens with extant *M. nigripes*. It is worth mentioning that the SCBC population appears to exhibit a relatively broad spectrum of individual variation as illustrated by the first 3 components of the PCA (Fig. 20). While this occurrence may be due to temporal differences in deposition and generations among individuals, a similar range was established in wild *N. vison*. However, captive black-footed ferrets exhibit markedly less intraspecific variability as illustrated by dense clustering (Fig. 20). These effects could reflect their morphological uniformity due to limited genetic variation and captive breeding as previously mentioned (Wisely et al. 2002a; Wisely et al. 2002b; Cain et al. 2011). On the contrary, such discrepancies may also be explained by regional vicariance among captive breeding facilities given the relatively short generation turnover among black-footed ferrets. Because individuals from only one breeding facility were included within this analysis, a restricted geographic sampling could generate morphological bias within these data as well. Other possibilities include, but are not limited to, physical modifications reflecting

environmental changes between the Late Pleistocene biome of eastern Nevada and habitats of *M. nigripes* today. Thus, a more comprehensive analysis that includes greater geographic and temporal ranges of captive and wild *M. nigripes* may be warranted, though it is beyond the scope of this project. Finally, it should be noted that a supplementary analysis was conducted in exclusion of m2_D and m2_W to determine if bias caused by low representation of the m_2 may have driven this dataset. This modification, however, did not change statistical outcomes.

These findings support the presence of *M. nigripes* within the SCBC paleofauna. Conversely, the occurrence of *N. vison* is not supported. The mustelid diversity of SCBC is accordingly reduced to 7 species, though additional specimens may benefit from reexamination as well (J. Mead, personal communication, April 2013). This locality subsequently represents one of at least 8 prehistoric sites, west of both *M. nigripes* and *Cynomys* spp. historic distributions, that contain black-footed ferrets, yet lack documented prairie-dog materials (Anderson et al. 1986; Owen et al. 2000) (Fig. 21). Given that 6 of the 11 *M. nigripes* specimens represent left dentaries (Table 2), the minimum number of individuals (MNI=6) is comparable to this number. SCBC therefore signifies the greatest abundance of black-footed ferrets among a *Cynomys*-absent fossil locality (Anderson 1968; Clark 1975; Anderson et al. 1986), and represents the second furthest westward occurrence of this taxon in the contiguous United States aside from Cathedral Cave located ~40 km further west (Owen et al. 2000) (Fig. 21). While Little Box Elder Cave (LBEC) has produced the greatest quantity of *M. nigripes* specimens yet reported (MNI=15), it also contains specimens of the genus *Cynomys* (Anderson 1968; Anderson et al. 1986).

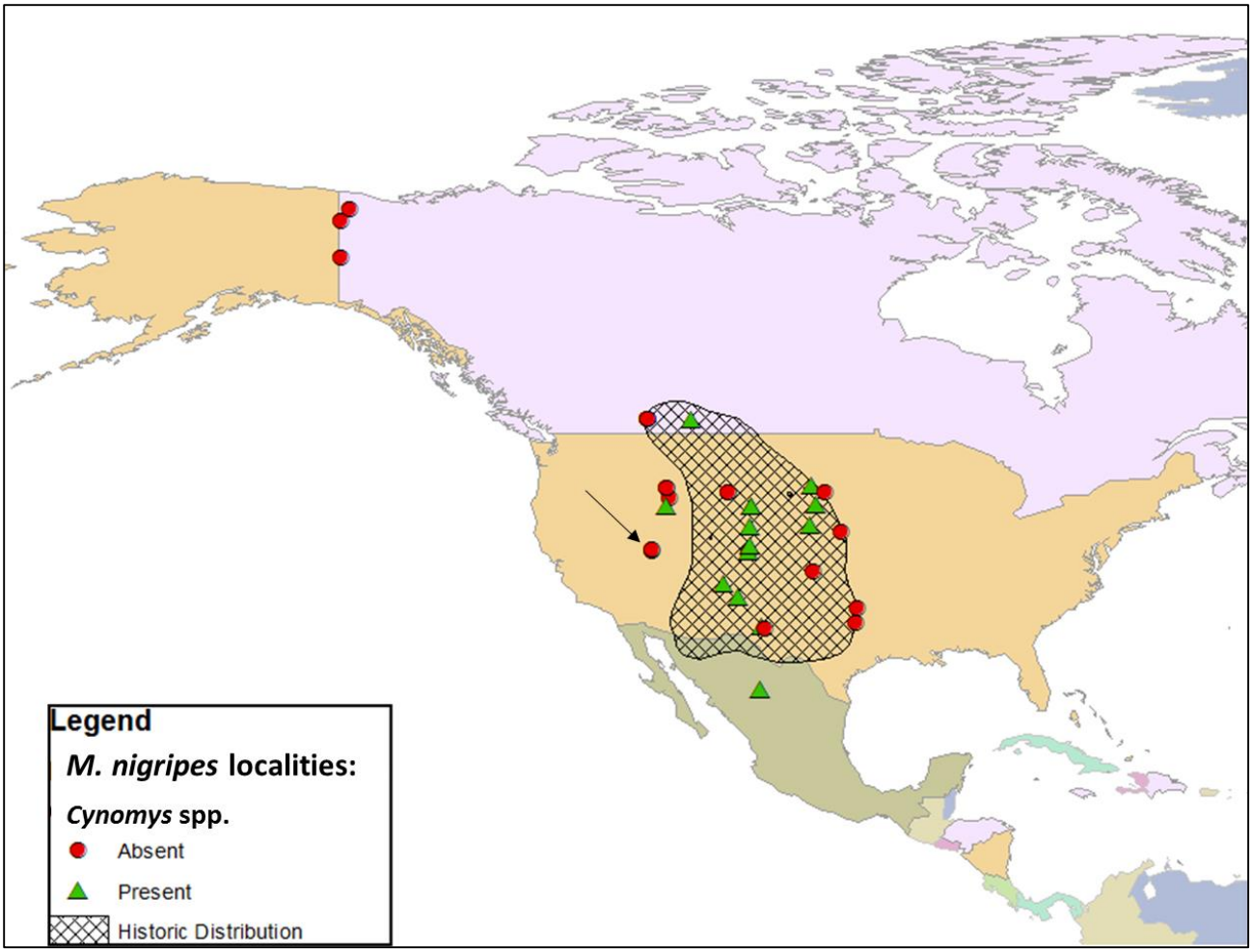

Figure 21. Map of North America illustrating 34 Pleistocene-Holocene localities associated with *Mustela nigripes* as listed in Table 4. Sites are labeled according to their presence (green triangles) or absence (red circles) of *Cynomys* taxa. SCBC and Cathedral Cave (overlapping) are indicated by the black arrow. Species range data from: Patterson et al. (2007).

In addition to SCBC, Anderson et al. (1986) noted that 11 of 21 prehistoric and precolonial North American localities containing *Mustela nigripes* materials lacked *Cynomys* spp., though alternate rodents and lagomorphs were often abundant. Likewise, Owen et al. (2000) address that while *M. nigripes* and *Cynomys* spp. are acknowledged as having an obligate predator-prey relationship, at least 42% of Pleistocene and Early Holocene localities yielding *M. nigripes* remain unassociated with *Cynomys* materials (Fig. 21). Data collected from a single *M. nigripes* specimen in Cathedral Cave, the westernmost locality associated with this taxon (~40 km from SCBC), suggest that current relationships between prairie-dogs and the black-footed ferret are derivative effects of colonization in regions heavily populated by *Cynomys* spp. (Owen et al. 2000). Although age estimates for Cathedral Cave were originally between 750,000-850,000 years BP (Owen et al. 2000), a more recent uranium-series analysis of flowstones sampled from Room 2 yielded dates between 146,020 +/- 2,584 and 153,700 +/- 6,400 years BP (Jass and Bell 2011). Accordingly, it was proposed that modern interactions between these taxa must have been established within the last 800,000 years (Owen et al. 2000), or alternatively between ~146,000 and ~154,000 years BP (Jass and Bell 2011). Occurrence of *M. nigripes* at SCBC, a *Cynomys*-lacking locality near Cathedral Cave yielding upper age limits of 15,100 +/- 700 years BP both support and refine these inferences. Specifically, data from this analysis imply that within select provinces of the Great Basin, modern ecological relationships between black-footed ferrets and prairie-dogs may have developed as recently as ~15,000 years BP or less.

Table 4. List of 34 prehistoric and precolonial North American localities yielding *Mustela nigripes* materials.

Site	Prov.	Lat.	Long.	Age	BFF ID	*C.*	*L.*	*Ma.*	*Mi.*	*S.*
Atlatl Cave	NM	36.1	-108	LHOL	*cf.*	**X**	**X**	-	**X**	-
BMC	NM	32.2	-104.5	LPLE		-	**X**	**X**	**X**	-
BFC I-III	YU	67.1	-140.8	LPLE		-	-	-	**X**	**X**
Burnet Cave	NM	32.4	-104.8	LPLE		**X**	-	**X**	**X**	**X**
Cathedral Cave	NV	39	-114.1	MPLE		-	**X**	-	**X**	**X**
Chimney Rock	CO	40.9	-105.8	HOPL		**X**	-	**X**	**X**	**X**
CWC	NE	41	-100.5	LPLE		**X**	N/I	N/I	N/I	N/I
CAM	KS	37.2	-100.3	MPLE	*cf.*	-	-	-	**X**	**X**
Duck Point	ID	42.6	-112.9	LPLE		**X**	**X**	-	**X**	**X**
Fort Washita	OK	34	-96.5	LHOL		-	-	-	-	-
Highway 74	NE	40.5	-97.9	MPLE		-	-	-	**X**	**X**
IC No. 2	NM	34.9	-106.8	HOPL		**X**	**X**	**X**	**X**	-
JC Hearth II	ID	44.3	-112.9	LPLE		-	-	-	-	-
JC Main Level	ID	44.3	-112.9	HOPL		-	-	-	-	-
JanC Level 3	AB	50.2	-114.5	LPLE		-	-	**X**	**X**	**X**
JanC Level 5	AB	50.2	-114.5	LPLE		-	**X**	**X**	**X**	**X**
JanC Level 6	AB	50.2	-114.5	LPLE		-	**X**	**X**	**X**	**X**
JanC Level 9	AB	50.2	-114.5	LPLE		-	-	**X**	**X**	**X**
Jimenez Cave	MX	27	-104.8	LPLE		**X**	-	-	**X**	**X**
LBEC-LGLA	WY	42.6	-105.6	LPLE		**X**	**X**	**X**	**X**	**X**
LBEC-PREB	WY	42.6	-105.6	EHOL		**X**	**X**	**X**	**X**	**X**
LCCC Atlantic	WY	43.9	-107.6	MHOL		-	**X**	**X**	**X**	-
LCCC LPLE	WY	43.9	-107.6	LPLE		-	**X**	**X**	**X**	-
MH Unit XIII	AB	50.1	-110.7	LPLE		**X**	-	-	**X**	**X**
Moonshiner	ID	43.4	-112.6	EHOL		-	**X**	**X**	**X**	**X**
Moore Pit	TX	32.7	-96.7	LPLE		-	-	-	**X**	**X**
OCR Loc. 65	YU	68.2	-140	LPLE		-	-	-	**X**	**X**
PC Loc. 1925	CO	38.7	-105.9	MPLE	*cf.*	**X**	**X**	**X**	**X**	**X**
PC Loc. 1927	CO	39.3	-105.7	MPLE		**X**	**X**	**X**	**X**	**X**
Sixtymile	YU	64	-140.8	LPLE		-	-	-	-	**X**
SFLF	NE	42.8	-100.1	LPLE		**X**	-	-	**X**	**X**
SCBC	NV	38.9	-114.1	LPLE		-	-	**X**	-	**X**
Spotted Bear	SD	44.5	-100.5	LHOL		**X**	-	-	-	-
Swanson	SD	43.9	-99.3	LHOL		-	-	-	-	-

Presence (**X**) /absence (-) or no information (N/I) of potential prey genera are indicated among these assemblages as well as their rough geographic coordinates. States and provinces follow universal abbreviations. Note that only assemblages containing 3 or more taxa were included to reduce underrepresentation of prey via reports of isolated *Mustela nigripes* materials. For site names and ages, see abbreviations section.

Data collected from *M. nigripes* fossil assemblages via primary literature (Harris and Findley 1964; Anderson 1968; Lyman 1983; Messing 1986; Mead and Mead 1989; Youngman 1994) and online databases (Graham and Lundelius 2010; http://fossilworks.org.) are in general agreement with the findings of Anderson et al. (1986) and Owen et al. (2000). Of the 34 prehistoric black-footed ferret localities evaluated throughout North America, 20 lack documented association with *Cynomys* spp. (58.9%) (Fig. 21, Table 4), yet other colonial rodents are often common among these deposits (Mead and Mead 1989; Owen et al. 2000). In addition to *Cynomys* spp., alternate rodent genera which may have functioned as prehistoric black-footed ferret prey were also recorded, such as: *Lemmiscus* spp., *Marmota* spp., *Microtus* spp., and *Spermophilus* spp. (Fig. 22).

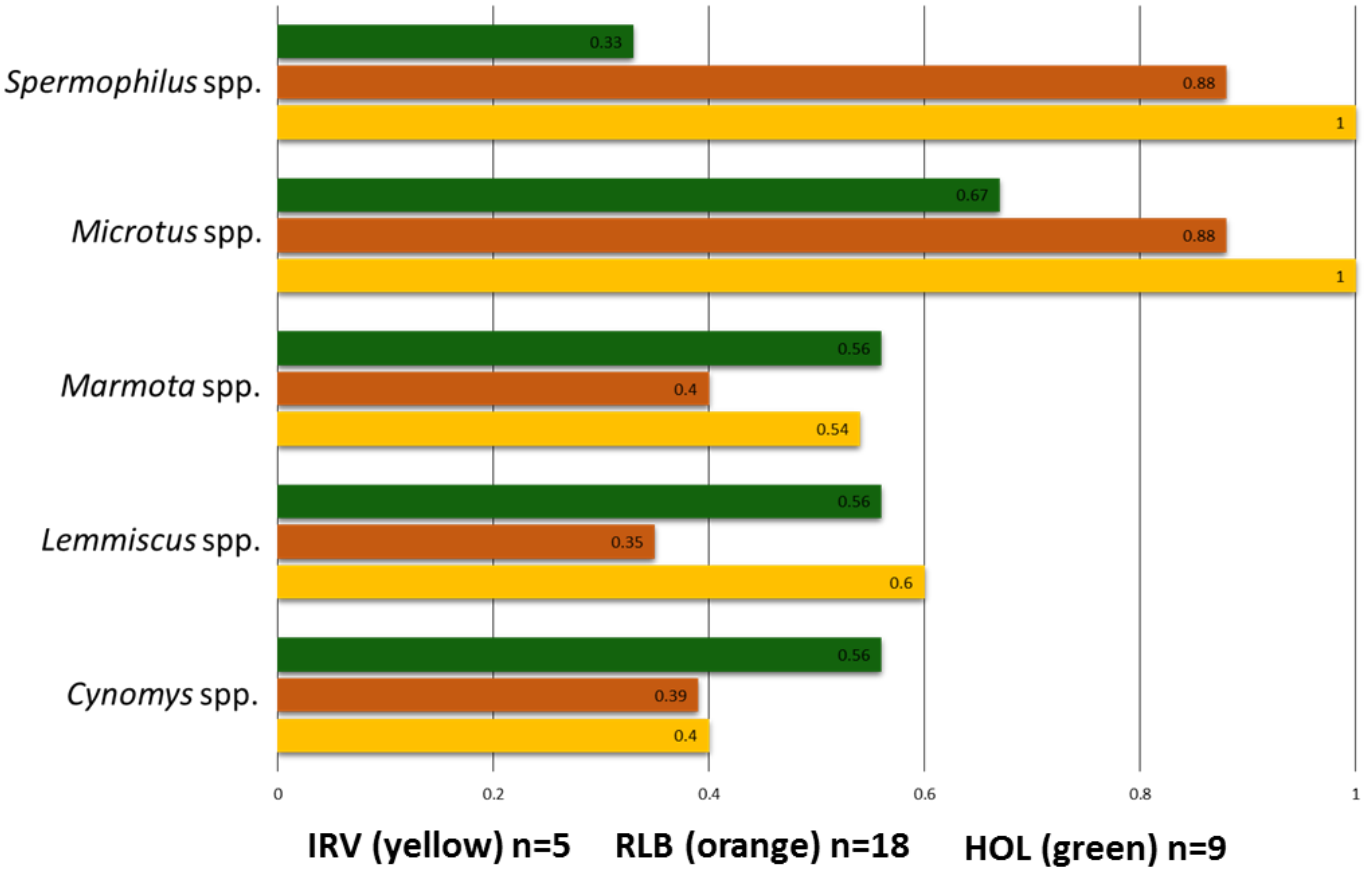

Figure 22. Comparative representation ratios of 5 rodent genera evaluated among the 34 *Mustela nigripes* localities. Data were compiled from presence/absence representation as seen in Table 4. Localities are grouped within the Irvingtonian (IRV), Rancholabrean (RLB), and Holocene (HOL) NALMAs according to information provided within primary literature (Harris and Findley 1964; Anderson 1968; Lyman 1983; Messing 1986; Mead and Mead 1989; Youngman 1994), and online databases (Graham and Lundelius 2010).

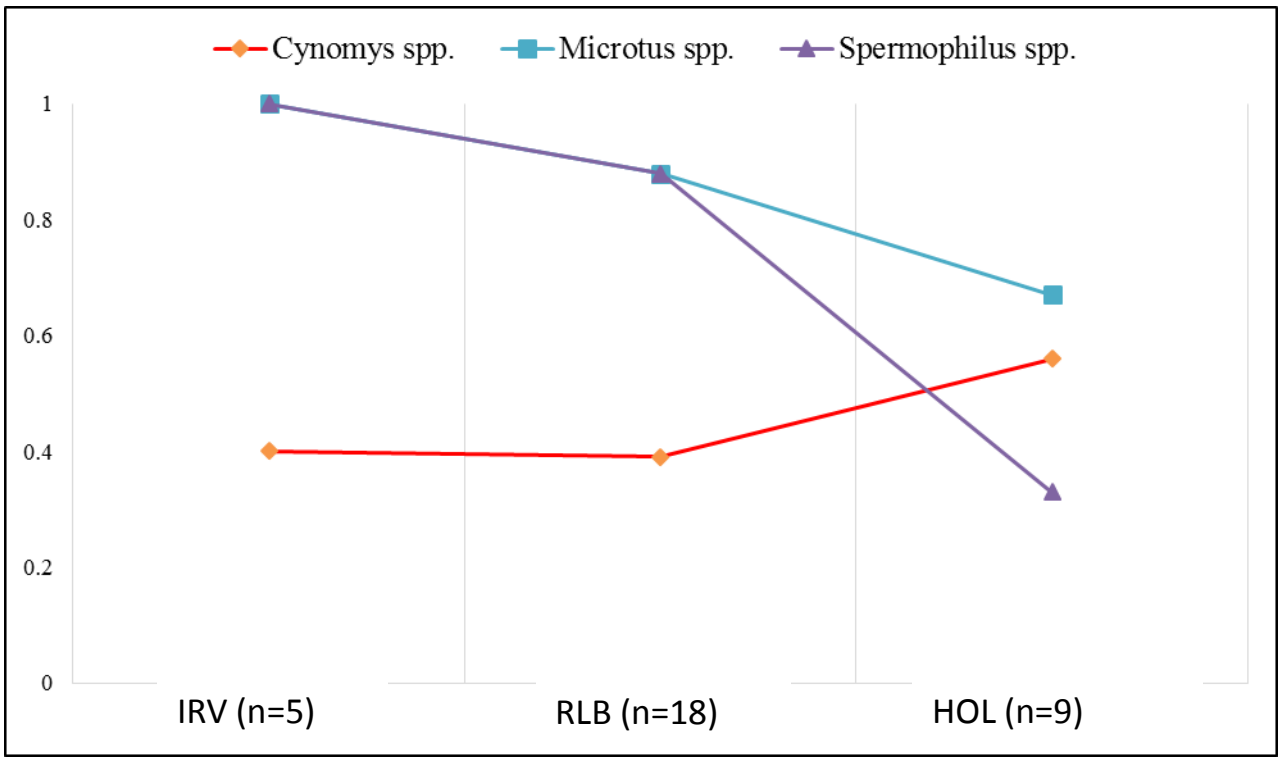

Figure 23. Relative linear temporal representation of *Cynomys* spp., *Microtus* spp. and *Spermophilus* spp. among 34 *Mustela nigripes* localities. Points follow presence/absence ratios depicted in Figure 22.

These data (Fig. 23) suggest an inverse relationship among several rodent genera, specifically during the Rancholabrean and Holocene. Interestingly, *Cynomys* spp. were among the most underrepresented genera analyzed overall, particularly within Pleistocene deposits (Figs. 22, 23, Table 4). Presence of this taxon increases markedly, however, among Holocene localities. While there is little trend temporally among *Marmota* spp. and *Lemmiscus* spp., *Spermophilus* spp. and *Microtus* spp. appear to dominate Irvingtonian and Rancholabrean localities, yet decrease in representation among Holocene localities (Figs. 22, 23, Table 4). However, given the broad scope of this data consensus, results must be assessed with a degree of caution. Differential methodologies, as well as collection and taphonomic biases, must be factored among these localities. Additionally, spatial variation, temporal unconformities, and time averaging effects should also be considered when interpreting these prehistoric assemblages (Owen et al. 2000; Varela et al. 2011). Due to these constraints, species absences among localities should be evaluated with particular caution given their likelihood of generating erroneous or misleading information (Varela et al. 2011), though, it seems unlikely that taphonomic events would preserve small rodent materials such as *Microtus* spp. over the comparatively large and robust elements of *Cynomys* spp. Admittedly, greater diversity in rodent genera and relative abundances (MNIs) of these taxa must be integrated to produce more conclusive results. Nevertheless, a temporal shift in prey representation is conspicuous among these data, and certainly warrants further examination.

Ecological Implications

While it is all but indisputable that extant *Mustela nigripes* populations prefer *Cynomys* spp. as their primary food source (e.g., Vargas and Anderson 1996), fossil evidence implies that this relationship was not facilitated until the recent geologic past (Anderson et al. 1986; Owen et

al. 2000). Rodent data compiled from prehistoric black-footed ferret assemblages support the inferences proposed by Owen et al. (2000) in that the prevalence of *M. nigripes* among *Cynomys* spp. colonies is unlikely a longstanding phenomenon. Furthermore, origins of modern predator-prey relationships between these taxa appears to have initiated or amplified sometime during the Late Pleistocene (Figs. 22, 23). Available data suggest that black-footed ferret diets were more diverse in the past than in recent times or as historically acknowledged, and that *Cynomys* spp. likely integrated a less substantial portion of this diet during the Pleistocene and precolonial Holocene than today.

Such evidence can be applied to modern conservation efforts given that highly specialized species are generally more vulnerable to extinction when confronted with environmental modification (Boyles and Storm 2007; Brickner et al. 2014). As consequence of their reduced genetic diversity, captive-bred black-footed ferrets may be at greater risk of extinction than species which demonstrate extreme niche specialization or have endured a population bottleneck exclusively (Cain et al. 2011). In light of these data, and as noted by Brickner et al. (2014), it may be of little coincidence why *M. nigripes* of Shirley Basin, WY are among the most successful reintroduced ferret populations given their marked dietary plasticity among a mosaic of white-tailed prairie-dogs, as well as alternative rodents and other small mammals. Therefore, while this study does not suggest that *M. nigripes* should be deterred from *Cynomys* populations; facilitating exposures to greater prey diversity may fortify their ecological resilience when faced with future adversities. Systematic analyses, regarding the consumption rate (e.g. Brickner et al. 2014) and sustainability of differential rodent genera among black-footed ferret reintroduction sites are therefore advocated. If necessary, preliminary data may be acquired through ecological surrogates such as the closely related Siberian polecat *M.*

eversmanii, prior to field assessments on this endangered taxon (Biggins et al. 2011b; Biggins et al. 2011c).

CHAPTER 4

DISCRIMINATING NORTH AMERICAN WEASELS USING CRANIOMANDIBULAR LANDMARK ANALYSIS.

Introduction

As with many common names, 'weasel' evokes a relatively ambiguous meaning that can vary markedly throughout regions (King and Powell 2007). This term has been used broadly for referencing all weasels, ferrets, and polecats; which may include species outside the genus *Mustela* (i.e., the African Striped weasel, *Poecilogale albinucha*). Conversely, 'weasel' can be used as explicitly as to define only the least-weasel, *M. nivalis* (King and Powell 2007). From a North American context, 'weasel' is often used for referencing any of 3 native mustelids within the subgenus *Mustela* including: *M. erminea*, *M. frenata*, and *M. nivalis*, and will therefore be defined as such hereafter. Establishment of this generic term is understandable, however, given the overwhelmingly similar morphologies expressed throughout these taxa (King and Powell 2007).

Most characters presently acknowledged for discriminating weasel species are superficial or behavioral; relying primarily on size, pelage, and/or reproductive patterns. Unfortunately, there remains a fundamental lack in osteologic apomorphies reported among these taxa as described in Chapter 2 (see North American Species Diagnosis). While soft-tissues and genetic analysis can be effective for phylogenetic inferences, they provide little assistance to field ecologists, zooarchaeologists, and paleontologists with respect to classifying bone material based on partial skeletons or isolated fragments. Anatomic data currently used for weasel classification generally include relative sizes, character ratios, and qualitative morphologies, the latter often being prone to subjective error. Establishing a reliable means for differentiating *Mustela* species

remains imperative, however, due to their sympatry throughout much of the United States and Canada (Ralls and Harvey 1985; Erlinge and Sandell 1988; Kurose et al. 2005; King and Powell 2007), which may result in a mixing of ostelogical materials between taxa. Thus, elements of one weasel species may easily be misclassified with those of another, especially for individuals of differential sex, ontogeny, temporal range, or region (Kurtén 1968; Anderson 1977).

Osteologic characters commonly used in weasel classification include: cranial-caudal length, skull ratios, relative tail length (Ralls and Harvey 1985; Dayan et al. 1989; Sheffield and Thomas 1997; Heptner et al. 2002; King and Powell 2007); and morphology of the baculum in males (Heptner et al. 2002; Baryshnikov and Bininda-Emonds 2003). However, fully articulated skeletons are relatively scarce in modern collections, and even less common among prehistoric assemblages. Consequently, body and caudal length measurements are often rendered inapplicable from a paleontological standpoint, leaving only dimensions of the cranium, and possibly baculum, as reliable proxies for classification. Moreover, well-preserved mammalian skulls are uncommon relative to the majority of postcranial elements (Lyman 1994), therefore limiting the utility of cranial features as well. While dentaries are significantly more robust, and thus, more common among death assemblages (Lyman 1994; Hillson 2005); inadequate literature could be found on their efficiency for weasel identification. Anderson (1977) noted that descriptive information regarding weasel dentaries were notably lacking despite overlap in morphometric data among extant *M. erminea* and *M. nivalis* jaws from Fairbanks, Alaska. Classification uncertainties within these taxa subsequently convoluted the identification of local Pleistocene materials (Anderson 1977). Nevertheless, successive publications aiming to improve weasel jaw discrimination could not be located for this study.

Weasel classification is further complicated given that *Mustela* taxa exhibit marked sexual dimorphism as mentioned in Chapter 2 (Moors 1980; Ralls and Harvey 1985; Gittleman and Van Valkenburgh 1997; Berdnikovs 2005) (Table 5). Consequently, females of one taxon may overlap with males of a typically smaller species (i.e., *M. frenata* ♀ and *M. erminea* ♂, or *M. erminea* ♀ and *M. nivalis* ♂) (McNab 1971; Dayan et al. 1989). Additional caveats to their classifications stem from intraspecific variation partially attributed to wide-ranging geographic distributions. Marked regional discrepancies have been observed in body size, morphology, and pelage among analogous species of weasels (Ralls and Harvey 1985; Reig 1997; Sheffield and Thomas 1997; Saarma and Tumanov 2006) thus resulting in the classification of multiple subspecies within each taxon. (Merriam 1896; Wozencraft 2005; Saarma and Tumanov 2006).

Size discrepancies among coexisting weasels have been documented throughout several studies including that of McNab (1971) who reported that in regions of sympatry, females often overlap in absolute length with males of the next smallest species. Likewise, a study conducted by Dayan et al. (1989) revealed extensive condylobasal overlap between sympatric male *M. erminea* and female *M. frenata* throughout 4 of 8 North American localities evaluated. One of these localities (Michigan) also exhibited overlap in homogenous sexes of *M. erminea* and *M. frenata* (see Dayan et al. 1989 figs 1, 2). Limited overlap occurred in skull length between sympatric *M. erminea* and *M. nivalis*, although, these data were restricted to 2 localities of Alaska and 1 in Michigan (Dayan et al. 1989). Thus, while size remains a major proxy for weasel species classification (Sheffield and Thomas 1997; King and Powell 2007), condylobasal length may not be adequate for taxonomic resolution. When applied to paleontological studies, such predicaments are appropriately summarized by a statement in Kurtén (1968, p. 103); “As regards fossil material, size is the only clue. The analysis is not facilitated by the fact that the female in

all weasels is smaller than the male…The identification of fossil weasels on the basis of incomplete material, perhaps only a few teeth and jaw fragments, is a tricky matter indeed."

Table 5. Average total skull length (TSL), total dentary length (TDL), and the respective male to female size ratios (MFR) for weasels sampled from ETVP, MCZ, and USNM collections.

Mean TSL	**Males**	**Females**	**MFR**
M. frenata	48.10 (n = 14)	42.79 (n = 9)	1.12
M. erminea	42.92 (n = 19)	36.84 (n = 10)	1.17
M. nivalis	32.73 (n = 14)	30.91 (n = 10)	1.06
Mean TDL			
M. frenata	27.30 (n = 14)	23.46 (n = 11)	1.16
M. erminea	22.55 (n = 20)	18.25 (n = 10)	1.23
M. nivalis	16.40 (n = 14)	15.12 (n = 11)	1.09

Length values are represented in millimeters. Interestingly, size dimorphism appears to be more prominent in dentaries versus skulls for all 3 species.

In light of these issues, the preliminary objectives of this study are to quantify whether interspecific overlap occurs between weasel taxa throughout their North American distributions. Accordingly, craniomandibular length measurements will be used to determine whether size-based species classification is applicable when subspecies and sex is unknown. The purpose of this modification is to construct a taxonomic scenario applicable to prehistoric material given that sex and/or subspecies information is often unknown among fossil assemblages. Data from 85 skull length (TSL) and 91 dentary length (TDL) measurements were compiled from extant weasels housed within the East Tennessee State University Vertebrate Paleontology (ETVP), Harvard Museum of Comparative Zoology (MCZ), and Smithsonian National Museum of Natural History (USNM) collections (Table 6). Measurements were conducted on North American species and subspecies exclusively using Mitutoyo Absolute IP67 digital calipers.

Table 6. North American subspecies and their respective localities for the 3 *Mustela* taxa evaluated.

Species	Locality
M. frenata	
M. f. alleni	WY
M. f. altifrontalis	OR, WA
M. f. arizonensis	AZ, NM
M. f. arthuri	LA
M. f. frenata	TX
M. f. inyoensis	CA
M. f. noveboracensis	CT, DE, GA, IL
M. erminea	
M. e. alascensis	AK
M. e. arctica	CAA, NT
M. e. bangsi	MN
M. e. cigognanii	MA, ME, ON, VT
M. e. fallenda	BC, WA
M. e. invicta	ID
M. e. kadiacensis	AK
M. e. polaris	East GL
M. e. richardsonii	AB, NL, YT
M. e. streatori	OR
M. nivalis	
M. n. allegheniensis	IN, NC, PA, VA
M. n. campestris	MO, SD
M. n. eskimo	AK
M. n. rixosa	AB, MT, ND, NT

Abbreviations follow those standardized for provinces of the United States, Canada, and Greenland.

Table 7. Total skull length (TSL) and total dentary length (TDL) of North American *Mustela frenata*, *M. erminea*, and *M. nivalis* obtained from ETVP, MCZ, and USNM collections.

Species	Skull #	Max	TSL Min	Range	Dentary #	Max	TDL Min	Range
M. frenata	n=27	56.38	38.67	17.71	n=31	32.70	21.21	11.49
M. erminea	n=31	46.76	32.43	14.33	n=32	25.41	15.55	9.86
M. nivalis	n=27	39.53	29.46	10.07	n=28	19.97	13.74	6.23

Values are represented in millimeters. Note the overlap in minimum and maximum measurements of *M. frenata* and *M. erminea*, as well as within *M. erminea* and *M. nivalis*.

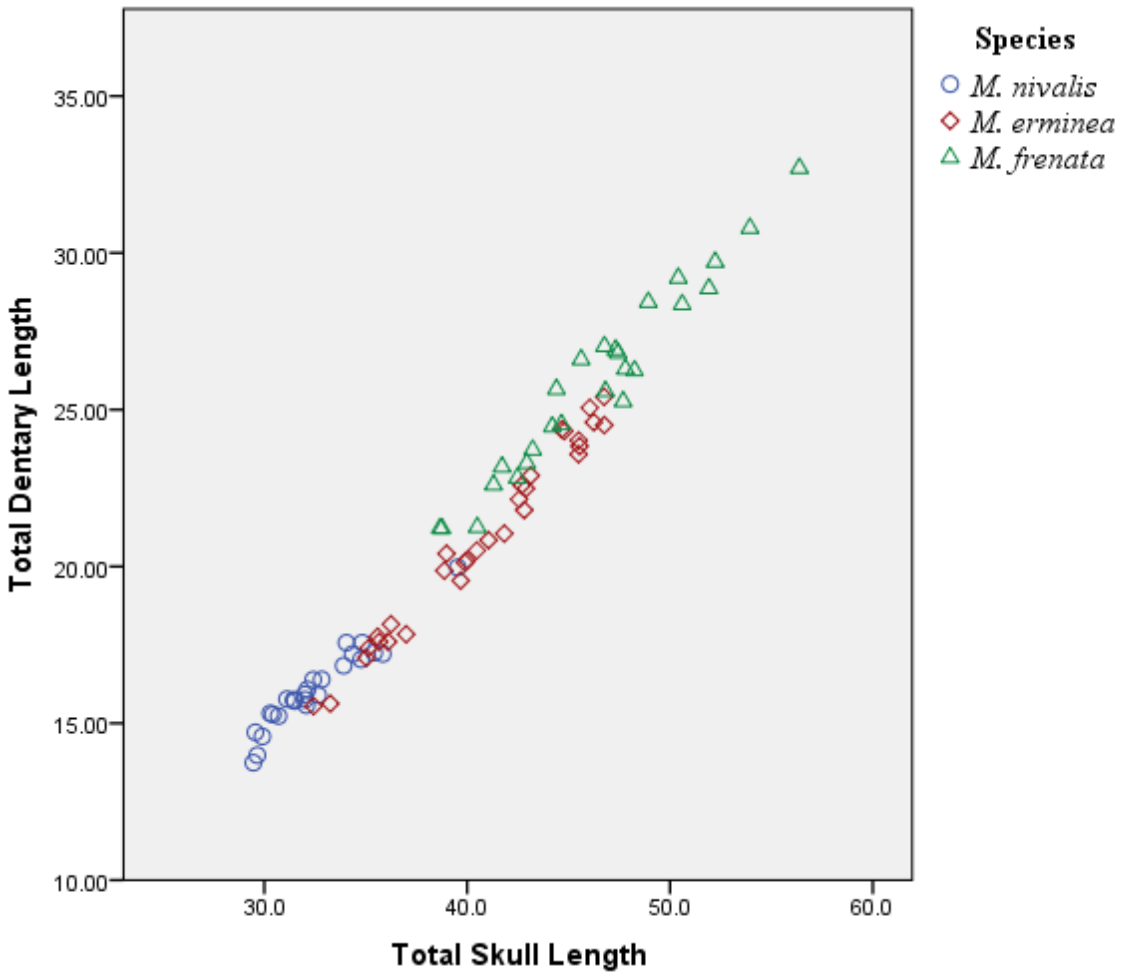

Figure 24. Bivariate plot of total skull length against total dentary length for extant North American *Mustela nivalis* (blue circles), *M. erminea* (red diamonds), and *M. frenata* (green triangles). Data were obtained from extant specimens within ETVP, MCZ, and USNM collections, with length values represented in millimeters. Subspecies and measurements within each taxon correlate with those listed in Tables 6 and 7 respectfully. Note the extreme overlap in size and linear morphologies throughout these species, despite their genetically discreet taxonomic statuses.

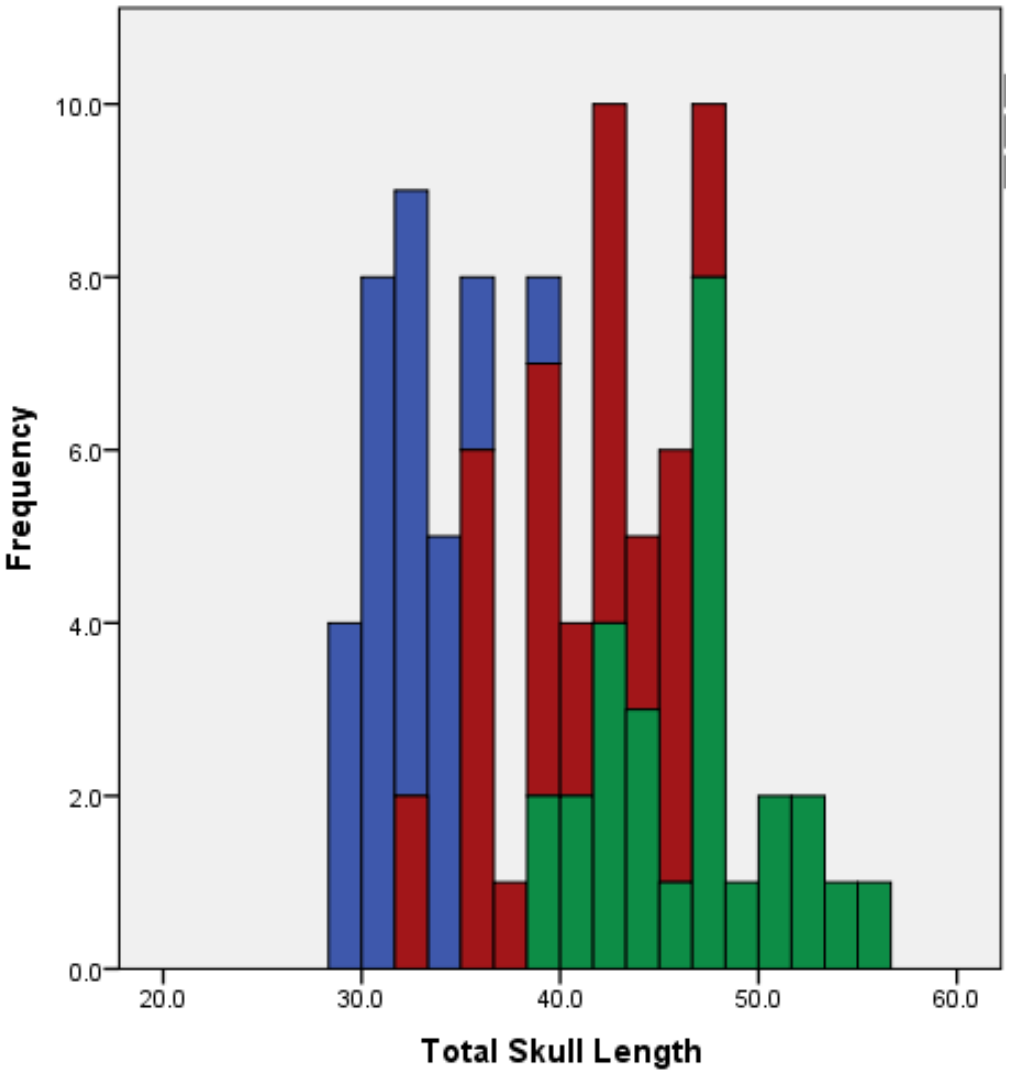

Figure 25. Total skull length (TSL) histogram of extant North American weasel taxa within ETVP, MCZ, and USNM collections. Blue = *Mustela nivalis* (n=27), red = *M. erminea* (n=31), and green = *M. frenata* (n=27). Subspecies and measurements within each taxon correlate with those listed in Tables 6 and 7 respectfully. Length values are represented in millimeters.

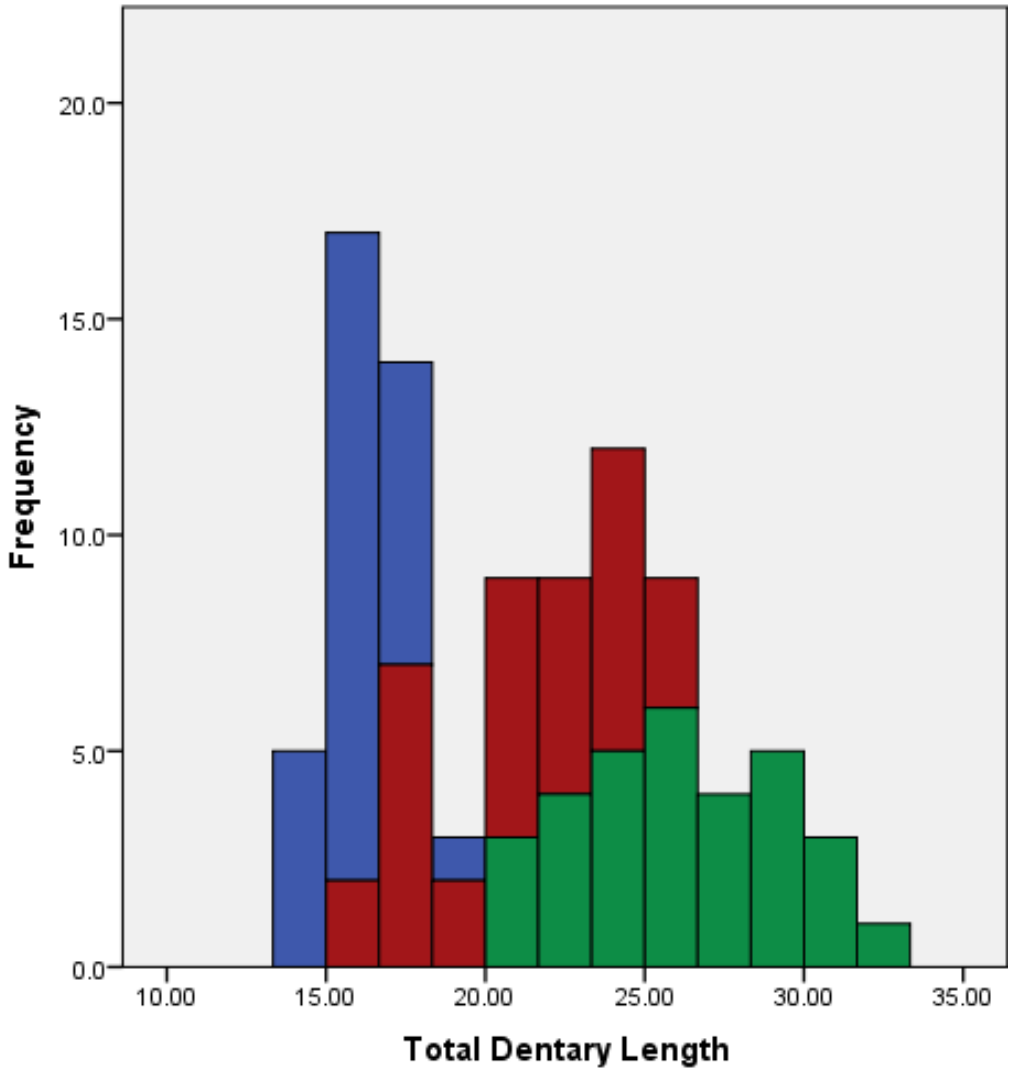

Figure 26. Total dentary length (TDL) histogram of extant North American weasel taxa within ETVP, MCZ, and USNM collections. Blue = *Mustela nivalis* (n=28), red = *M. erminea* (n=32), and green = *M. frenata* (n=31). Subspecies and measurements within each taxon correlate with those listed in Tables 6 and 7 respectfully. Length values are represented in millimeters.

Empirical data established marked overlap in TSL and TDL among *M. frenata* and *M. erminea* as well as within *M. erminea* and *M. nivalis* (Table 7, Figs. 24-26), therefore confirming that craniomandibular length cannot be used as a reliable proxy for weasel classification when sex and subspecies are unknown. Consequently, the intent of this study is to facilitate a more reliable means for weasel identification in North America using landmark-based geometric morphometric (GM) analyses. Such methods have been applied to a broad range of vertebrate animals (e.g. Cavalcanti et al. 1999; Wallace 2006; Figueirido et al. 2009), including several studies within the Mustelidae (e.g. Reig 1998; Loy et al. 2004; Meyers 2007; Peters et al. 2010). Ultimately, this approach aims to quantify interspecific variation within the skull and jaw morphologies of each taxon regardless of, or indicative to, region (subspecies) and sex. If successful, corresponding methods will be applied to prehistoric *Mustela* spp. from Snake Creek Burial Cave in an effort to classify these taxa as well.

Materials and Methods

Landmark-based (GM) are a class of statistical analyses that quantify shape and shape change within objects using spatial displacement of discreet loci (Bookstein 1991; Zelditch et al. 2004). Conversely, traditional GM are based primarily on linear distances and ratios that can be highly correlated among differential measurements as a result of size bias (Bookstein 1991; Zelditch et al. 2004). Thus, landmark-based GM could be suitable for weasel classification where size overlap and lack of osteologic apomorphies are among the principal taxonomic issues. This study may also benefit from such methods given that significant variables do not require *a priori* establishment as in traditional GM (Zelditch et al. 2004). On the contrary, the intent of landmark-based analyses are to quantify the variability and significance of each locus within the study and,

therefore, may be advantageous over traditional GM when group-discriminating characters are yet to be established (Zelditch et al. 2004).

Spatial data are acquired from landmark analyses through Cartesian coordinates of biologically homologous features that must be identifiable throughout all objects (Bookstein 1991; Zelditch et al. 2004; Webster and Sheets 2010). As defined by Bookstein (1991), these loci can be grouped into 3 broad categories: discreet juxtapositions (type 1), minima/maxima of curvature (type 2), and extremal points (type 3). Type 1 landmarks are most efficient because they can be analyzed independently from surrounding structures, whereas type 3 landmarks are the most subjective, and generally, uninformative (Bookstein 1991; Reig 1998; Zelditch et al. 2004). Likewise, type 2 landmarks are intermediately effective at quantifying shape change between types 1 and 3 (Bookstein 1991; Zelditch et al. 2004).

In evaluating 3-dimensional digitizing precision and error, Reig (1998) noted that type 1 landmarks are exceedingly difficult to establish among weasel skulls due to their overall lack of type 1 features such as well-defined sutures and bony processes. Likewise, landmarks used herein are primarily type 2 (Tables 8-10). Nevertheless, Reig (1998) was able to achieve adequate separation among weasel crania through Canonical Variate analysis of landmarks from 2 subspecies of *M. erminea*, and 1 of *M. frenata*. Consequently, landmarks used within this analysis were selected for illuminating species-level variation as noted in previous literature (e.g. rostral length (Kurtén and Anderson 1980); shape of the auditory meatus (Reig 1998); shape of the infraorbital foramen (Heptner et al. 2002)…etc.), and to characterize discernable morphologic features (e.g., shape of the auditory bullae, m_1 carnassial blades, P^4 protocone…etc.). Several cranial loci in this analysis were adapted from other mustelid GM studies, including works of: Reig (1998); Loy et al. (2004), and Meyers (2007). All included loci

are defined in Tables 8-10. It is worth noting, however, that some landmarks may transcend types between specimens (Bookstein 1991) (Tables 8-10). For example, the maximum posterior curvature of the palatine (Table 10, LM 32) is a type 2 landmark as defined in this analysis for specimens lacking a well-defined midpalatal suture. However, this loci becomes type 1 when the medial suture is present as characterized by a 3-way juxtaposition bisecting the posterior curvature of the palatine with the midpalatal suture.

Table 8. Landmark types, numerical sequence, and descriptions of the 18 anatomic loci analyzed from the lateral plane of the left dentary.

Lateral Landmarks	Number	Type	Description
Upper mandibular symphysis	(omitted)	2	Anterodorsal most curvature of the dentary at the mandibular symphysis
c1 alveolus, anterior	(omitted)	2	Anterior most curvature of the alveolus at the c1
c1 alveolus, posterior	1	2	Posterior most curvature of the alveolus at the c1
p3 alveolus, anterior	2	2	Anterior most curvature of the alveolus at the p3
p3 alveolus, posterior	3	2	Posterior most curvature of the alveolus at the p3
p4 occlusal ridge	4	2	Dorsal most curvature of the occlusal ridge at the p4, labial side
p4 alveolus, posterior	5	2	Posterior most curvature of the alveolus at the p4
Carnassial invagination	6	1-2	Ventral most curvature of the posterior paraconid and anterior protoconid; trisection between the paraconid, protoconid, and superior boundary of the carnassial notch
m1 occlusal ridge	7	2	Dorsal most curvature of the occlusal ridge at the m1, labial side
m1 talonid invagination	8	1-2	Ventral most curvature at the base of the m1 protoconid and anterior origin of the talonid
m1 talonid, posterior	9	1	Intersection between the posteroventral most margin of the m1 talonid and the dorsal surface of the dentary
Posterior m2 alveolus	10	2	Posterior most curvature of the alveolus at the m2
Coronoid apex	11	2	Dorsal most curvature of the coronoid process
Post-coronoid convexity	12	2	Maximum curvature at the posterior base of the coronoid and anterior margin of the condyloid processes
Condyle apex, posterior	13	2	Posterior most curvature of the condyloid condyle
Angular apex, posterior	14	2	Posteroventral most curvature of the angular process
Masseteric fossa, anterior	15	2	Anterior most curvature of the masseteric fossa indentation
Dentary at the p3, ventral	16	3	Ventral margin of the dentary adjacent to the labial side p3 occlusal ridge

Table 9. Landmark types, numerical sequence, and descriptions of the 15 anatomic loci analyzed from the occlusal plane of the left dentary.

Occlusal Landmarks	Number	Type	Description
c1 alveolus, posterior	1	2	Posterior most curvature of the alveolus at the c1
p3, posterior	2	2	Maximum curvature of the posterior occlusal surface at the p3
p4 medial constriction	3	2	Maximum mesial curvature of the p4 enamel, lingual
p4, posterior	4	2	Maximum curvature of the posterior occlusal surface at the p4
m1 medial constriction	5	2	Maximum mesial curvature of the m1 enamel, lingual
Anterior talonid, lingual	6	2	Maximum curvature of the outer enamel margin at the base of the m1 protoconid and anterior of the m1 talonid, lingual
Anterior talonid, labial	7	2	Maximum curvature of the outer enamel margin at the base of the m1 protoconid and anterior of the m1 talonid, labial
m2 alveolus, anterior	8	3	Anterolingual most curve of the m2 (alveolus)
m2 alveolus, posterior	9	3	Posterolabial most curve of the m2 (alveolus)
Lateral condyle apex	10	2	Maximum lateral curvature of the lateral codyloid condyle
Medial condyle apex	11	2	Maximum lateral curvature of the medial codyloid condyle
Pre-condyloid convexity	12	2	Maximum point of curvature anterior to the medial condyloid condyle
Posterior symphysis	13	1-2	Posterior extent of the lingual curvature at the mandibular symphysis; juxtaposition between the anterolingual margins of the two dentaries at the mandibular symphysis and the posterior extent of the mandibular suture
m1, anterior	14	2	Maximum anterior most curvature of the m1 occlusal surface
m1, posterior	15	2	Maximum posterior most curvature of the m1 occlusal surface

Table 10. Landmark types, numerical sequence, and descriptions of the 43 anatomic loci analyzed from the left ventral plane of the skull.

Ventral Landmarks	Number	Type	Description
I1, mesial	1	1	Juxtaposition between the posteromesial occlusal surfaces of the medial incisors
Incisive foramen, anterior	2	2	Maximum anteromedial curvature of the incisive foramen
Incisive foramen, posterior	3	2	Maximum posterolateral curvature of the incisive foramen
C^1 alveolus, posterior	4	2	Maximum posterior curvature of the C^1 alveolus
P^2, posterior	5	2	Maximum curvature of the posterior occlusal surface at the P^2
P^3 medial constriction	6	2	Maximum mesial curvature of the P^3 enamel, lingual
P^3, posterior	7	2	Maximum curvature of the posterior occlusal surface at the P^3
Infraorbital foramen, anterior	8	2	Maximum anterior curvature of the infraorbital foramen
Infraorbital foramen, posterior	9	2	Maximum posterior curvature of the infraorbital foramen
P^4 parastyle, anterior	10	2	Maximum anterior curvature of the P^4 parastyle
P^4 curvature, posterior	11	2	Maximum posterior curvature between the P^4 parastyle and protocone
P^4 protocone, anterior	12	2	Maximum anterolingual curvature of the P^4 protocone
P^4 curvature, lingual	13	2	Maximum labial curvature at the base of the P^4 protocone, lingual
P^4- M^1 intersection, lingual	14	1	Juxtaposition between the P^4 and M^1 occlusal surfaces, lingual side
P^4-M^1 intersection, labial	15	1	Juxtaposition between the P^4 and M^1 occlusal surfaces, labial side
M^1, posterior	16	2	Maximum curvature between the M^1 protocone and metacone, posterior side
M^1 protocone, posterior	17	1	Juxtaposition between the posterior curvature of the M^1 protocone and the posterior boundary of the maxilla
M^1 protocone, anterior	18	2	Maximum anterior of the M^1 protocone
Glenoid fossa, anterior	19	2	Maximum curvature of the anterodorsal margin of the glenoid fossa

Table 10 (continued).

Ventral Landmarks	Number	Type	Description
Glenoid fossa, lateral	20	2	Maximum anterolateral curvature of the glenoid fossa
Glenoid fossa, posterior	21	2	Maximum curvature of the posteroventral margin of the glenoid fossa
Glenoid fossa, medial	22	2	Maximum medial curvature of the glenoid fossa
Auditory meatus, posterior	23	2	Maximum posterior curvature of the auditory meatus
Auditory foramen, lateral	24	2	Maximum anterior curvature of the auditory foramen, lateral side
Auditory bullae, posterior	25	2	Maximum posterior curvature of the auditory bullae
Auditory bullae, medial	26	2	Anterior most depression of the posteromedial auditory curvature
Auditory foramen, medial	27	2	Maximum anterior curvature of the auditory foramen, medial side
Occipital condyle, posterior	28	2	Maximum curvature of the posterior apex at the occipital condyle
Occipital condyle, medial	29		Maximum curvature of the medial projection at the occipital condyle, inferior
Foramen magnum, inferior	30	2	Anterior most curvature of the inferior margin at the foramen magnum
Pterygoid hamulus apex	31	2	Posterior most curvature of the pterygoid hamulus
Palatine, posterior	32	1-2	Maximum curvature of the posterior palatine above the vomer; juxtaposition between the maximum point of curvature of the palatine and the midpalatal suture
I^3, lateral	33	1	Juxtaposition between the lateral I^3 margin and the anterior boundary of the premaxillae
Premaxillae, anterior	34	2	Maximum anterolateral curvature of the premaxillae
Rostrum, posterior	35	2	Maximum curvature of the posterior boundary at the rostrum and the base of the zygomatic arch
Zygoma, anterior	36	2	Maximum anterior curvature of the zygomatic arch, medial
Zygoma, posterior	37	2	Maximum posterior curvature of the zygomatic arch, medial
Mastoid process, lateral	38	2	Lateral most curvature of the mastoid process

Table 10 (continued).

Ventral Landmarks	Number	Type	Description
Palatal curvature, posterior	39	2	Maximum posterior curvature of the palatine, left side
Palatal curvature, anterior (left)	40	2	Maximum anterior curvature of the palatine, left side
Palatal curvature, anterior (right)	41	2	Maximum anterior curvature of the palatine, right side
Infraorbital foramen, medial	42	2	Maximum medial curvature of the infraorbital foramen
Infraorbital foramen, lateral	43	2	Maximum lateral curvature of the infraorbital foramen
Glenoid fossa, anteromedial	44	2	Maximum anteromedial curvature of the glenoid fossa

Craniomandibular landmark series were plotted in coplanar orientation due to the challenges of 2-dimensional analyses for quantifying depth in 3-dimensional objects (Zelditch et al. 2004; Webster and Sheets 2010). Therefore, landmarks were entered in tpsDig2 using loci from lateral and occlusal views of the dentary (Fig. 27), as well as a ventral profile of the skull (Fig. 28). While 3-dimensional digitizers are available to reduce the limitations of two-dimensional landmarks, such materials tend to be expensive (Zelditch et al. 2004). Consequently, a 2-dimensional analysis was designated to maximize the replicability and utility of these methods for future studies. All morphometric software were acquired from the freely accessible programs on the SUNY Stony Brook Morphometrics website: http://life.bio.sunysb.edu/morph/index.html, while digital photographs were taken using the corresponding 85 weasel skulls and 91 dentaries previously measured (Table 7, Figs. 24-26)

using a Panasonic ZS19 Lumix digital camera. Adult specimens were digitized exclusively based on fully erupted permanent dentition, lack of cranial/mandibular sutures, and catalogue information.

To minimize individual bias, left skull and dentary characters were digitized exclusively from extant taxa. However, to compensate for fossil materials that represent both left and right specimens, those of the right side were flipped to portray left characters. Moreover, specimens digitized in occlusal view of the dentary and ventral view of the skull were stabilized prior to photographing using clay foundations after obtaining permission from their respective housing facilities. This was implemented to minimize lateral rotation, which can significantly modify coordinate output from 2-dimensional images. Likewise, clay pedestals were erected to support the anterior jaw of fused mandibles photographed in lateral view in an effort to mimic the lateral resting position of isolated dentaries. Lastly, elevation bubbles were used along with a photographing stand to insure that all images were taken from a uniform angle.

After digital photographs of each specimen were acquired, landmarks were plotted over these images using tpsDig2 and superimposed via a least-squares Generalized Procrustes Analysis (GPA) in tpsSUPER. Species consensuses were then generated from superimposed data to average-out the intraspecific variation within each weasel taxon. Thin-plate spline (TPS) orthogonal deformation grids were subsequently interpolated from these consensuses to visually quantify interspecific variation among *Mustela* species. These warp grids were generated using a consensus of *M. erminea* referenced against the respective consensuses of *M. nivalis* and *M. frenata* for morphological comparison (Figs. 29-31).

After superimposing the designated landmark variables, stepwise discriminant analyses (SDA) and principal component analyses (PCA) were performed in SPSS (version 21) to

quantify the significance of each anatomic loci for species classification. A discriminant function is a type of multivariate analysis used to sort unknown data into 1 of 2 or more groups based on a set of independent variables selected *a priori* (Lachenbrunch and Goldstein 1979). When group memberships of a reference dataset are known beforehand, a discriminant function can estimate the reliability of these variables for correctly classifying specimens of unknown group membership. In short, a SDA performs much like a discriminant function analysis in evaluating the percentage of correctly predicted group memberships using the most significant of the allotted variables for separation (Lachenbrunch and Goldstein 1979). Conversely, a PCA uses orthogonal transformation to plot each unsegregated specimen in multivariate space according to the components that account for the greatest percentages of variation among groups (Abdi and Williams 2010). Thus, a PCA can be beneficial for illustrating the relative similarity, or variability, among specimens as illustrated by the density and overlap of their respective group clusters.

It is also worth mentioning that 2 anterior landmarks of the lateral jaw as defined in Table 8 were removed prior to SDA and PCA analyses. These landmarks were excluded due to their relatively thin and fragile corresponding loci to allow for several nearly complete SCBC dentaries to be included within these analyses. Nevertheless, the 2 landmarks proved highly variable and taxonomically insignificant among extant specimens in preliminary SDA. This removal subsequently facilitated the classification of an additional 17 fossils without inhibiting extant predicted group memberships. These characters were retained, however, within the lateral thin-plate splines for visual reference of the anterior jaw structure (Fig. 29).

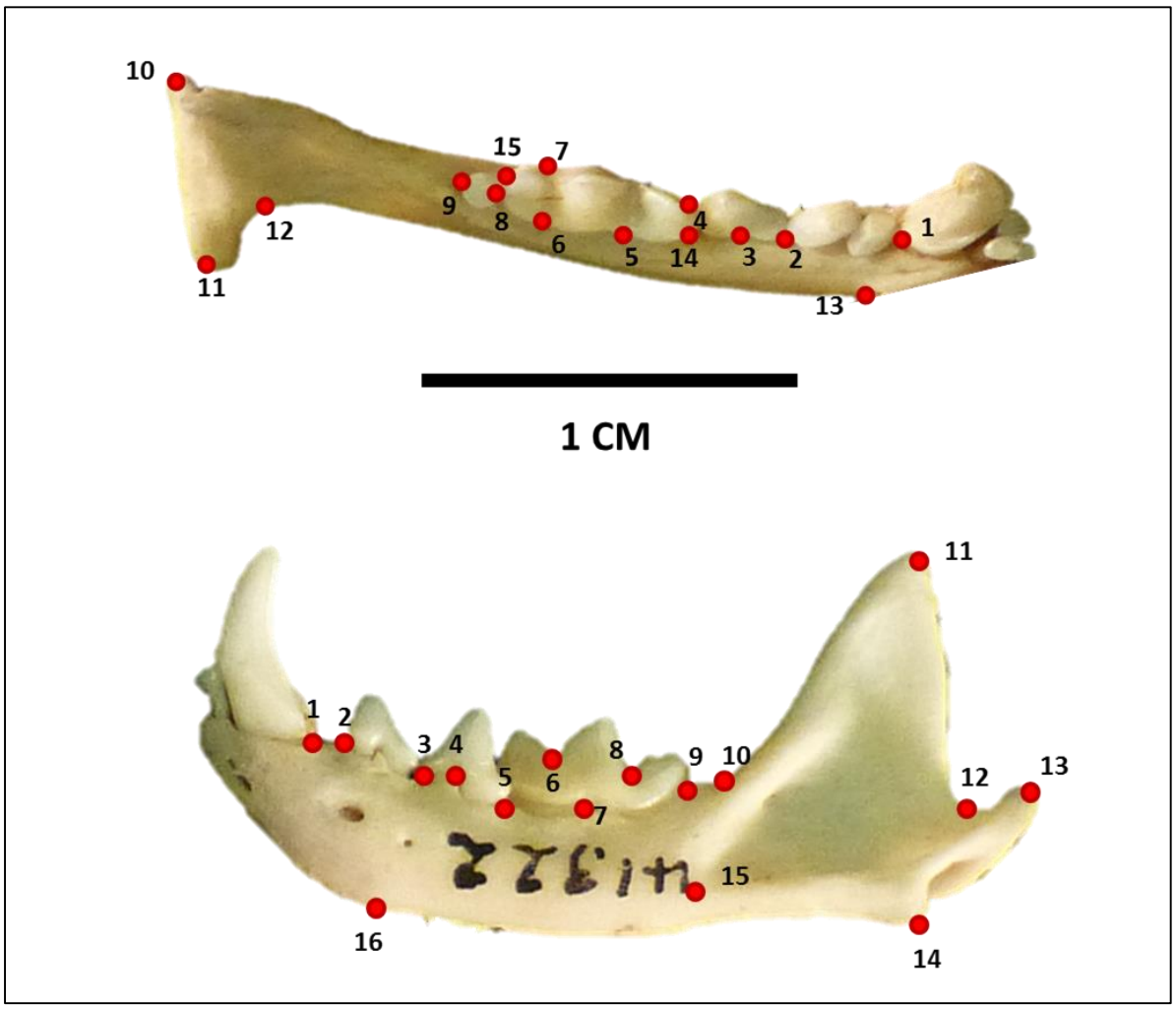

Figure 27. Occlusal (top) and lateral (bottom) landmarks of the dentary (*Mustela erminea* MCZ12652 and *M. erminea* MCZ41322 in top and bottom profiles respectively) used for extant weasels and SCBC specimens. Landmark numbers correspond with types and definitions as described in Tables 8 and 9.

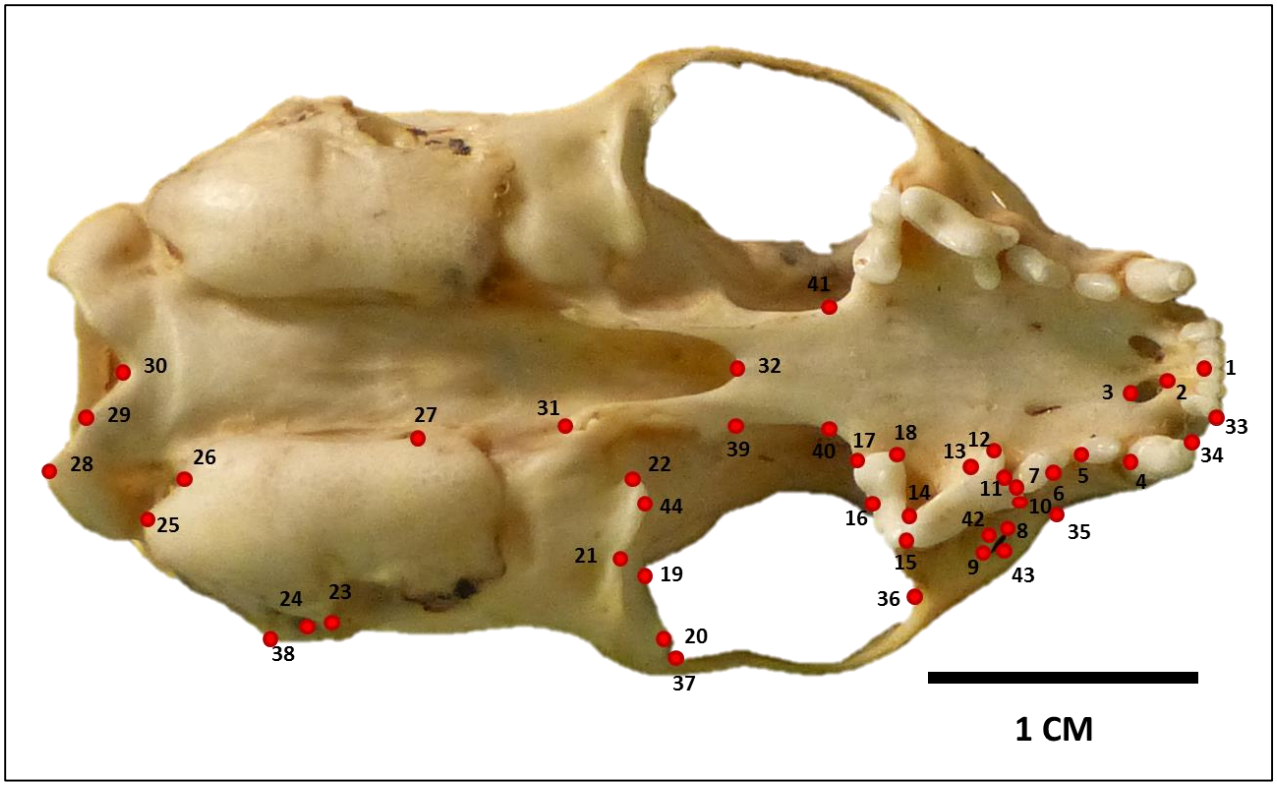

Figure 28. Landmarks of the ventral skull (*Mustela erminea* MCZB788) used for extant weasels and SCBC specimens. Landmark numbers correspond with types and definitions as described in Table 10.

Results

Extant Species Classification

Thin-plate splines from Generalized Procrustes consensuses illustrate a marked contrast in variation between jaw morphologies (Figs. 29, 30), and that of the skull (Fig. 31). Loci of the dentary in both occlusal and lateral views tend to exhibit far less displacement among *M. erminea-M. nivalis*, and *M. erminea-M. frenata* than ventral skull characters between these taxa. Nevertheless, subtle changes are expressed within the posterior dentition and mandibular condyle of the dentary. Such changes appear relatively consistent in both lateral (Fig. 29), and occlusal (Fig. 30) views. However, slight discrepancies are exhibited between species in both profiles of the dentary (Figs. 29, 30). Conversely, ventral skull loci demonstrate far greater interspecific displacement overall. Regions including the incisive foramina, maxillary toothrow, palatine, temporomandibular joint, and auditory bulla vary significantly between *M. erminea* and *M. nivalis* (Fig. 31a). Such displacement is further exacerbated among *M. erminea* and *M. frenata* throughout several of these regions (Fig. 31b).

Stepwise discriminant analysis (SDA) using 32 variables from 16 anatomic loci of the lateral dentary conveyed 95.0% and 88.8% correctly separated original and cross-validated predicted group memberships respectively among all three *Mustela* species (Table 11, Fig. 32). Results correctly classified 20/21 *M. nivalis*, 29/31 *M. erminea*, and 27/28 *M. frenata* specimens. These data were statistically significant at $p = .000$, with a Wilks' Lamba value of .074 and .333 for the first and second functions respectively. Two functions with Eigenvalues of 3.467 and 2.006 accounted for 63.3% and 36.7% of the total variance individually within these data. This analysis selected 12 significant variables for discriminating taxa. Chosen variables in descending significance were: Y4, X5, Y13, X7, Y12, Y2, Y7, Y9, X1, X2, Y5, and X6. Additionally, one

ETVP specimen (NAUSP2048) classified as "cf. *M. frenata*" was entered as an unknown. Stepwise results subsequently classified this specimen within extant *M. frenata* (Fig. 32). The first 3 components of the principal component analysis explained 53.893% of the total variance at 28.873%, 16.864%, and 8.156% respectively. Three-dimensional scatterplots of these components illustrate marked overlap among species, though distinct group clustering is established as well (Fig. 33).

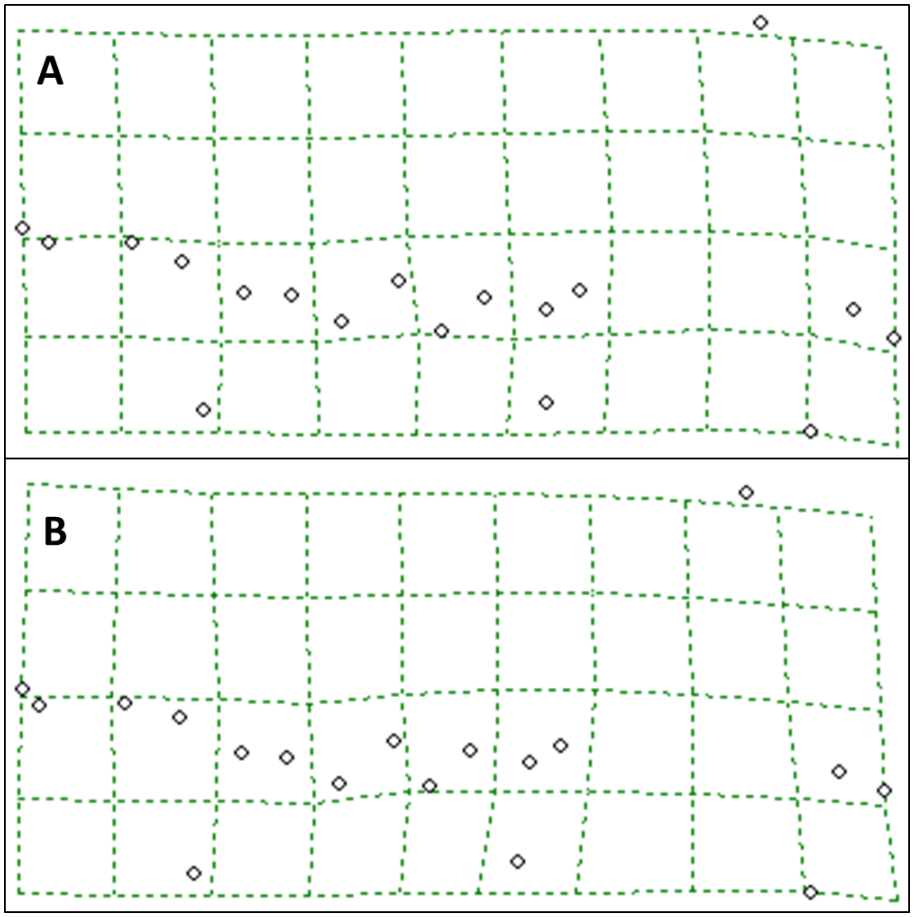

Figure 29. Thin-plate splines from superimposed consensuses of extant *Mustela erminea-M. nivalis* (A), and *M. erminea-M. frenata* (B) left dentaries in lateral view. Deformation grids illustrate the relative variation among 18 anatomic loci as defined in Table 8, and exhibited in Fig. 27.

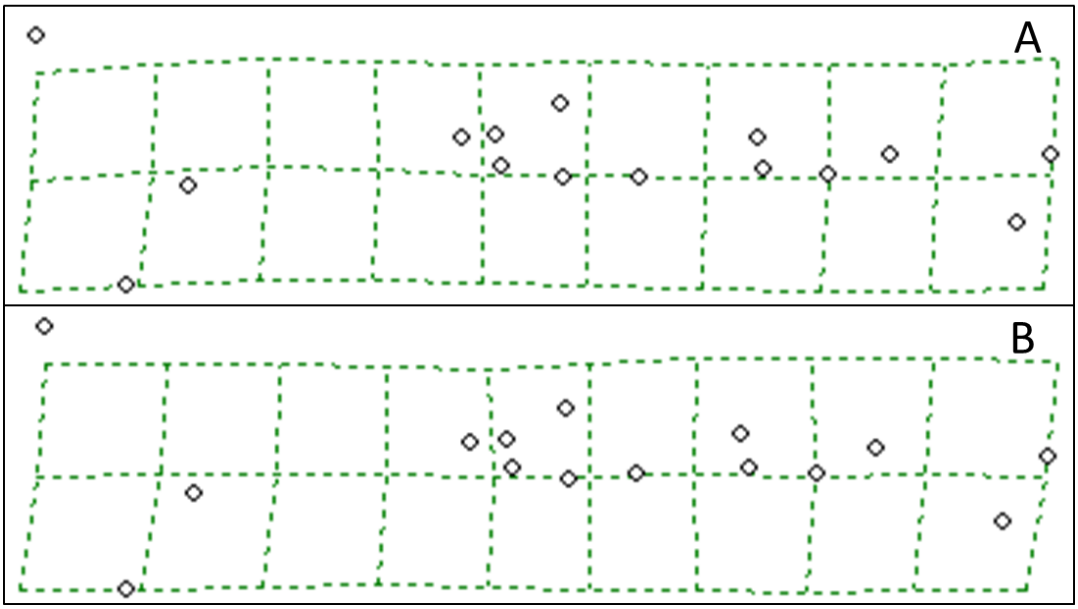

Figure 30. Thin-plate splines from superimposed consensuses of extant *Mustela erminea-M. nivalis* (A), and *M. erminea-M. frenata* (B) left dentaries in occlusal view. Deformation grids express the variation among 15 anatomic loci as defined in Table 9, and illustrated in Fig. 27.

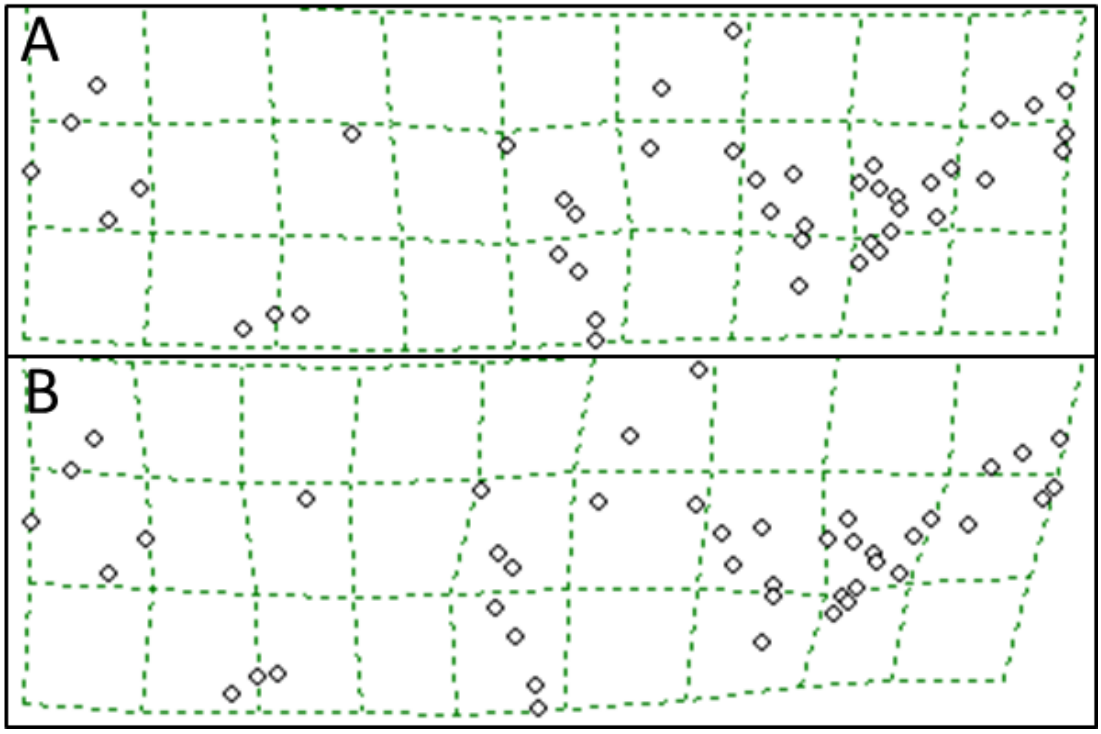

Figure 31. Thin-plate splines of extant *Mustela erminea-M. nivalis* (A), and *M. erminea-M. frenata* (B) skulls in left side ventral view. Warp grids illustrate the variation among 44 anatomic loci from the left side of the skull as defined in Table 10, and depicted in Fig. 28.

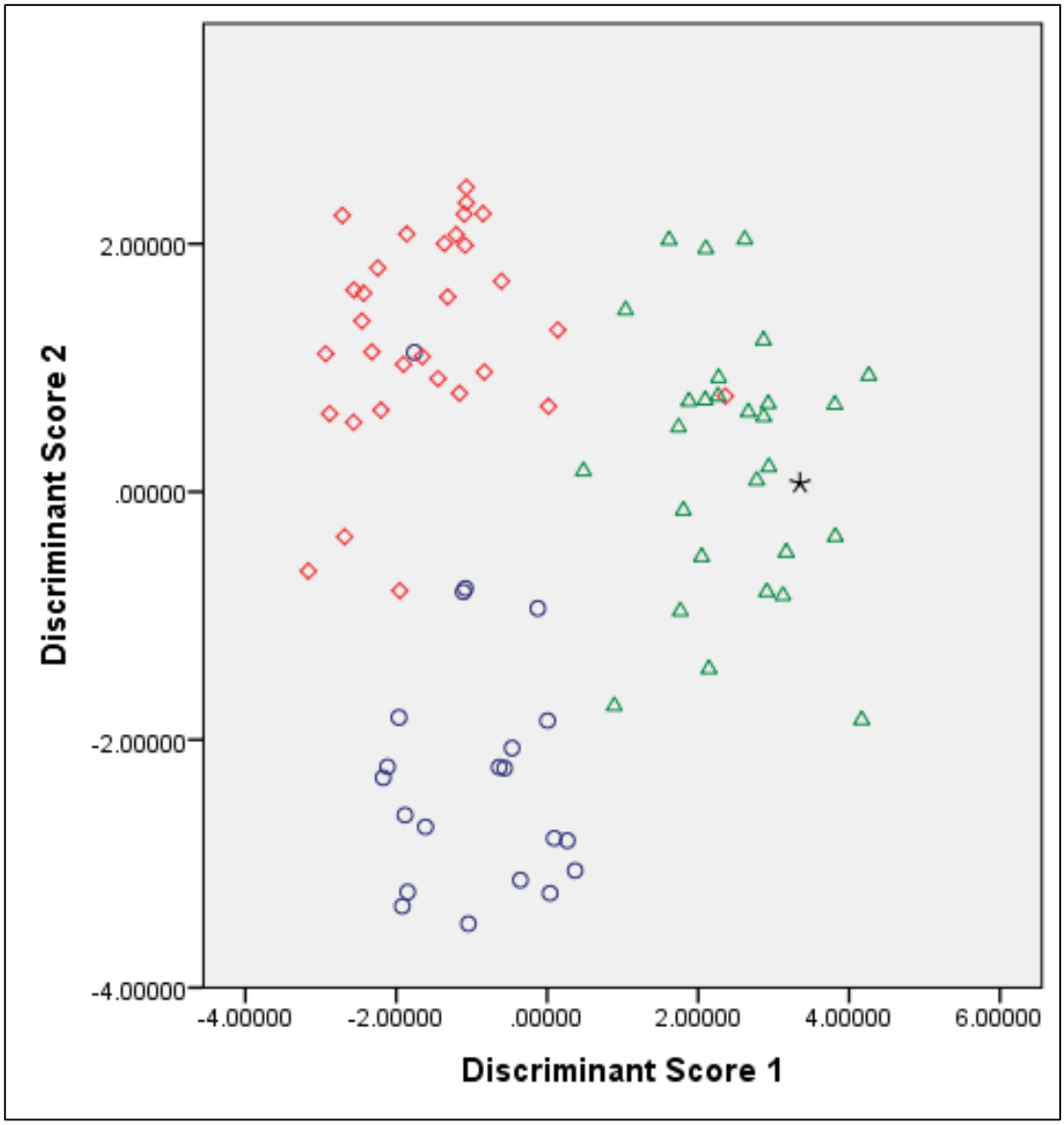

Figure 32. Stepwise discriminant scores for extant weasel dentaries in lateral profile from ETVP, MCZ, and USNM collections. Circles = *Mustela nivalis* (n=21), diamonds = *M. erminea* (n=31), and triangles = *M. frenata* (n=28). Star = an unknown extant dentary from ETVP collections.

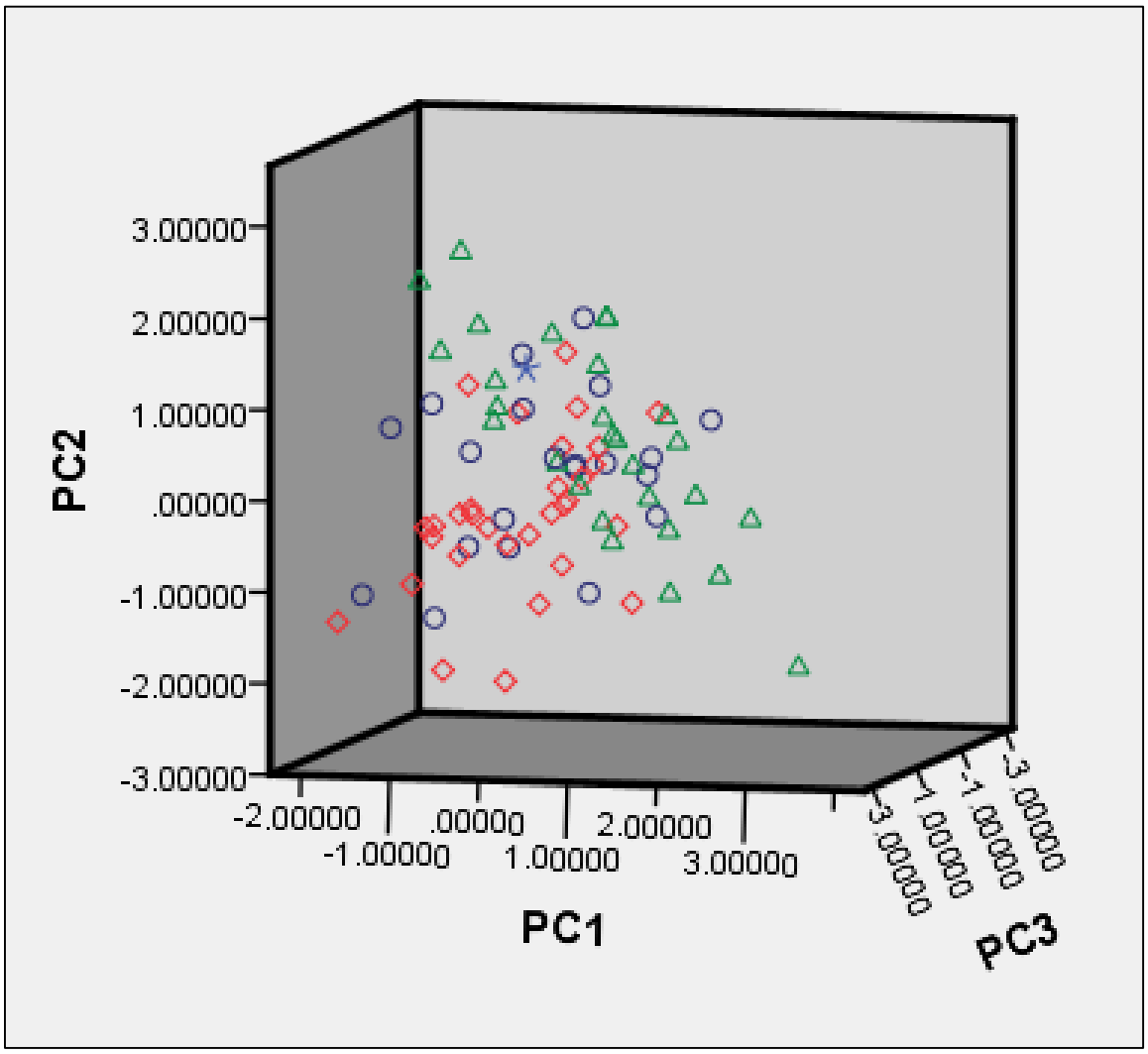

Figure 33. Three-dimensional principal component analysis illustrating the first 3 variation components of the lateral dentary for extant *Mustela nivalis* n=21 (circles), *M. erminea* n=31 (diamonds), *M. frenata* n=28 (triangles), and an unknown extant ETVP specimen (star).

Analysis of 30 variables from 15 anatomic loci of the occlusal dentary proved marginally less efficient in extant species classification. SDA correctly classified 89.2% and 86.7% of original and cross-validated group memberships respectively among weasel taxa (Fig. 34). Results correctly classified 21/24 *M. nivalis*, 26/30 *M. erminea*, and 27/29 *M. frenata* specimens. Data were statistically significant at $p = .000$, with a Wilks' Lamba value of .158 and .476 for the first and second functions respectively. Two functions with Eigenvalues of 2.015 and 1.099 accounted for 64.7% and 35.3% of the total variance among these data, however, only 4 variables were chosen for species discrimination. Selected variables in descending significance were: X4, X5, X11, and X7. Despite using nearly equivalent specimens, discriminant scores of the occlusal dentary (Fig. 34) demonstrated significantly more species overlap than scores generated from lateral variables (Fig. 32). Note that the number of extant specimens varies slightly between lateral and occlusal data. This inconsistency is due to variations in character availability based on different loci used between these profiles. PCA of the occlusal jaw explained 50.603% of the total variance at 28.406%, 13.258%, and 8.939% respectively in the first 3 components. Three-dimensional scatterplots of these components exhibit marked overlap among taxa similar to the lateral dentary PCA, though, groups still appear relatively unified by clusters (Fig. 35).

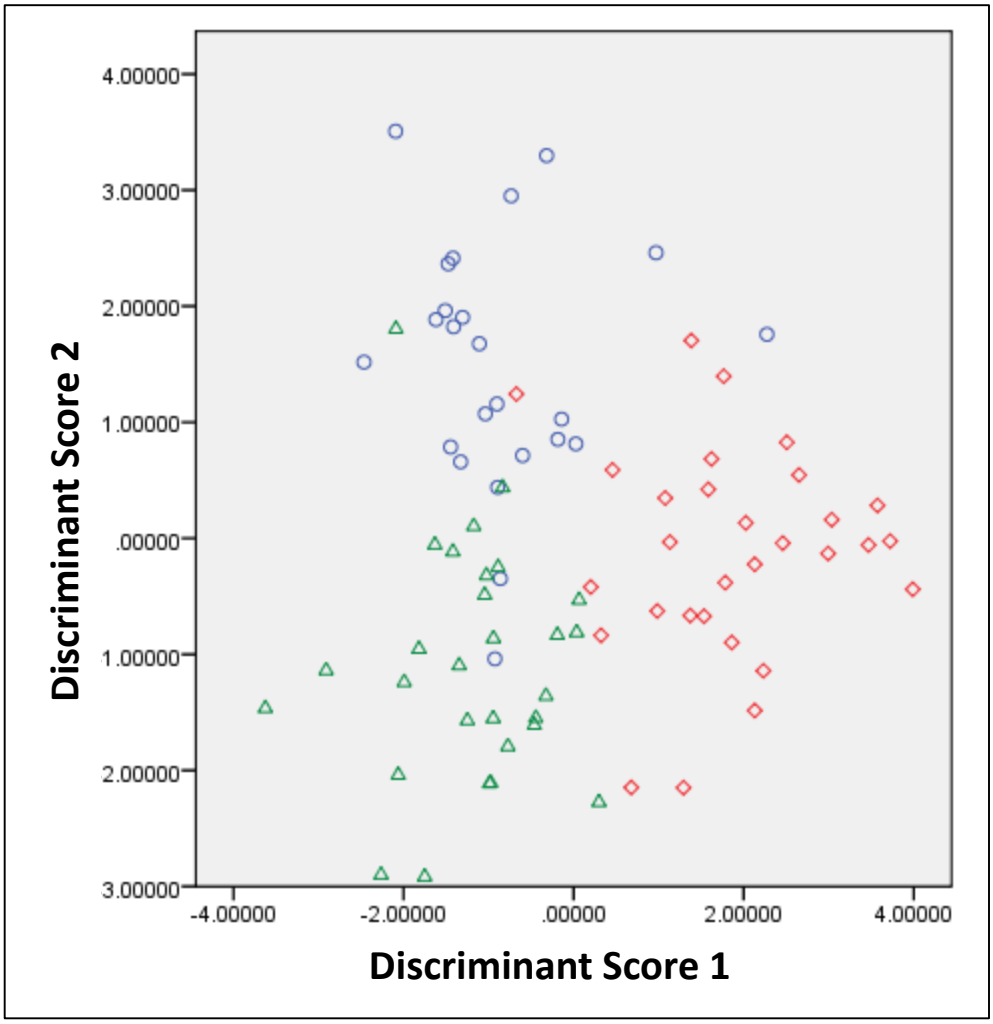

Figure 34. Stepwise discriminant scores for extant *Mustela nivalis* (circles) n=24, *M. erminea* (diamonds) n=30, and *M. frenata* (triangles) n=29 dentaries in occlusal profile from ETVP, MCZ, and USNM collections.

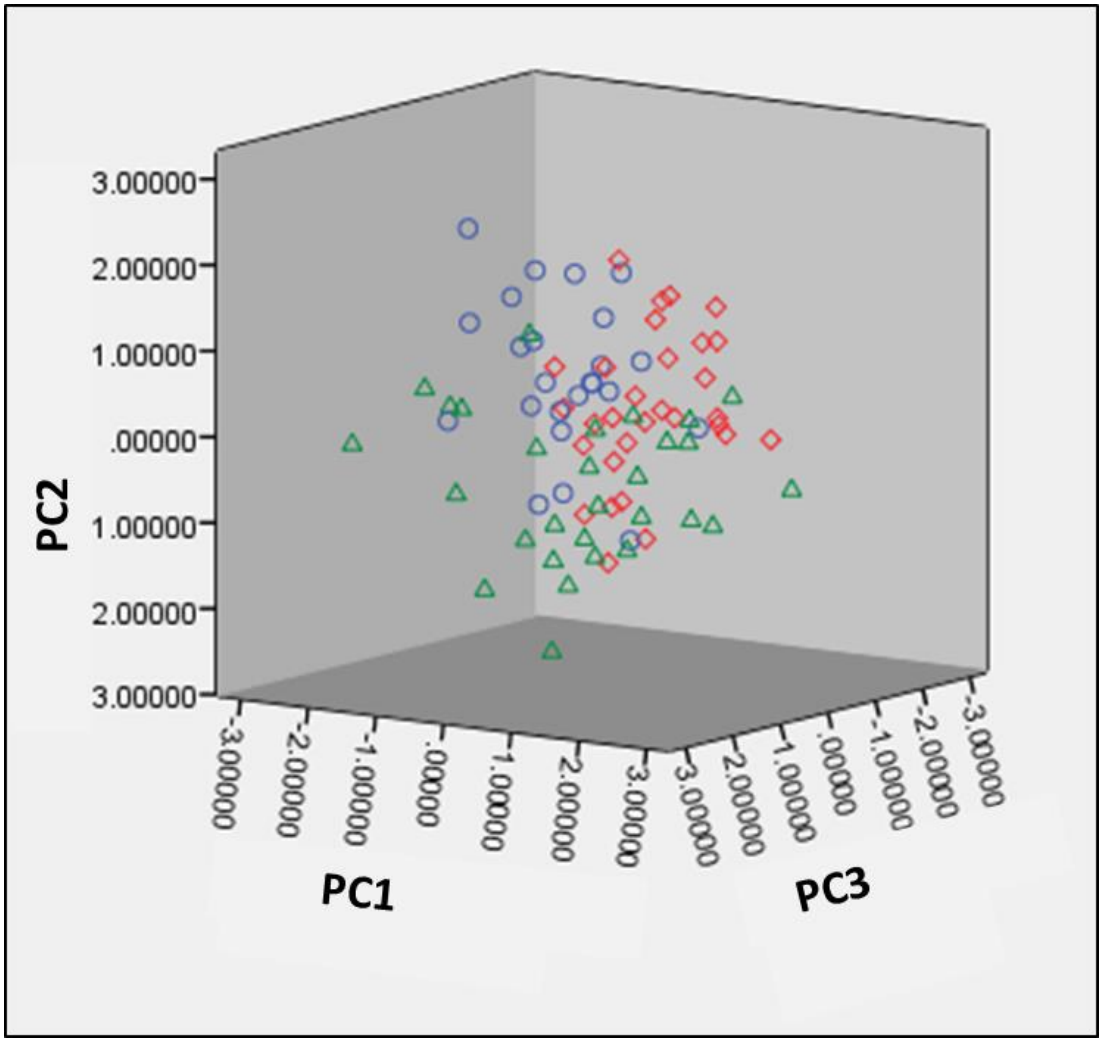

Figure 35. First three principal components for the occlusal jaw of extant *Mustela nivalis* (circles) n=24, *M. erminea* (diamonds) n=30, and *M. frenata* (triangles) n=29.

Stepwise discriminant analysis of 88 variables from 44 anatomic loci of the skull in ventral view demonstrated markedly superior group classification relative to those of the dentary. Results correctly predicted 100% of group memberships for both original and cross-validated specimens (Table 12). Additionally, discriminant scores of the skull illustrated more distinct group partitioning than dentaries in either occlusal or lateral profile (Fig. 36). These data were statistically significant at $p = .000$, with a Wilks' Lamba value of .013 for the first function and .165 in the second. Two Eigenvalues of 11.290 and 5.065 accounted for 69.0% and 31.0% of the total variance respectively. Eleven variables were selected by SDA for discriminating these groups. Variables in descending significance were: X26, X41, X6, X3, X42, X30, Y19, X23, Y6, X2, and Y31. A PCA of the ventral skull data explained 49.017% of the total variance in data at 31.859%, 9.736%, and 7.422% for the first, second, and third components respectively. Three-dimensional scatterplots of these components illustrated more distinct separation between species than PCAs from either view of the dentary (Fig. 37). Furthermore, group clusters of *M. erminea* and *M. frenata* exhibited more variation relative to *M. nivalis* despite the inclusion of all 3 North American subspecies of the latter taxon (Fig. 37).

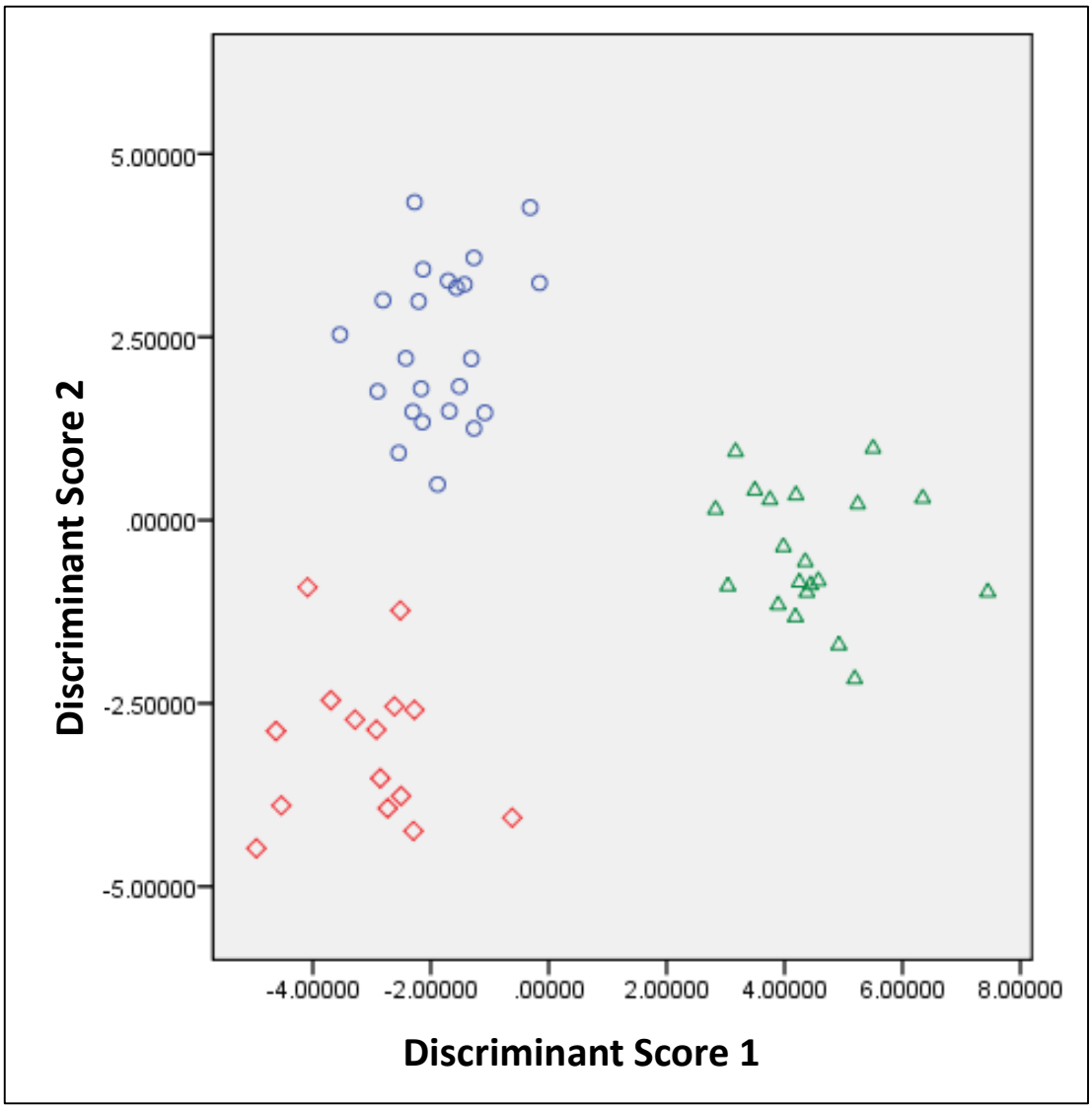

Figure 36. Stepwise discriminant scores of ventral skulls for extant *Mustela nivalis* (circles) n=23, *M. erminea* (diamonds) n=15, and *M. frenata* (triangles) n=20 from MCZ, and USNM collections.

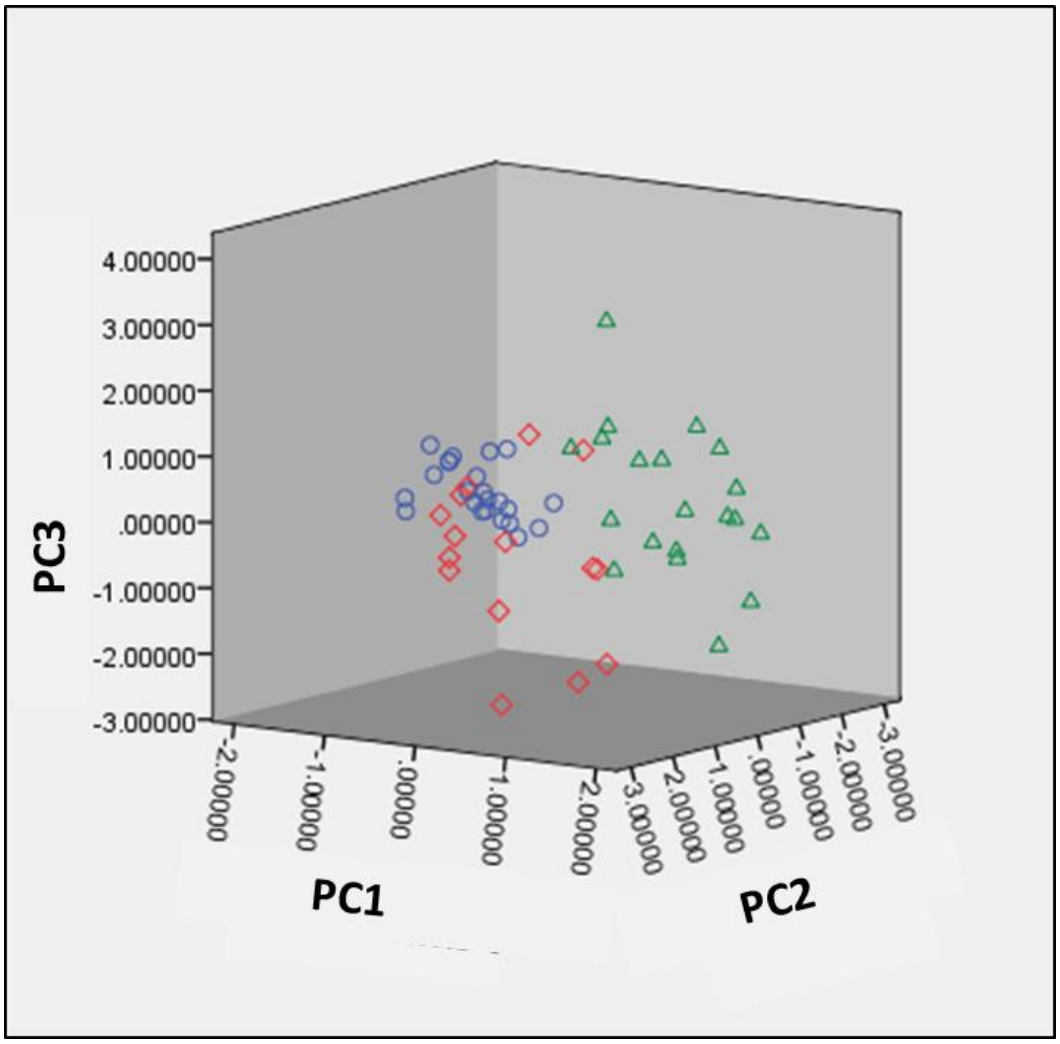

Figure 37. Three-dimensional scatterplot illustrating the first 3 principal component scores for the ventral skull of extant *Mustela nivalis* (circles) n=23, *M. erminea* (diamonds) n=15, *M. frenata* (triangles) n=20 from MCZ, and USNM collections.

.

SCBC Classification

Of the 90 Snake Creek Burial Cave (SCBC) *Mustela* spp. dentaries stored in ETVP collections, 79 are within or near the size and phenotypic range of extant weasels. An effort was made to classify as many specimens as possible using 16 landmarks of the lateral dentary as previously demonstrated. Loci from this orientation of the dentary were selected over the occlusal view due to their marginally greater classification efficiency and group segregation. Eleven of the 90 dentaries (NAUQSP8711/115 - NAUQSP8711/125) were reserved for separate analysis (see CHAPTER 3) because they exceed the size range of extant male *M. frenata* and demonstrate morphologies atypical of the subgenus *Mustela* (i.e., comparatively more robust jaws, markedly diminutive m_2 or m_2 alveoli (Anderson et al. 1986), and more numerous, yet often smaller mental foramina). In addition to these dentaries, 14 skull and maxillary specimens exhibiting weasel-like morphology and size were reevaluated using the 44 ventral skull loci previously analyzed. Fossil data acquisition follow the same methodologies used for extant specimens.

A total of 51 complete and nearly complete SCBC fossil dentaries retaining all 16 lateral loci were included within SDA using extant specimens as group proxies. Of these fossils, 8, 3, and 40 were classified as *M. nivalis* (n=8), *M. erminea* (n=3), and *M. frenata* (n=40) respectively (Table 11, Fig. 38). Specimens were included within the lateral dentary PCA as well to determine their unbiased multivariate orientation. Results advocate that SCBC specimens indeed share close affinity to extant weasels (Fig. 39). Within the first 2; and first 3 PCA components respectively, the vast majority of SCBC members appear to plot parallel (Fig. 39a) or intersect (Fig. 39b) along the morphospace of extant *M. frenata*. Furthermore, a minority of SCBC specimens seem to overlap with extant *M. nivalis*, and possibly *M. erminea* as well. PCA is,

therefore, in general agreement with the classification statistics generated by SDA (Table 11, Figs. 38, 39).

Table 11. Original and cross-validated predicted group membership (PGM) statistics for extant *Mustela nivalis* (1), *M. erminea* (2), and *M. frenata* (3) using 16 landmarks of the lateral dentary.

			PGM			
Results (a, b)		Species	*M. nivalis*	*M. erminea*	*M. frenata*	Total
Original	#	1	20	1	0	21
		2	1	29	1	31
		3	1	0	27	28
		Ungrouped cases	8	3	40	51
	%	1	95.2%	4.8%	0	100%
		2	3.2%	93.5%	3.2%	100%
		3	3.6%	0	96.4%	100%
		Ungrouped cases	15.7%	5.9%	78.4%	100%
Cross-validated	#	1	19	2	0	21
		2	2	27	2	31
		3	1	2	25	28
	%	1	90.5%	9.5%	0%	100%
		2	6.5%	87.1%	6.5%	100%
		3	3.6%	7.1%	89.3%	100%

a.95.0% of original grouped cases correctly classified

b.88.8% of cross-validated grouped cases correctly classified

These data include predicted group memberships of 51 well-preserved Snake Creek Burial Cave dentaries entered as ungrouped cases.

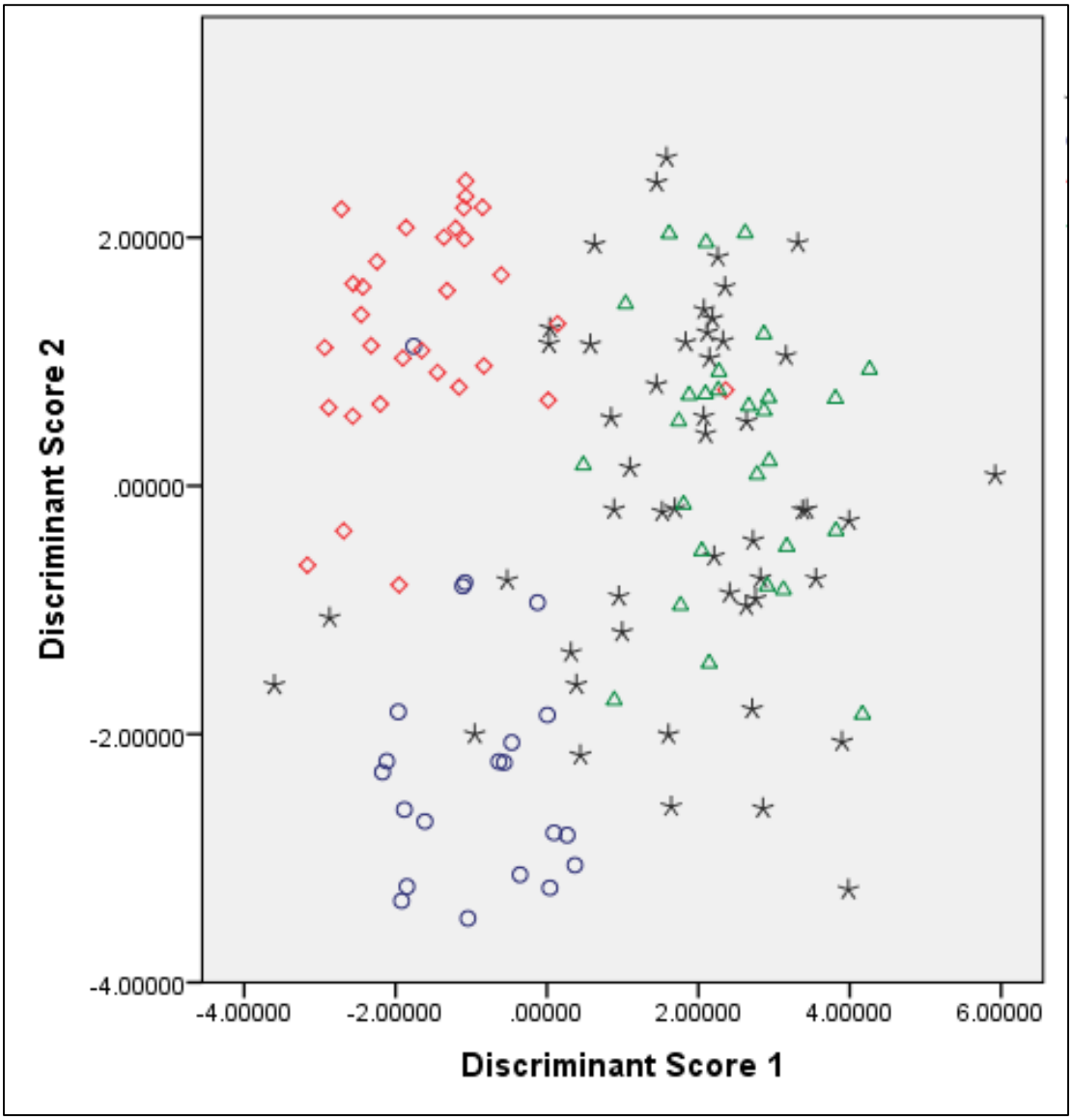

Figure 38. Stepwise discriminant scores of the lateral dentaries from extant *Mustela nivalis* (circles) n=21, *M. erminea* (diamonds) n=31, *M. frenata* (triangles) n=28, and Snake Creek Burial Cave (SCBC) specimens (stars) n=51 from ETVP, MCZ, and USNM collections.

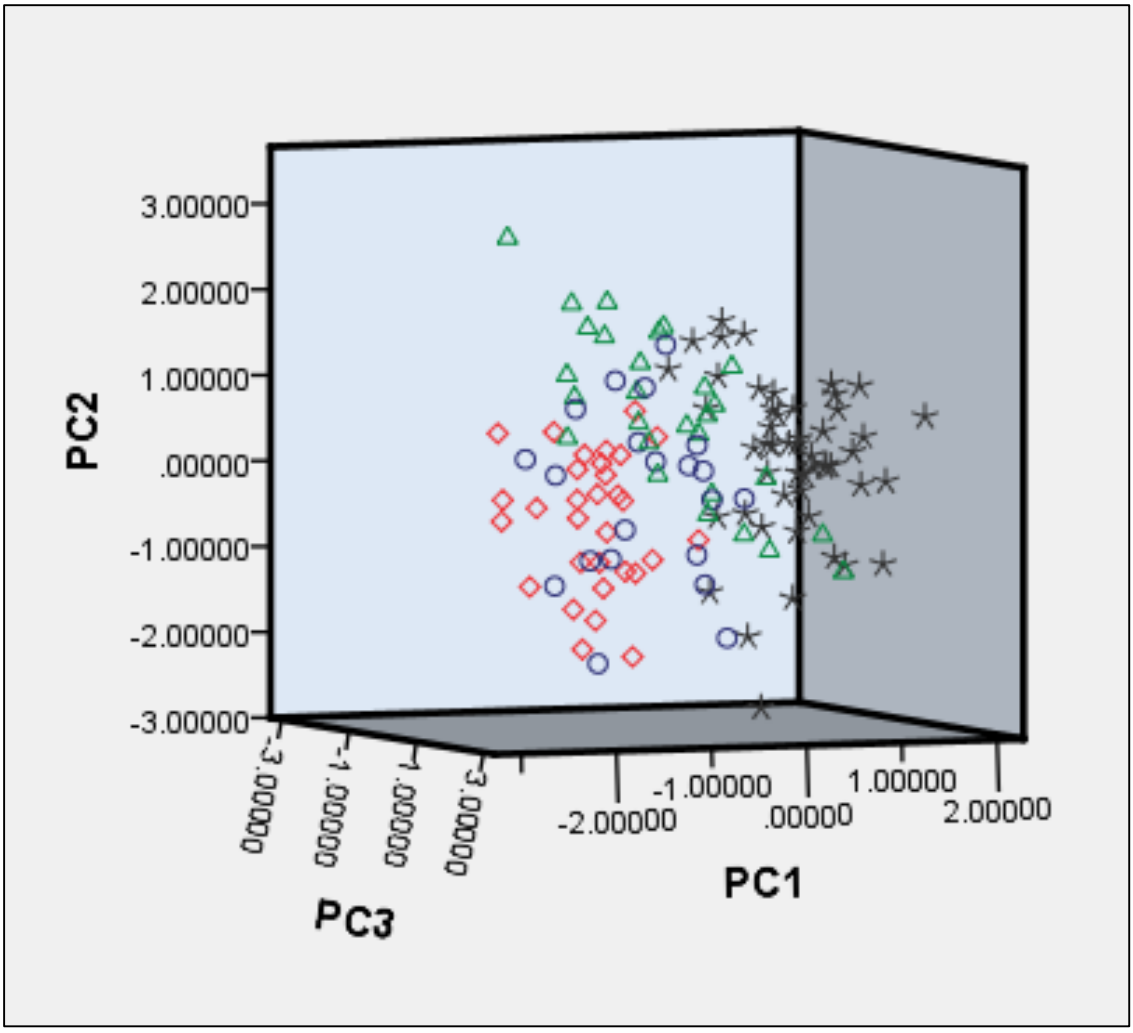

Figure 39. Scatterplot of the first three principal components from the lateral dentaries of extant *Mustela nivalis* (circles) n=21, *M. erminea* (diamonds) n=31, *M. frenata* (triangles) n=28, and SCBC specimens (stars) n=51.

Classifying SCBC cranial materials proved challenging due to markedly differential preservation among specimens. Conditions of these materials range from nearly complete, to maxillary and palatal fragments (Table 13, Appendix B). In order to compensate for such variation, discrete analyses were conducted based on the relative condition of each specimen. All 44 landmarks that achieved 100% correctly predicted group memberships in extant taxa were included for the analysis of a nearly complete fossil skull NAUQSP197 (Tables 12, 13). However, these loci were subsequently reduced relative to the degradation of each additional SCBC specimen. While some morphometric programs can interpolate missing landmarks with group averages, this method was avoided due to the inherent bias of a discriminant function given that such analyses sort unknown members into pre-designated groups of best fit despite how insufficient these data may be. Nevertheless, running a case-by-case analysis for extant and fossil specimens at differential levels of landmark reduction would generate separate statistics for each dataset, thus providing more detailed information for the classification reliability of each unknown specimen relative to the landmarks used. Consequently, the latter method was selected for this analysis, and, much like the SDA outcome of fossil dentaries, these findings suggest that *M. frenata* was the dominant weasel taxon among the SCBC paleofauna (Table 13). However, it is worth mentioning that significant discrepancies were present among specimens evaluated with the parietal region intact and those that did not retain a braincase (Table 13, Figs. 40, 41).

Table 12. Original and cross-validated group membership (PGM) statistics of extant *Mustela nivalis* (1), *M. erminea* (2), and *M. frenata* (3) using 44 landmarks of the ventral skull.

			PGM			
Results (a, b)		Species	*M. nivalis*	*M. erminea*	*M. frenata*	Total
Original	#	1	23	0	0	23
		2	0	15	0	15
		3	0	0	20	20
		Ungrouped cases	0	0	1	1
	%	1	100%	0	0	100%
		2	0	100%	0	100%
		3	0	0	100%	100%
		Ungrouped cases	0	0	100%	100%
Cross-validated	#	1	23	0	0	23
		2	0	15	0	15
		3	0	0	20	20
	%	1	100%	0	0	100%
		2	0	100%	0	100%
		3	0	0	100%	100%

a.100% of original grouped cases correctly classified.

b.100% of cross-validated grouped cases correctly classified.

These data also include classification results of the most complete Snake Creek Burial Cave cranial specimen (NAUQSP197) retaining all 44 loci of the skull, and entered as an ungrouped case.

Table 13. Predicted group memberships (PGMs) using stepwise discriminant analysis for 14 Snake Creek Burial Cave cranial specimens as individually classified based on the maximum number of ventral skull landmarks (LM) available.

Specimen #	General Description	Current ID	# of LM Analyzed	Extant Class. Accuracy-Xval	PGM
NAUQSP195	Near complete skull	*M. frenata*	35/44	100% - 94.8%	*M. frenata*
NAUQSP197	Complete Skull	*M. frenata*	44/44	100% - 100%	*M. frenata*
NAUQSP198	Partial skull	*M. frenata*	35/44	100% - 94.8%	*M. frenata*
NAUQSP201	Partial skull	*Mustela* sp.	19/44	100% - 98.3%	*M. frenata*
NAUQSP204	Partial skull	*Mustela* sp.	11/44	91.4% - 89.7%	*M. frenata*
NAUQSP206	Complete premaxilla, maxilla, palatine	*M. nivalis*	25/44	100% - 100%	*M. erminea**
NAUQSP207	Right premaxilla, maxilla, anterior zygoma	*M. frenata*	21/44	100% - 93.1%	*M. nivalis**
NAUQSP208	Right maxilla and palate	*M. erminea*	08/44	81.0% - 77.6%	*M. erminea**
NAUQSP209	Right maxilla, anterior zygoma	*M. frenata*	08/44	81.0% - 77.6%	*M. erminea**
NAUQSP210	Right maxilla, palate	*M. frenata*	5/44	N/A	Data insuff.
NAUQSP211	Left maxilla	*M. frenata*	13/44	86.4% - 81.4%	*M. frenata**
NAUQSP212	Right maxilla, palate	*M. frenata*	10/44	84.7% - 83.1%	*M. nivalis**
NAUQSP213	Right maxilla, palate	*M. frenata*	09/44	76.3% - 74.6%	*M. frenata**
NAUQSP216	Partial skull	*Mustela* sp.	11/44	91.4% - 89.7%	*M. frenata*

* Indicate specimens unsupported by an intact braincase. Case-by-case percentages of correctly classified extant species over correct cross-validations (Xval) are portrayed as well.

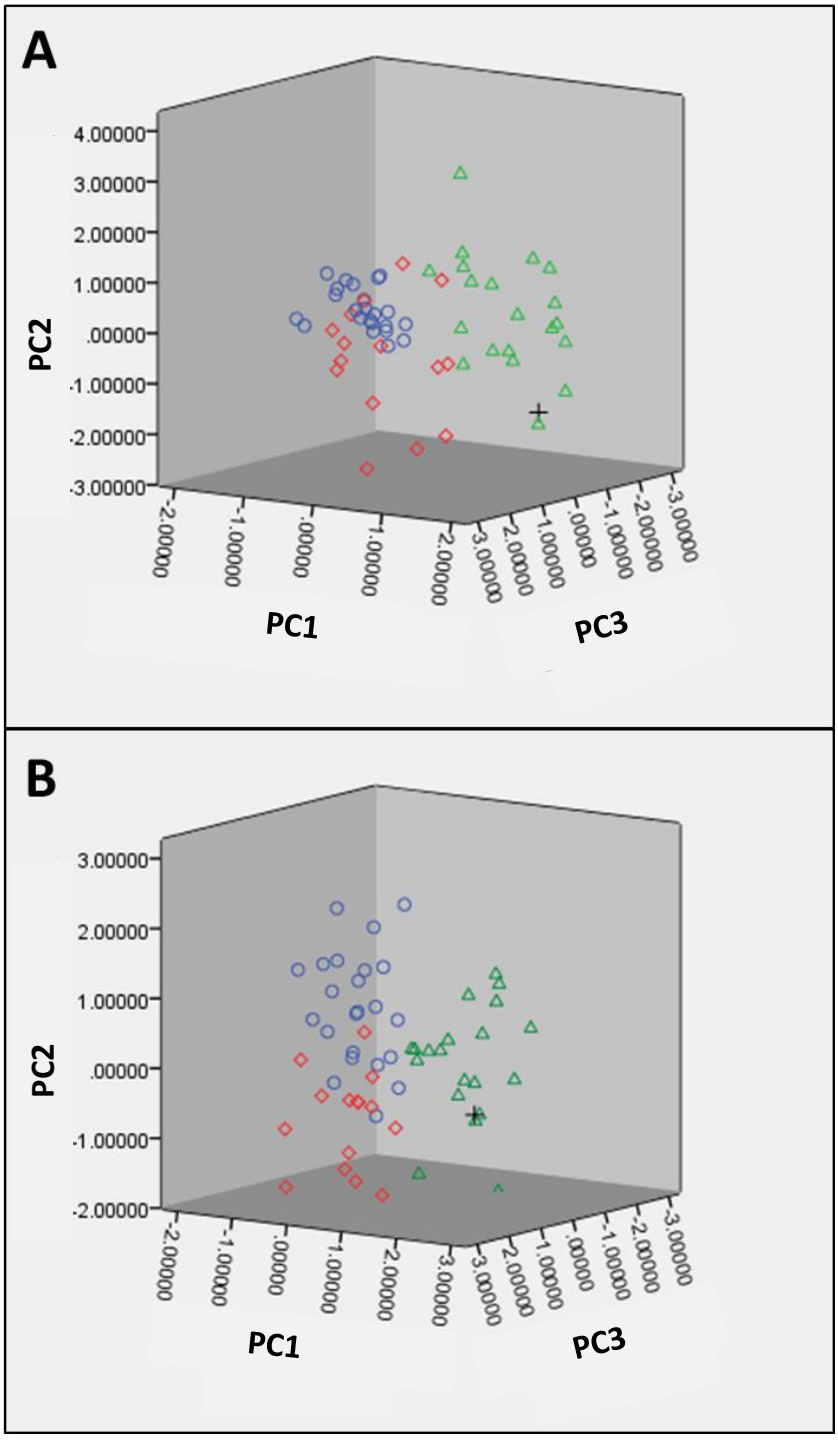

Figure 40. Three-dimensional scatterplots illustrating the first 3 principal component scores in the ventral skull of extant *Mustela nivalis* (circles), *M. erminea* (diamonds), *M. frenata* (triangles) as well as fossil specimens (crosses) from individual analyses of NAUQSP8711/197b using 44/44 landmarks (A), and NAUQSP8711/201b using 19/44 landmarks (B), according to their respective conditions. Despite marked variations in preservation, both specimens retain an intact braincase (Appendix B), and cluster within extant populations.

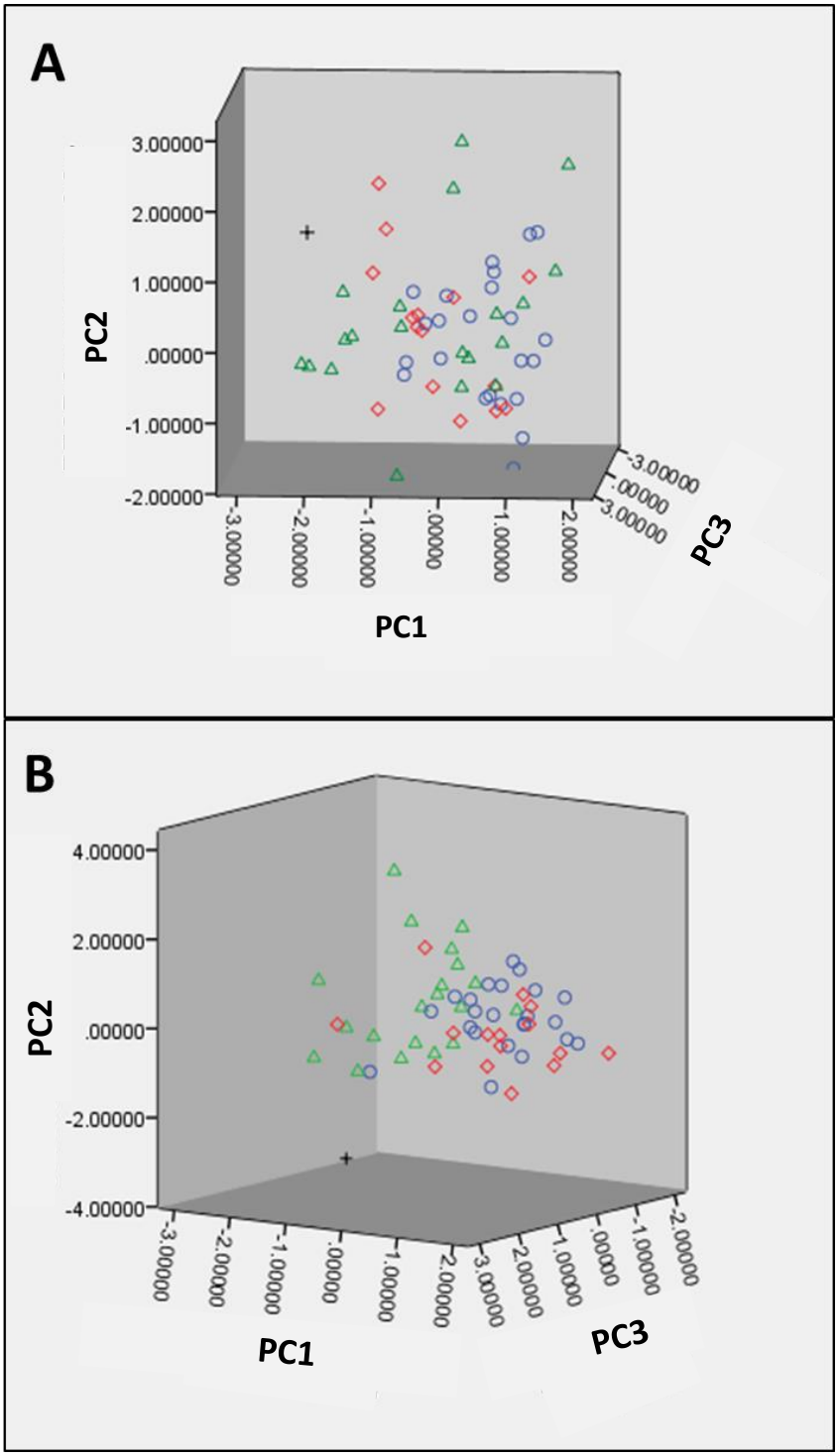

Figure 41. Three-dimensional scatterplots illustrating the first 3 principal components for the ventral skulls of extant *Mustela nivalis* (circles), *M. erminea* (diamonds), *M. frenata* (triangles), as well as fossils (crosses) of NAUQSP8711/206b using 25/44 landmarks (A), and NAUQSP8711/207b using 21/44 landmarks (B). Both specimens represent maxillary and palatal fragments unsupported by a braincase in ventral position (Appendix B), and exhibit marked displacement from extant groups.

Discussion

Taxonomic Implications

Landmark analyses of the cranium and dentary have proven useful in classifying extant New World weasel materials of *Mustela erminea*, *M. frenata*, and *M. nivalis*. Although sexual dimorphism and regional plasticity are prominent among these taxa, specimens were evaluated irrespectively of sex, subspecies, or province, notwithstanding a confine to North America. Such modifications were facilitated to compile species-explicit data that can be applied to the classification of isolated craniomandibular elements. Results found interspecific skulls significantly more variable than dentaries as demonstrated by morphologic overlap and occasional misclassification of the latter in PCA and SDA respectfully. Landmark displacement between taxa, as illustrated in TPS deformation grids, complement these inferences (Figs. 29-31).

Several morphologic trends conveyed throughout these landmark datasets should be addressed as well. For example, Ralls and Harvey (1985) mention that North American subspecies of *M. nivalis* tend to exhibit less size variation relative to *M. erminea* and *M. frenata*. Linear measurements acquired herein support their observations (Table 7). Interestingly, a similar pattern was exhibited within the PCA of extant weasel skulls (Fig. 37). Results depict subspecies of *M. nivalis* clustering more densely than *M. erminea* and *M. frenata* that exhibit markedly greater orthogonal dispersal. Consequently, these data may infer that *M. nivalis* is more conservative in both size and cranial morphology relative to other weasels. Furthermore, TPS of the skull and dentary illustrated more deformation overall in *M. frenata* warped against *M. erminea*, than in *M. nivalis* (Figs. 29-31). These results imply that *M. frenata* express greater morphologic deviation from *M. erminea* and *M. nivalis*. Such data may be expected, however,

given the exclusively New World distribution of the long-tailed weasel, versus the inferred Old World origins of least-weasels and stoats (Kurtén 1968; Sheffield and Thomas 1997).

In addition to these general trends, discreet variation was established through each of the three craniomandibular profiles evaluated. Landmarks plotted on the lateral plane of the dentary proved more efficient for species classification than occlusal characters in achieving 95.0% versus 89.2 % predicted group memberships in the former and latter orientation respectively (Table 11, Figs. 32, 34). Furthermore, SDA of characters in lateral view generated more significant variables for species discrimination than in occlusal view. Twelve variables representing 5 morphologic features were selected for classification of the lateral dentary as listed in Table 8, including: c_1 (X1), p_3 (X2, Y2), p_4 (Y4, X5, Y5), m_1 (X6, X7, Y7), and the mandibular condyle (Y12, Y13). Conversely, only 4 variables from 3 characters were selected for classification of the dentary in occlusal view that, as defined in Table 9, included: p_4 (X4), m_1 (X5, X7), and the inner mandibular condyle (X11). Even with preemptive efforts, subtle changes in the resting orientation of weasel dentaries could have displaced 2-dimensional coordinates enough to facilitate species misclassifications as a result of their markedly similar morphologies (Figs. 29, 30). Such occurrences may have been especially problematic for standardizing resting orientations between fused mandibles and isolated dentaries. Caution is therefore advised against integrating both fused and unfused jaw elements in future two-dimensional landmark analyses. Nevertheless, landmarks plotted throughout 44 loci of the ventral cranium achieved 100% correctly predicted group memberships, and strong separation among taxa (Table 12, Figs. 36, 37). Eleven significant variables representing 8 skull characters were selected as viewed in Table 10, including: foramen magnum (X30), auditory bulla (X23, X26), pterygoid hamulus (X31), palatine (X41), glenoid fossa (Y19), P^3 (X6,Y6), infraorbital foramen (X42), and incisive

foramen (X2, X3). Although ventral characters were sufficient for the intent of this study, accumulating supplementary data from dorsal and lateral views of the skull may illuminate additional characters for species discrimination in future works.

Despite 100% accurate separation of weasel crania, classification of fossil skulls proved significantly more problematic. Though individual analyses were modified according to the preservation of each specimen, marked discrepancies appeared between partial skulls and maxillary elements. The latter specimens often plotted in isolation of extant groups, while the former generally grouped within extant clusters (Figs. 40, 41). Surprisingly, extant species classification maintained relatively accurate predicted group memberships despite substantial reductions to landmarks correlated with fossil fragments (Table 13). One could argue that landmark degradation may have been a critical factor in the ambiguous data generated from several fossil specimens (Table 13, Fig. 41). However, these influences appear less relevant due to extant group clustering of several partial SCBC skulls that exhibited relatively poor preservation, and thus, significant landmark reduction (Table 13, Fig. 40). In light of this trend, it seems reasonable to assume that differential orientation among specimens may have been a fundamental influence in grouping discrepancies. Although efforts were made for each fragmentary specimen to mimic the horizontal orientation of a complete skull in ventral view, corresponding vertical orientations could not be so easily replicated without support from the underlying basicranium. Moreover, while postorbital constrictions were used as a standard focal point in extant skulls, estimated alignments of fossils lacking this central locus may have resulted in horizontal dislocation as well. Thus, linear GM, or 3-dimensional GM, may be preferable over 2-dimensional analyses for other studies that intend to evaluate specimens of markedly differential conditions.

Ecomorphological and Functional Inferences

Landmark displacement exhibited by TPS correlated strongly with variables chosen by stepwise discriminant analyses. From loci of the lateral dentary; the posterior p_4 boundary, intersection of the lower carnassial blades, m_1 occlusal ridge, and relative positioning of the mandibular condyle all illustrated significant displacement among *M. erminea-M. nivalis* (Fig. 29a) and *M. erminea-M. frenata* (Fig. 29b). These features are associated with variables from landmarks 5, 6, 7, and 13 of which one or both Cartesian coordinates were deemed significant in species classification as mentioned above (Fig. 27). In lateral orientation, the posterior c_1 alveolus (Table 8, LM 1) demonstrates more posterior displacement in *M. frenata* over *M. erminea* while the posterior margin of the p_4 occlusal surface (Table 8, LM 5) appears more posteriorly extended in *M. nivalis* and *M. frenata* relative to *M. erminea* (Fig. 29a, b). Moreover, the superior boundary of the carnassial notch (Table 8, LM 6) is more dorsally displaced in lateral view among *M. nivalis* and *M. frenata* over *M. erminea*, while the m_1 occlusal ridge (Table 8, LM 7) is more posteriorly oriented in each of these taxa relative to *M. erminea* (Fig. 29a, b). The lateral side apex of the mandibular condyle (Table 8, LM 13) also appears more ventrally and anteriorly displaced in *M. nivalis* (Fig. 29a) and *M. frenata* (Fig. 29b) respectively in comparison to *M. erminea*, while the apex of the angular process (Table 8, LM 14) exhibits more anterodorsal (Fig. 29a), and posterodorsal orientation in *M. nivalis* and *M. frenata* individually (Fig. 29b). Lastly, the anterior curvature of the massetric fossa (Table 8, LM 15) appears more anterodorsally positioned in *M. frenata*, and to a more subtle degree in *M. nivalis*, relative to *M. erminea* (Fig. 29a, b). However, this landmark was not significant in SDA, perhaps due to excessive intraspecific variability.

In occlusal view of the dentary, interspecific landmark displacement can be observed among the p_4, m_1, and mandibular condyle (Fig. 30a, b) as conveyed in species discrimination though corresponding variables of landmarks 4, 5, 7, and 11 (Fig. 27). From this orientation, the medial curvature (Table 9, LM 3) and posterior margin of the p_4 occlusal surface (Table 9, LM 4) is anteriorly and posteriorly displaced respectively in *M. frenata* (Fig. 30b), and to a lesser extent in *M. nivalis*, over *M. erminea* (Fig. 30a). This may suggest that a comparatively larger p_4 is present in the former 2 taxa. Moreover, the m_1 occlusal ridge (Table 9, LM 5) exhibits more posterior orientation in *M. frenata* relative to *M. erminea*, while the breadth of the m_1 talonid (Table 9, LMs 6, 7) appears comparatively wider in *M. frenata*, and narrower in *M. nivalis*, relative to *M. erminea* as demonstrated by labial and lingual displacement of the lateral talonid margin (Table 9, LM 7) in *M. frenata* (Fig. 30b) and *M. nivalis* (Fig. 30a) respectively. Lastly, the medial apex of the mandibular condyle (Table 9, LM 11) exhibits more posterior orientation in both *M. frenata* and *M. nivalis* relative to *M. erminea* (Fig. 30a, b).

Landmark displacement was amplified in several regions of the skull including: incisive foramen, infraorbital foramen, maxillary toothrow (particularly the upper carnassial), palatine, apex of the pterygoid hamulus, as well as morphologies of the glenoid fossa, auditory bulla, and foramen magnum (Fig. 31a, b). Again, these characters interpolate nicely with the 11 selected stepwise variables as mentioned previously. At least one variable from each of these loci was determined significant in SDA. The incisive foramen (Table 10, LMs 2, 3) of *M. nivalis* (Fig. 31a), and *M. frenata* (Fig. 31b) are comparatively smaller relative to *M. erminea* as demonstrated in TPS. Positioning of the posterior C^1 alveolus (Table 10, LM 4) also appears more anteriorly displaced in *M. frenata* relative to *M. erminea*, yet not in *M. nivalis* (Fig. 31a, b). Much like the lower jaw, however, variables of this landmark were not significant in SDA. Additionally, 4 loci

surrounding the infraorbital foramen (Table 10, LMs 8, 9, 42, and 43) are markedly compressed in *M. nivalis* (Fig. 31a), this expression is further amplified within *M. frenata* (Fig. 31b). Data herein accordingly support interpretations of *M. erminea* and *M. nivalis* in the Old World such that the infraorbital foramen in stoats is comparatively rounded and larger relative to (least) weasels (Heptner et al. 2002). These observations appear to correspond with North American taxa as well, and, more explicitly between stoats and long-tailed weasels.

Positioning of the rostral-zygomatic curvature (Table 10, LM 35) was greatly displaced posteroventrally in *M. frenata*, thus advocating the presence of an overall more elongate rostrum over *M. erminea* or *M. nivalis* as observed by Kurtén and Anderson (1980). However, this landmark was not deemed significant by SDA among all 3 species, likely because its displacement is not significantly expressed in *M. nivalis* (Fig. 31a). A similar phenomenon is demonstrated in the adjacent landmark (Table 10, LM36) representing the anterior curvature of the zygomatic arch (Fig. 31a, b). Many loci of the posterior cheek-teeth (Table 10, LMs 6, 7 and 10-18) exhibit an overall anterodorsal shift in *M. nivalis* and *M. frenata* relative to *M. erminea* (Fig. 31a, b). Although, individual displacements are somewhat difficult to interpret due to the high density in landmarks of this region. Loci encompassing the glenoid fossa (Table 10, LMs 19-22, and 44) are proportionally compacted both anteroposteriorly and dorsoventrally, as well as anteriorly shifted in *M. nivalis* relative to *M. erminea*. Conversely, this region is comparatively more elongate, wider, posteriorly displaced medially, and anteriorly displaced laterally in *M. frenata* (Fig. 31b). These findings appear to complement the slight anterior displacement of the lateral side mandibular condyle in *M. frenata* (Fig. 29b) and its posterior displacement from the medial side (Fig. 30b). Moreover, lateral curvature of the palatal regions (Table 10, LMs 39, 40, 41) exhibit anteroposterior expansion and posterior displacement in *M.*

nivalis relative to *M. erminea* (Fig. 31a). These features are also anteroposteriorly extended, yet anteriorly shifted in *M. frenata*, with marked anterior shifting of the posterior palatal curvature (Table 10, LM 32) in the latter taxon as well (Fig. 31b).

With regard to the postglenoid region of the skull, the apex of the pterygoid hamulus (Table 10, LM 31) exhibits a slight posteroventral displacement in *M. nivalis* (Fig. 31a), and a marked anterior shift in *M. frenata* relative to *M. erminea* (Fig. 31b). Additionally, the posterior curvature of the auditory meatus (Table 10, LM 23) and relative position of the mastoid (Table 10, LM 38) appear more posterodorsally oriented, and anteroposteriorly expanded in *M. nivalis* (Fig. 31a). Likewise, these features exhibit anteroposterior expansion, yet anterodorsal orientation in *M. frenata* compared to *M. erminea* (Fig. 31b). Furthermore, positioning of the medial auditory foramen (Table 10, LM 27) is posteriorly displaced in *M. nivalis* (Fig. 31a) and anteriorly oriented in *M. frenata* (Fig. 31b); however, an inverse orientation is exhibited in the posteromedial curvature of the auditory bulla (Table 10, LM 26) between these taxa relative to *M. erminea* (Fig. 31a, b). Lastly, the relative positioning of the inferior curvature of the foramen magnum (Table 10, LMs 29, 30) demonstrates a slightly posterior, and markedly posterior displacement in *M. nivalis* (Fig. 31a) and *M. frenata* (Fig. 31b) respectively over *M. erminea*.

Interestingly, landmarks in regions articulating between the skull and dentary are a) significant in all species from ventral, lateral, and occlusal views, and b) exhibit marked displacement throughout each of the TPS deformation girds. These loci incorporate portions of the mandibular condyle, and glenoid fossa of the skull, that together form the temporomandibular joint (TMJ). Moreover, several loci of the carnassials (P^4 and m_1) exhibit discernible variation across all species as depicted in TPS. Because carnassial teeth and the TMJ function as the primary food processing and masticating apparatuses respectfully within

carnivorans (Ewer 1973), these data may support claims of interspecific resource partitioning given that TPS morphologies have been averaged over multiple subspecies, and both sexes within each taxon. However, comprehensive analyses must be initiated before such conclusions are justified that include the full range of North American weasel subspecies, and specifically evaluate masticatory function in these taxa. Related studies of craniomandibular form and function in alternate groups of mustelids could be used as experimental benchmarks (e.g., Riley 1985). These assumptions may be complemented by interspecific modifications of the tympanum as well (Fig. 31), which could suggest differential auditory capabilities among these taxa. Although, limited information is known regarding the function of this character within carnivorans (Ewer 1973).

Additional variations such as the relative positioning of the foramen magnum, which exhibits markedly posterior displacement in *M. frenata* (Fig. 31b), may convey differential loading capabilities throughout the anterior cervical vertebra. These highly modified elements in weasels are thought to facilitate prey transport and cashing within narrow passages (King and Powell 2007). Data may therefore suggest differential prey exploitation among taxa. Of course, such inferences are merely speculative until systematic analyses are conducted throughout these anatomic regions and their associated musculatures using an extensive geographic subset of specimens. Consequently, a geometric morphometric evaluation of the atlas and axis morphologies in these taxa may be worth investigating in future analyses. It is also worth mentioning that average size dimorphism was more prominent in dentaries over skulls throughout all specimens evaluated (Table 5). Given that mandibles function almost exclusively as instruments for food acquisition and processing, these data would appear to support arguments that sexual dimorphism in weasels is facilitated by intraspecific resource partitioning as opposed

to sexual selection (see "Geographic Variation and Sympatry" section of Chapter 2 for discussion). Consequently, this analysis advocates for more comprehensive studies regarding craniomandibular form and function throughout North American weasel taxa.

Paleontological Significance

Review of these data support all 3 North American weasel species (*M. erminea*, *M. frenata*, and *M. nivalis*) among the SCBC paleofauna, with an overwhelming majority of specimens belonging to the long-tailed weasel *M. frenata* (Table 11, 13, Figs. 38-40). Presence of the least weasel *M. nivalis* among this assemblage (Table 11) is particularly significant given that SCBC lies well outside the western boundary of its historic distribution (Mead and Mead 1989) (Fig. 1), and therefore, represents the greatest displacement of *M. nivalis* from its modern range within the contiguous United States. It is suggested, however, that skull materials without a supportive basicranium are revisited using alternative methods due to a possible classification bias as consequence of differential landmark orientations (Table 13, Fig. 41).

While it is possible that some maxillary fragments may represent an extinct weasel taxon dissimilar to extant forms, this circumstance seems unlikely. First, only *M. frenata* is thought to have originated in the New World. Fossils examined thus far indicate that *M. erminea* and *M. nivalis* already exhibited modern morphologies by the time they crossed the Bering Strait into North America (Kurtén and Anderson 1980; King and Powell 2007). Second, evidence for a more basal *Mustela* taxon seems unlikely due to the age of this locality near the Pleistocene-Holocene boundary (9,460 +/- 160 to 15,100 +/- 700 years BP) (Mead and Mead 1989). Additionally, the suggested ancestral taxon of *M. frenata*, *M. rexroadensis*, has not been reported in fossil deposits younger than Pliocene-age (Kurtén and Anderson 1980).

This study highlights a functional tradeoff in the taxonomic application of landmarks from both skulls and mandibles of weasels. Characters of the skull, though effective in species-discriminating analyses, are less frequently preserved among paleontological localities (Lyman 1994). The quantity of moderately complete *Mustela* spp. skulls compared to dentaries among this assemblage may be a testament of this phenomenon. While dentaries are far more common in the fossil record, these materials are also more constrained in their taxonomic utility. This incidence may be due, in part, to the somewhat modest degree of interspecific variation expressed in their morphologies as illustrated among TPS (Figs. 29, 30) and PCA (Figs. 33, 35) of the dentary in both lateral and occlusal views. Furthermore, this reduction in classification efficiency may result from less type 1 and type 2 landmarks available relative to the skull (Figs 27, 28). It is acknowledged, however, that characters selected from either jaw profile were by no means exhaustive. Therefore, more scrutinous analyses of weasel dentaries, while overwhelmingly disregarded in literature thus far, may promote new understandings of their ecomophological and taxonomic utility for future paleontological and zoological studies.

CHAPTER 5

CONCLUSIONS

Geometric Morphometric Utility

In light of these analyses, both linear and landmark-based geometric morphometrics (GM) have demonstrated substantial taxonomic utility for classifying the skulls and dentaries of small mustelids. Although ferret-sized dentaries evaluated through linear GM achieved greater separation relative to weasel dentaries using 2-dimensional landmarks, all showed promise. Inconsistencies among methods may be an effect of differential variation between the black-footed ferret and American mink relative to interspecific variation in weasels. Moreover, linear GM facilitated the discrimination of 2 groups, while landmark-based GM separated 3 closely related taxa. Landmark analyses were quite successful, however, at discriminating weasel skulls that offered a greater number of discreet loci over characters of the corresponding dentaries. Such methods also proved effective for visually quantifying morphological variation among taxa within thin-plate spline deformation grids. However, the utility of 2-dimensional landmark analysis for classifying fossil specimens of markedly differential preservation was somewhat limited. Consequently, linear or 3-dimensional GM analyses are recommended unless homologous loci, and features providing structural support to each specimen are preserved. Finally, while both linear and landmark-based GM generated sufficient data for the purposes of this study, it may be worth comparing the utility of these methods by analyzing equivalent specimens using both types of analyses.

Interpretation of the SCBC Paleofauna

Snake Creek Burial Cave is a unique Late Pleistocene valley-bottom deposit within the Great Basin of western North America. This well-stratified locality has been interpreted as a

somewhat open vegetation-rich community, possibly of lacustrine and grassland affinity due to the presence of colonial ground squirrels, lagomorphs and other open-expanse inhabitants (Mead and Mead 1989). Review of *Mustela* spp. specimens collected from this locality support the occurrence of every *Mustela* taxon native to North America, including the long-tailed weasel *M. frenata*, ermine *M. erminea*, and least weasel *M. nivalis*, as well as the black-footed ferret *M. nigripes*. Presence of the latter 2 taxa (*M. nivalis, M. nigripes*) warrant prehistoric range extensions west of their modern and historic distributions respectfully (Fig. 1). While the American mink *Neovison vison* was formerly identified within this assemblage, its presence is not supported here. In juxtaposition with 3 additional mustelids (*Martes americana*, *M. noblis*, and *Gulo gulo*) reported among this assemblage (Mead and Mead 1989; Meyers 2007), SCBC yields a total of 7 species within the Mustelidae. Confirmation of *M. nigripes* and *M. nivalis* maintain support for a relatively open vegetational habitat during the Late Pleistocene in this region.

REFERENCES

Abdi H, Williams LJ. 2010. Principle component analysis. Wiley Interdisciplinary Reviews: Computational Statistics 2: 433-459.

Abramov AV. 2000. A taxonomic review of the genus *Mustela* (Mammalia, Carnivora). Zoosystematica Rossica 8: 357-364.

Abramov AV, Meschersky IG, Aniskin VM, Rozhnov VV. 2013. The mountain weasel *Mustela kathiah* (Carnivora: Mustelidae): molecular and karyological data. Biology Bulletin 40: 52-60.

Altizer S, Harvell D, Friedle E. 2003. Rapid evolutionary dynamics and disease threats to biodiversity. Trends in Ecology and Evolution 18: 589-596.

Anderson E. 1968. Fauna of the Little Box Elder Cave Converse County, Wyoming: the Carnviora. University of Colorado Studies, Series in Earth Sciences 6: 1-60.

Anderson E. 1977. Pleistocene Mustelidae (Mammalia, Carnivora) from Fairbanks, Alaska. Bulletin Museum of Comparative Zoology 148: 1-21.

Anderson E, Forrest SC, Clark TW, Richardson L. 1986. Paleobiology, biogeography, and systematics of the black-footed ferret, *Mustela nigripes* (Audubon and Bachman), 1851; pp. 11-62 *In* S. L. Wood, ed., The Black-footed Ferret. Great Basin Naturalist Memoirs Number 8. Brigham Young University, Provo, Utah.

Anderson E. 1989. The phylogeny of mustelids and the systematics of ferrets; pp. 10-20 *In* U. S. Seal, E. T. Thorne, M. A. Bogan, S. H. Anderson, eds., Conservation Biology and the Black-footed Ferret. Yale University Press, New Haven, Connecticut.

Aunapuu M, Oksanen T. 2003. Habitat selection of coexisting competitors: a study of small mustelids in northern Norway. Evolutionary Ecology 17: 371-392.

Baryshnikov GF, Bininda-Emonds OR, Abramov AV. 2003. Morphological variability and evolution of the baculum (os penis) in Mustelidae (Carnivora). Journal of Mammalogy 84: 673-690.

Bell CJ, Mead JI. 1998. Late Pleistocene microtine rodents from Snake Creek Burial Cave, White Pine County, Nevada. Great Basin Naturalist 58: 82-86.

Berdnikovs S. 2005. Evolution of sexual dimorphism in mustelids. Ph.D. dissertation, University of Cincinnati, Cincinnati, Ohio, 201 pp.

Biggins DE, Vargas A, Godbey JL, Anderson SH. 1999. Influence of prerelease experience on reintroduced black-footed ferrets (*Mustela nigripes*). Biological Conservation 89: 121-129.

Biggins DE, Livieri TM, Breck SW. 2011a. Interface between black-footed ferret research and operational conservation. Journal of Mammalogy 92: 699-704.

Biggins DE, Hanebury LR, Miller BJ, Powell RA. 2011b. Black-footed ferrets and Siberian polecats as ecological surrogates and ecological equivalents. Journal of Mammalogy 92: 710-720.

Biggins DE, Miller BJ, Hanebury LR, Powell RA. 2011c. Mortality of Siberian polecats and black-footed ferrets released onto prairie dog colonies. Journal of Mammalogy 92: 721-731.

Bininda-Emonds OR, Gittleman JL, Purvis A. 1999. Building large trees by combining phylogenetic information: a complete phylogeny of the extant Carnivora (Mammalia). Biological Reviews 74: 143-175.

Bookstein FL. 1991. Morphometric Tools for Landmark Data: Geometry and Biology. Cambridge University Press, New York, 435 pp.

Boyles JG, Storm JJ. 2007. The perils of picky eating: dietary breadth is related to extinction risk in insectivorous bats. PLoS ONE 2: e672.

Brickner KM, Grenier MB, Crosier AE, Pauli JN. 2014. Foraging plasticity in a highly specialized carnivore, the endangered black-footed ferret. Biological Conservation 169: 1-5.

Brown WL, Wilson EO. 1956. Character displacement. Systematic Zoology 5: 49-64.

Brown WC. 1966. Comparative osteology of *Mustela vison* Schreber and *Martes americana* Turton. M. S. thesis, University of Utah, Salt Lake City, Utah.

Bryant HN, Russell AP, Fitch WB. 1993. Phylogenetic relationships within the extant Mustelidae (Carnivora): appraisal of the cladistic status of the Simpsonian subfamilies. Zoological Journal of the Linnaean Society 108: 301-334.

Cain CM, Livieri TM, Swanson BJ. 2011. Genetic evaluation of a reintroduced population of black-footed ferrets (*Mustela nigripes*). Journal of Mammalogy 92: 751-759.

Campbell TM, III, Clark TW, Richardson L, Forrest SC, Houston BR. 1987. Food habits of Wyoming black-footed ferrets. American Midland Naturalist 117: 208-210.

Cavalcanti MJ, Monteiro LR, Duarte Lopes PR. 1999. Landmark-based morphometric analysis in selected species of serranid fishes (Perciformes: Teleostei). Zoological Studies 38: 287-294.

Clark TW. 1975. Some relationships of prairie dogs, black-footed ferrets and paleo- and modern Indians. Plains Anthropologist 20: 71-74.

Clark TW. 1986. Some guidelines for management of the black-footed ferret. Great Basin Naturalist Memoirs 8: 160-168.

Dayan T, Simberloff D, Tchernov E, Yom-Tov Y. 1989. Inter-and intraspecific character displacement in mustelids. Ecology 70: 1526-1539.

Dayan T, Simberloff D. 1994. Character displacement, sexual dimorphism, and morphological variation among British and Irish mustelids. Ecological Society of America 75: 1063-1073.

Digital Morphology a National Science Foundation Digital Library at the University of Texas at Austin [Internet]. 2002-2005. Austin (Texas): The University of Texas at Austin. [updated 2013 Mar 16; cited 2014 Jan 11]. Available from: http://www.digimorph.org/index.phtml

Dragoo JW, Honeycutt RL. 1997. Systematics of mustelid-like carnivores. Journal of Mammalogy 78: 426-443.

Eads DA, Millspaugh JJ, Biggins DE, Livieri TM, Jachowski DS. 2011. Postbreeding resource selection by adult black-footed ferrets in Conata Basin, South Dakota 92: 760-770.

Erlinge S. 1979. Adaptive significance of sexual dimorphism in weasels. Oikos 33: 233-245.

Erlinge S, Sandell M. 1988. Coexistence of stoat, *Mustela erminea*, and weasel, *M. nivalis*: social dominance, scent communication, and reciprocal distribution. Oikos 53: 242-246.

Ewer RF. 1973. The Carnivores. Cornell University Press, Ithaca, New York, 494 pp.

Fagerstone KA. 1987. Black-footed ferret, long-tailed weasel, short-tailed weasel, and least weasel; pp. 548-573 *In* M. Novak, J. A. Baker, M. E. Obbard, and B. Malloch, eds., Wild Furbearer Management and Conservation in North America. Ontario Ministry of Resources, Toronto, Canada.

Figueirido B, Palmqvist P, Pérez-Claros A. 2009. Ecomorphological correlates of craniodental variation in bears and paleobiological implications for extinct taxa: an approach based on geometric morphometrics. Journal of Zoology 277: 70-80.

Flesness NR. 1989. Mammalian extinction rates: background to the black-footed ferret drama; pp. 3-9 *In* U. S. Seal, E. T. Thorne, M. A. Bogan, and S. H. Anderson, eds., Conservation Biology and the Black-footed Ferret. Yale University Press, New Haven, Connecticut.

Flynn JJ, Finarelli JA, Zehr S, Hsu J, Nedbal MA. 2005. Molecular phylogeny of the Carnivora (Mammalia): assessing the impact of increased sampling on resolving enigmatic relationships. Systematic Biology 54: 317-337.

Gittleman JL, Van Valkenburgh B. 1997. Sexual dimorphism in the canines and skulls of carnivores: effects of size, phylogeny, and behavioral ecology. Journal of Zoology 242: 97-117.

Grafodatsky AS, Volobuev VT, Ternovsky DV, Radzhabli SI. 1976. G-banding of the chromosomes in seven species of Mustelidae (Carnivora). Genetika 13: 2123-2128.

Graham RW, Lundelius EL, JR. 2010. FAUNMAP II: new data for North America with a temporal extension for the Blancan, Irvingtonian and early Rancholabrean. FAUNMAP II Database, version 1.0 this website.

Grant PR. 1972. Convergent and divergent character displacement. Biological Journal of the Linnean Society 4: 39-68.

Grayson DK. 1987. The biogeographic history of small mammals in the Great Basin: some observations on the last 20,000 years. Journal of Mammalogy 68: 359-375.

Hall ER. 1981. The Mammals of North America, Second Edition. John Wiley & Sons, Inc., New York 2: 601-1181+90 pp.

Harding LE, Smith FA. 2009. *Mustela* or *Vison*? Evidence for the taxonomic status of the American mink and a distinct biogeographic radiation of American weasels. Molecular Phylogenetics and Evolution 52: 632-642.

Harrington, E. Eh Illustration [Internet]. Missoula (MT) [cited 2013 Sep 24]. Available from: http://www.ehillustration.com/ehillustration_about.html

Harris AH, Findley JS. 1964. Pleistocene-recent fauna of the Isleta Caves, Bernalillo County, New Mexico. American Journal of Science 262: 114-120.

Heaton TH. 1987. Initial investigation of vertebrate remains from Snake Creek Burial Cave, White Pine County, Nevada. Current Research in the Pleistocene 4: 107-109.

Heptner VG, Naumov NP, Yurgenson PB, Sludskii AA, Chirkova AF, Bannikov AG. 2002. Mammals of the Soviet Union, Volume II, part 1b. Smithsonian Institution Libraries and National Science Foundation, Washington, D. C, 1552 pp.

Hibbard CW. 1950. Mammals of the Rexroad Formation from Fox Canyon, Kansas. Contributions from the Museum of Paleontology University of Michigan 8: 113-192.

Hillman CN, Clark TW. 1980. *Mustela nigripes*. Mammalian Species 126: 1-3.

Hillson S. 2005. Teeth, Second Edition. Cambridge University Press, New York, 373 pp.

Hosoda T, Suzuki H, Harada M, Tsuchiya K, Han S, Zhang Y, Kryukov A, Lin L. 2000. Evolutionary trends of the mitochondrial lineage differentiation in species of genera *Martes* and *Mustela*. Genes and Genetic Systems 75: 259-267.

Jachowski DJ, Lockhart JM. 2009. Reintroducing the black-footed ferret *Mustela nigripes* to the Great Plains of North America. Small Carnivore Conservation 41: 58-64.

Jass CN, Bell CJ. 2011. Arvicoline rodent fauna from the room 2 excavation in Cathedral Cave, White Pine County, Nevada, and its biochronologic significance. Journal of Vertebrate Paleontology 31: 684-699.

King CM, Moors PJ. 1979. On co-existence, foraging strategy and the biogeography of weasels and stoats (*Mustela nivalis* and *M. erminea*) in Britain. Oecologica 39: 129-150.

King CM. 1983. *Mustela erminea*. Mammalian Species 195: 1-8.

King CM. 1989. The advantages and disadvantages of small size to weasels, *Mustela* species; pp. 302-334 *In* J. L. Gittleman, ed., Carnivore Behavior, Ecology, and Evolution. Cornell University Press, Ithaca, New York.

King CM, Powell RA. 2007. The Natural History of Weasels and Stoats: Ecology, Behavior, and Management. Oxford University Press, New York, 446 pp.

Klebanoff A, Minta S, Hastings A, Clark TW. 1991. Age-dependent predation model of black-footed ferrets and prairie dogs. SIAM Journal on Applied Mathematics 51: 1053-1073.

Koepfli K, Wayne RK. 2003. Type I STS markers are more informative than cytochrome *b* in phylogenetic reconstruction of the Mustelidae (Mammalia: Carnivora). Systematic Biology 52: 571-593.

Koepfli K, Deere KA, Slater GJ, Begg C, Begg K, Grassman L, Lucherini M, Veron G, Wayne RK. 2008. Multigene phylogeny of the Mustelidae: resolving relationships, tempo and biogeographic history of a mammalian adaptive radiation. BMC Biology 6: 10.

Korpimäki E, Norrdahl K, Rinta-Jaskari T. 1991. Responses of stoats and least weasels to fluctuating food abundances: is the low phase of the vole cycle due to mustelid predation? Oecologia 88: 552-561.

Kurose N, Abramov AV, Masuda R. 2000. Intrageneric diversity of the cytochrome *b* gene and phylogeny of Eurasian species of the genus *Mustela* (Mustelidae, Carnivora). Zoological Science 17: 673-679.

Kurose N, Abramov AV, Masuda R. 2005. Comparative phylogeography between the ermine *Mustela erminea* and the least weasel *M. nivalis* of Palaearctic and Nearctic regions, based on analysis of mitochondrial DNA control region sequences. Zoological Science 22: 1069-1078.

Kurose N, Abramov AV, Masuda R. 2008. Molecular phylogeny and taxonomy of the genus *Mustela*, (Mustelidae, Carnivora), inferred from mitochondrial DNA sequences: new perspectives on phylogenetic status of the back-striped weasel and American mink. Mammal Study 33: 25-33.

Kurtén B. 1968. Pleistocene Mammals of Europe. Transaction Publishers, Piscataway, New Jersey, 317 pp.

Kurtén B, Anderson E. 1980. Pleistocene Mammals of North America. Columbia University Press, New York, 442.

Lachenbruch PA, Goldstein M. 1979. Discriminant analysis. Biometrics 35: 69-85.

Lariviére S. 1999. *Mustela vison*. Mammalian Species 608: 1-9.

Lawlor TE. 1998. Biogeography of Great Basin mammals: paradigm lost? Journal of Mammalogy 79: 1111-1130.

Levine HJ. 1997. Rest heart rate and life expectancy. Journal of the American College of Cardiology 30: 1104-1106.

Lin LK, Motokawa M, Harada M. 2010. A new subspecies of the least weasel *Mustela nivalis* (Mammalia, Carnivora) from Taiwan Mammal Study. 35: 191-200.

Loy A, Spinosi O, Carlini R. 2004. Cranial morphology of *Martes foina* and *M. martes* (Mammalia, Carnivora, Mustelidae): the role of size and shape in sexual dimorphism and interspecific differentiation. Italian Journal of Zoology 71: 27-35.

Lyman RL. 1983. Prehistoric extralimital records for *Pappogeomys castanops* (Geomyidae), in northwestern New Mexico. Journal of Mammalogy 64: 502-505.

Lyman RL. 1994. Vertebrate Taphonomy. Cambridge University Press, New York, 524 pp.

Mandahl N, Fredga K. 1980. A comparative chromosome study by means of G-, C-, and NOR-bandings of the weasel, the pygmy weasel and the stoat (*Mustela*, Carnivora, Mammalia). Hereditas 93: 75-83.

Marmi J, López-Giráldez JF, Domingo-Roura X. 2004. Phylogeny, evolutionary history and taxonomy of the Mustelidae based on sequences of the cytochrome *b* gene and a complex repetitive flanking region. Zoologica Scripta 33: 481-499.

McDonald RA. 2002. Resource partitioning among British and Irish mustelids. Journal of Animal Ecology 71: 185-200.

McNab BK. 1971. On the ecological significance of Bergmann's Rule. Ecology 52: 845-854.

Mead EM, Mead JI. 1989. Snake Creek Burial Cave and a review of the Quaternary mustelids of the Great Basin. Great Basin Naturalist 49: 143-154.

Mead JI, Spiess AE, Sobolik KD. 2000. Skeleton of extinct North American sea mink (*Mustela macrodon*). Quaternary Research 53: 247-262.

Meiri S, Simberloff D, Dayan T. 2011. Community-wide character displacement in the presence of clines: a test of Holarctic weasel guilds. Journal of Animal Ecology 80: 824-834.

Merriam CH. 1896. Synopsis of the weasels of North America. North American Fauna 1: 1-45.

Messing HJ. 1986. A Late Pleistocene-Holocene fauna from Chihuahua, Mexico. The Southwestern Naturalist 31: 277-288.

Meyers JI. 2007. Basicranial analysis of *Martes* and the extinct *Martes nobilis* (Carnivora: Mustelidae) using geometric morphometrics. M.S. thesis, Northern Arizona University, Flagstaff, Arizona, 156 pp.

Moors PJ. 1980. Sexual dimorphism in the body size of mustelids (Carnivora): the roles of food habits and breeding systems. Oikos 34: 147-158.

Murphy EC, Dowding JE. 1995. Ecology of the stoat in *Nothofagus* forest: home range, habitat use and diet at different stages of the beech mast cycle. New Zealand Journal of Ecology 19: 97-109.

Nowark RM. 1999. Walker’s Mammals of the World, Volume I, Sixth Edition. John Hopkins University Press, Baltimore, Maryland 838 pp.

Owen PR, Bell CJ, Mead EM. 2000. Fossils, diet, and conservation of black-footed ferrets (*Mustela nigripes*). Journal of Mammalogy 81: 422-433.

Patterson BD, Ceballos G, Sechrest W, Tognelli MF, Brooks T, Luna L, Ortega P, Salazar I, Young BE. 2007. Digital Distribution Maps of the Mammals of the Western Hemisphere, version 3.0. NatureServe, Arlington, Virginia, USA.

Peters JE, Axtell RW, Kohn LA. 2010. Morphometric evaluation of the two mink subspecies in Illinois. Journal of Mammalogy 91: 1459-1466.

Pocock RI. 1921. On the external characters and classification of the Mustelidae. Proceedings of the Zoological Society of London 91: 803-837.

Powell RA, Zielinski WJ. 1983. Competition and coexistence in mustelid communities. Acta Zoologica Fennica 174: 223-227.

Ralls K, Harvey PH. 1985. Geographic variation in size and sexual dimorphism of North American weasels. Biological Journal of the Linnean Society 25: 119-167.

Reig S. 1997. Biogeographic and evolutionary implications of size variation in North American least weasels (*Mustela nivalis*). Canadian Journal of Zoology 75: 2036-2049.

Reig S. 1998. 3d digitizing precision and sources of error in the geometric analysis of weasel skulls. Acta Zoologica Academiae Scientiarum Hungaricae 44: 61-72.

Riley MA. 1985. An analysis of masticatory form and function in the three mustelids (*Martes americana*, *Lutra canadensis*, *Enhydra lutris*). Journal of Mammalogy 66: 519-528.

Rosenzweig ML. 1966. Community structure in sympatric Carnivora. Journal of Mammalogy 47: 602-612.

Saarma U, Tumanov IL. 2006. Phylogenetic evaluation of three subspecies from the *Mustela nivalis* group. Zoological Studies 45: 435-442.

Sandell M. 1989. Ecological energies, optimal body size and sexual size dimorphism: a model applied to the stoat, *Mustela erminea* L. Functional Ecology 3: 315-324.

Santymire RM, Wisely SM, Livieri TM, Howard J. 2012. Using canine width to determine age in the black-footed ferret *Mustela nigripes*. Small Carnivore Conservation 46: 17-21.

Sato JJ, Hosoda T, Wolsan M, Tsuchiya K, Yamamoto M, Suzuki H. 2003. Phylogenetic relationships and divergence times among mustelids (Mammalia: Carnivora) based on nucleotide sequences of the nuclear interphotoreceptor retinoid binding protein and mitochondrial cytochrome *b* genes. Zoological Science 20: 243-264.

Sato JJ, Wolsan M, Prevosti FJ, D'Elía G, Begg C, Begg K, Hosoda T, Campbell KL, Suzuki H. 2012. Evolutionary and biogeographic history of weasel-like carnivorans (Musteloidea). Molecular Phylogenetics and Evolution 63: 745-757.

Seal US, Thorne ET, Bogan MA, Anderson SH (eds.). 1989. Conservation Biology and the Black-footed Ferret. Yale University Press, New Haven, Connecticut, 302 pp.

Sheffield SR, King CM. 1994. *Mustela nivalis*. Mammalian Species 454: 1-10.

Sheffield SR, Thomas HH. 1997. *Mustela frenata*. Mammalian Species 570: 1-9.

Simpson GG. 1945. The principles of classification and a classification of mammals. Bulletin of the American Museum of Natural History 85: 1-350.

Varela S, Lobo JM, Hortal J. 2011. Using species distribution models in paleobiogeography: a matter of data, predictors and concepts. Paleogeography, Paleoclimatology, and Paleoecology 310: 451-463.

Vargas A, Anderson SH. 1996. Effects of diet on captive black-footed ferret (*Mustela nigripes*) food preference. Zoo Biology 15: 105-113.

Wallace SC. 2006. Differentiating *Microtus xanthognauthus* and *Microtus pennsylvanicus* lower first molars using discriminant analysis of landmark data. Journal of Mammalogy 87: 1261-1269.

Webster M, Sheets HD. 2010. A practical introduction to landmark-based geometric morphometrics; pp. 163-188 *In* J. Alroy and G. Hunt, eds., Quantitative Methods in Paleobiology. The Paleontological Society Papers, Volume 16.

Wisely SM, Buskirk SW, Fleming MA, McDonald DB, Ostrander EA. 2002a. Genetic diversity and fitness in black-footed ferrets before and during a bottleneck. The American Genetic Association 93: 231-237.

Wisely SM, Buskirk SW, Fleming MA, McDonald DB, Ostrander EA. 2002b. Morphological changes to black-footed ferrets (*Mustela nigripes*) resulting from captivity. Canadian Journal of Zoology 80: 1562-1568.

Wozencraft WC. 2005. Order Carnivora; pp. 282-293 *In* D. E. Wilson and D. M. Reeder, eds., Mammal Species of the World: a Taxonomic and Geographic Reference. John Hopkins University Press, Baltimore, Maryland.

Youngman PM. 1994. Beringian ferrets: mummies, biogeography, and systematics. Journal of Mammalogy 75: 454-461.

Zelditch ML, Swiderski DL, Sheets HD, Fink WL. 2004. Geometric Morphometrics for Biologists: a Primer. Elsevier Academic Press, New York and London, 469 pp.

APPENDICES

Appendix A

SCBC specimens: NAUQSP8711/115B-NAUQSP8711/125B

* Each scale bar square = 1cm.

NAUQSP 8711/115B: Relatively large incomplete left dentary fractured anterolabialy at the c_1 alveolus. Lower dentition is primarily absent aside from m_1; however, alveoli are preserved throughout all lower cheek-teeth.

NAUQSP 8711/116B: Relatively large complete left dentary. Posterior cheek-teeth p_3 - m_2 remain intact with preservation of the p_2 alveolus. Lower canine alveolus is fairly complete aside from a missing fragment of the anterolingual edge.

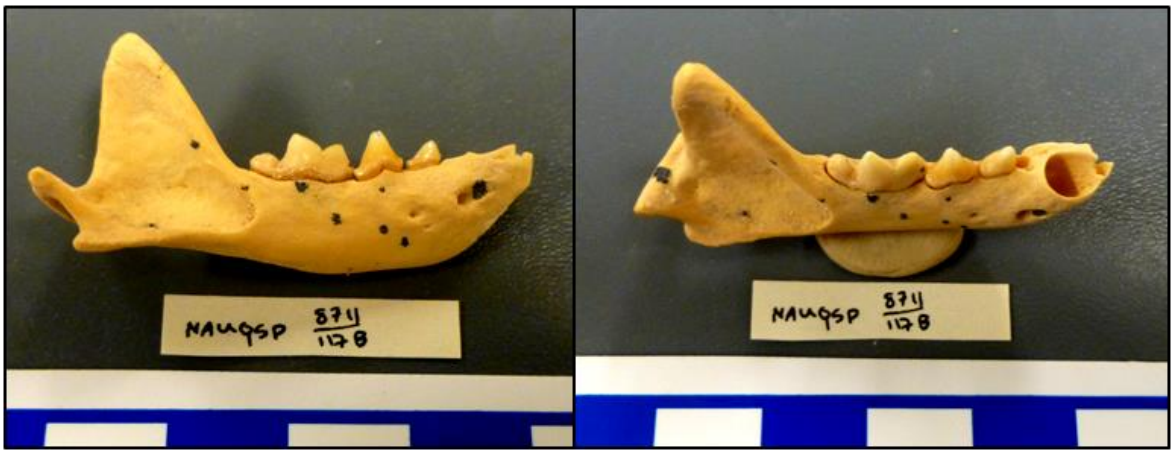

NAUQSP 8711/117B: Relatively large complete right dentary. Cheek-teeth p_3 -m_1 are intact with preservation of the p_2 alveolus. C_1 alveolus is fairly complete aside from a small anteromedial fracture. M_2 is absent, with alveolus completely sealed.

NAUQSP 8711/118B: Moderately sized complete right dentary. Cheek-teeth p_2 - m_1 remain intact with preservation of the c_1 alveolus. Majority of m_2 is absent, fractured at the root within the alveolus.

NAUQSP 8711/119B: Moderately sized complete left dentary. Cheek-teeth p_3 - m_1 remain intact with preservation of the p_2 and c_1 alveoli. M_2 is absent with alveolus completely sealed apart from a shallow occlusal depression.

NAUQSP 8711/120B: Relatively large and overall complete right dentary. Both lingual and labial ends of the condyloid process have been fractured, though medial portion centered along the axis of the coronoid process remains. Alveoli are preserved throughout all lower cheek-teeth and at the c_1, however, only m_1 remains intact.

NAUQSP 8711/121B: Relatively small incomplete left dentary. Anterior end fractured posteroventraly from the posterior edge of the c_1 alveolus. Dorsal end of the coronoid process is fractured medially. Lower p_4 and m_1 remain intact with preservation of the p_2 and p_3 alveoli. Lower m_2 alveolus is completely sealed.

NAUQSP 8711/122B: Moderately sized complete left dentary. P_4 and m_1 remain intact with p_3 and m_2 alveoli preserved. C_1 alveolus is relatively complete aside from a small anteromedial fracture. P_2 alveolus is completely fused.

NAUQSP 8711/123B: Relatively small complete right dentary. P_3 - m_1 remain intact with preservation of the c_1, p_2, and m_2 alveoli.

NAUQSP 8711/124B: Relatively large and fairly complete right dentary. Majority of the coronoid process has fractured off. Only m_1 remains intact, with all other cheek-teeth alveoli preserved. C_1 alveolus is relatively complete aside from a small anterolingual fracture.

NAUQSP 8711/125B: Relatively small incomplete left dentary. Anterior end of the mandibular symphysis is fractured posterolabialy down through the c_1 and p_2 alveoli breaking off the anterior edge of the p_3 enamel. Labial plane of the condyloid process is broken. Only p_4 remains completely intact with m_1 fractured approximately half way through the trigonid. M_2 is absent, with alveolus completely sealed.

Linear Data

Linear measurements for extant *Neovison vison* (n=21).

Spec. ID #	TDL	DP_p3	DP_m1	p4_H	p4_W	m1_L	m1_TalW	m2_D	m2_W	MTR
ETMNH011	41.02	7.88	7.27			8.08	3.25	2.17	2.08	20.43
ETMNH012	34.67	6.89	5.96	3.46	2.22	7.48	2.92	2.13	1.92	18.72
ETMNH013	38.40	7.41	6.83		2.35	8.27	3.51	2.58	2.44	20.43
ETMNH014	39.40	8.24	7.21	4.08	2.42	8.97	3.52	2.57	2.50	21.51
ETMNH016	42.30	8.35	8.37	3.77	2.88	9.07	3.66	2.54	2.49	22.02
ETMNH017	34.82	6.91	6.64	2.95	2.40	7.57	3.00	2.12	1.96	18.21
ETMNH018	38.22	7.52	6.61		2.49	8.01	3.05	2.42	2.26	20.08
ETMNH019	36.20	7.68	6.45	3.42	2.51	7.70	3.12	2.37	2.21	19.62
ETMNH438	40.15	7.70	7.25	3.61	2.58	8.72	3.33	2.29	2.22	20.71
ETMNH496	43.87	8.75	7.22	3.93	2.78	8.57	3.57	2.41	2.27	21.72
ETMNH599	39.63	8.11	8.09	3.42	2.44	7.72	3.14	2.27	2.21	19.25
ETVP5543	35.35	6.63	6.44	2.75	1.98	6.88	2.36	1.96	1.74	18.13
ETVP5542	41.61	8.20	7.39	3.68	2.69	8.10	3.30	2.18	2.23	21.24
NAUQSP2053	39.66	8.12	7.71	3.58	2.62	8.06	3.42	2.57	2.51	20.97
NAUQSP2054	35.07	7.16	6.13	3.43	2.28	7.63	3.28	2.26	1.90	18.04
NAUQSP2055	42.85	8.82	7.72	3.78	2.56	8.7	3.34	2.12	2.02	21.10
NAUQSP6611	41.42	7.97	7.15	3.83	2.74	8.13	3.36			
NVPL7062	41.28	8.26	7.24	3.82	2.77	8.93	3.43	2.46	2.61	21.72
NVPL7063	35.62	7.42	5.76	3.01	2.35	7.04	2.69	2.12	2.03	18.52
NVPL7064	36.67	7.34	6.29	3.45	2.56	7.36	3.02	1.95	1.82	18.87
NVPL7065	36.98	7.33	6.72	3.43	2.67	7.70	2.90	2.00	2.02	19.33

Values are represented in millimeters. Blank spaces indicate missing or fragmentary features averaged according to species. Symbols correspond with abbreviations in Table 1.

Linear measurements for extant *Mustela nigripes* specimens (n=38).

Spec. ID #	TDL	DP_p3	DP_m1	p4_H	p4_W	m1_L	m1_TalW	m2_D	m2_W	MTR
ETVP3146	38.65		7.48	3.03	2.41	7.98	2.39	1.07	0.98	17.26
ETVP7261	41.70	8.94	8.09	3.88	2.60	8.81	2.45	1.77	1.60	19.37
ETVP7262	40.34	9.00	8.16		2.54	8.40	2.41	1.19	1.22	18.65
ETVP7263	37.78	8.81	7.57		2.40	7.99	2.32			
ETVP7264	41.98	8.93	8.51		2.80	8.94	2.45			
ETVP7265	36.89	8.43	6.89	3.10	2.44	7.57	2.22			
ETVP7266	38.62	8.25	7.27		2.47	8.19	2.32			
ETVP7267	37.46	8.50	7.41		2.29	8.16	2.30	1.97	1.81	17.46
ETVP7268	41.98	9.42	8.49	3.72	2.76	8.65	2.39	1.62	1.47	19.46
ETVP7269	41.74	9.31	7.78	3.47	2.65	8.68	2.43	1.80	1.62	19.57
ETVP7270	38.67	9.10	7.63	3.46	2.50	8.05	2.36	1.08	0.94	17.57
ETVP7271	41.95	9.31	8.06	3.59	2.84	8.60	2.56	1.62		19.07
ETVP7272	38.85	8.61	7.89	3.17	2.39	7.94	2.29	1.60	1.48	17.76
ETVP7273	41.10	9.20	8.00	3.40	2.67	8.83	2.57	1.34		
ETVP7310	41.23	9.26	8.45	3.43	2.64	8.43	2.38	1.70		19.04
ETVP7311	42.58	9.04	8.40			8.91	2.53	1.96	1.84	19.85
ETVP3146	43.06	9.54	8.68	3.73	2.81	8.78	2.31	1.75	1.70	
NVPL6902	39.34	8.80	7.42			8.17	2.29	1.45	1.50	18.18
NVPL6903	38.30	8.10	7.35		2.43	8.16	2.27	1.65	1.60	17.94
NVPL6904	44.37	10.37	8.77		2.78	8.80	2.60			
NVPL6906	38.12	8.46			2.53	7.92	2.32	1.38	1.25	17.36
NVPL6907	39.15	8.84	7.74		2.40	8.49	2.30	1.75	1.58	17.61
NVPL6910	38.35	8.31	7.34		2.40	8.00	2.28	1.57	1.42	17.32
NVPL6911	40.10	8.70	7.95		2.41	8.15	2.22			
NVPL6912	39.34	9.36	7.56	3.31	2.69	8.11	2.31			
NVPL6913	38.35	8.32	7.45			8.17	2.25	1.75	1.62	17.89
NVPL6914	42.72	9.95	8.57	3.95	2.85	8.83	2.45	1.91	1.70	19.71
NVPL6915	42.92	9.54	8.79	3.10	2.92	8.92	2.54		1.41	19.55
NVPL6919	39.03	8.90	7.53	3.35	2.51	8.00	2.32	1.60	1.52	18.33
NVPL7009	42.48	9.85	7.84		2.63	8.67	2.43	1.47	1.47	
NVPL7010	38.36	8.14	7.11	3.02	2.42	8.01	2.31	1.56	1.42	17.57
NVPL7012	39.31	8.48	7.72		2.42	8.13	2.29			
NVPL7013	39.02	8.48	7.50		2.47	8.15	2.17			
NVPL7014	40.86	8.79	8.25		2.46	8.39	2.41	1.41	1.41	18.59
NVPL7068	37.70	8.13	7.48	2.98	2.38	7.78	2.15	1.63	1.54	17.67
NVPL7069	37.95	8.77	7.68	3.39	2.43	8.02	2.46	1.68	1.64	17.74
NVPL7070	41.76	9.64	7.89		2.68	8.71	2.41			
NVPL7072	39.57	9.04	7.80	3.07	2.59	8.91	2.53	1.78	1.67	18.39

Values are represented in millimeters. Blank spaces indicate missing or fragmentary features averaged according to species. Symbols correspond with abbreviations in Table 1.

Appendix B

SCBC weasel crania

NAUQSP8711/195B

NAUQSP8711/197B

NAUQSP8711/198B

NAUQSP8711/201B

NAUQSP8711/204B

NAUQSP8711/206B

NAUQSP8711/207B

NAUQSP8711/208B

NAUQSP8711/209B

NAUQSP8711/210B

1 CM

NAUQSP8711/211B

1 CM

NAUQSP8711/212B

1 CM

NAUQSP8711/213B

VITA

NATHANIEL S. FOX

Education:	Rockport High School, Rockport, Massachusetts 2007
	B.S. Biology, geology minor, University of Massachusetts, Amherst, Massachusetts 2011
	M.S. Geosciences East Tennessee State University, Johnson City, Tennessee 2014
Professional Experience:	Lab Volunteer, Marine Science Center, University of New England, Biddeford, Maine 2007
	Lab Volunteer, Biology Department, University of Massachusetts, Amherst, Massachusetts 2009
	Intern, The Mammoth Site of Hot Springs, South Dakota 2011
	Intern, Denver Museum of Nature and Science, Denver, Colorado 2011
	Field Assistant, Gray Fossil Site, Johnson City, Tennessee 2012-13
	Teaching Associate and Research Assistant, Department of Geosciences, East Tennessee State University, Johnson City, Tennessee 2012-14
Presentations:	Fox, N. S. Interpretation of Early Mesozoic Ichnology in Holyoke, MA**.** Southeast Association of Vertebrate Paleontology, Boone, North Carolina 2012.
	Fox, N. S., S. C. Wallace, and J. I. Mead. Partitioning of *Mustela nigripes* and *Neovison vison* dentaries from Snake Creek Burial Cave, NV**.** Tenth North American Paleontological Convention, Gainesville, Florida 2014.

Honors and Awards:	Full Graduate Assistantship, ETSU 2012-13
	University Honors, University of Massachusetts, Amherst 2011
	Eagle Scout, Boys Scouts of America 2007
Affiliations:	
	American Society of Mammalogists
	Ecological Society of America
	Golden Key International Honor Society
	ETSU Graduate and Professional Student Association
	Don Sundquist Center of Excellence in Paleontology
	Society of Vertebrate Paleontology